

**THE ANNEALING STUDIES ON THE STRUCTURE
AND PROPERTIES OF ELECTROLESS AMORPHIC
TRANSITION METAL-METALLOID SYSTEM: Ni₁₀**

A THESIS

submitted in fulfilment of the
requirements for the award of the d
of
DOCTOR OF PHILOSOPHY
in
PHYSICS

By

S. V. S. TYAGI



**DEPARTMENT OF PHYSICS
UNIVERSITY OF ROORKEE
ROORKEE-247 667 (INDIA)**

December, 1986


TO MY BELOVED WIFE

SAROJ


CANDIDATE'S DECLARATION

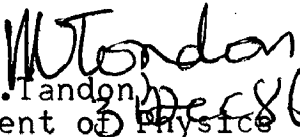
I hereby certify that the work which is being presented in thesis entitled 'THE ANNEALING STUDIES ON THE STRUCTURE AND PROPERTIES OF ELECTROLESS AMORPHOUS TRANSITION METAL-METALLOID SYSTEM: Ni_{100-x}P_x' in fulfilment of the requirement for the award of the Degree of Doctor of Philosophy, submitted in the Department of Physics of the University is an authentic record of my own work carried out during a period from December 1979 to October 1986 under the supervision of Dr. V.K.Tandon, Prof. V.K.Srivastava and Dr. S.Ray.

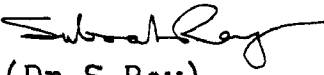
The matter embodied in this thesis has not been submitted by me for the award of any other degree.


(S.V.S.Tyagi)

This is to certify that the above statement made by the candidate is correct to the best of our knowledge.


(Prof.V.K.Srivastava)
Department of Physics
University of Roorkee
Roorkee.


(Dr.V.K.Tandon)
Department of Physics
University of Roorkee
Roorkee.


(Dr.S.Ray)
Reader

Department of Met. Engineering
University of Roorkee
Roorkee-247 667
INDIA.

Dated
31. 12. 86

ACKNOWLEDGEMENT

It has been a matter of privilege for me to join research under Dr.V.K.Tandon, Prof.V.K.Srivastava and Dr.S.Ray, my thesis supervisors, for their expert guidance. I express my heartfelt gratitude and deep appreciation for their continuous interest, discussions and encouragement throughout the period of this work.

It has been a pleasure to work with Dr.S.K.Barathwal, who guided me at each and every step in the preparation of Resistivity set up and measurements. He has always been available for the remedy of our experimental problems.

I take the opportunity to express my thanks to Dr.R.C.Bemby, Department of Chemistry for his help in the analysis of samples. My thanks are also due to Dr.O.V.Singh, Dr.Mala Tyagi and Dr.R.Singh for providing help in the elemental analysis.

It is a matter of pleasure to thank Dr. Kailash Chandra, Director USIC for providing all facilities to work in the University Service and Instrumentation Centre, even after working hours. I am thankful to Mr.Jagdish Saini for VSM studies, Mr.N.C.Saini for TEM and Mr.Brahm Pal for carrying out X-ray diffraction studies and other staff members of the Centre for their helping and cooperative attitude.

I am thankful to Prof.S.K.Joshi, Prof.B.P.Singh, Prof.N.C.Varshneya and Prof.S.N.Gupta for providing me all the facilities for executing the research work in the Physics Department, University of Roorkee, Roorkee.

I also record my appreciation and thankfulness to all the staff members and research scholars of Physics Department, for providing me congenial atmosphere and cooperation during my stay at this place.

I express my thanks to Mr.Arvind K.Jain, Dr.K.S.Balyan, Miss Kiran Jain, Sri R.K.Sharma and Kamyar Ajdari for helping me in the thesis work even at the crucial stage of their work.

My thanks also due to Dr.R.R.Mehrotra, former principal, D.J.College, Baraut for granting me study leave and financial assistance for the purchase of books etc..

To reach at this cherished stage of my life, I have been extremely fortunate in getting unreserved love and affection from my parents-in-law, mother and my family members. My daughter and niece also extended cooperation and son Amitabh has also been of great help.

I donot have words to express my idebtedness to Saroj, my wife, who took utmost care of my health and welfare. Without her encouragement and cooperation, I would have never embarked upon research career.

In the last I am thankful to Mr. D.P.Tyagi and Mr.S.P. Singh for a good typing of this thesis.



(.S.V.S.Tyagi)

SYNOPSIS

Amorphous metallic alloys, characterised by the absence of a long range atomic order, have emerged as an important class of materials of widespread scientific and industrial interest. These materials have unique magnetic, electrical transport, mechanical and other physical properties as a direct consequence of their non-crystalline structure.

There are two important classes of magnetic amorphous alloys- the transition metal-metalloid system and rare earth transition metal system. The transition metal-metalloid amorphous alloys have been prepared by various techniques, like rapid quenching from the melt, sputtering, electrodeposition and electroless deposition. The transition metal-metalloid amorphous alloys prepared by a relatively simple technique like electroless deposition have not been investigated in detail. Also, the thermal stability of these alloys as revealed by annealing studies and the modes of crystallization may, to an extent, depend on the technique used in their preparation.

In the present investigation, we undertake the annealing studies of the amorphous transition metal-metalloid system of $\text{Ni}_{100-x}\text{P}_x$ with the following objectives :

- (i) To prepare Ni-P alloys of different phosphorus content ranging from a few atomic percent to as high as twenty three atomic percent using electroless deposition technique.

(ii) To characterize the magnetic and resistivity behaviour of these alloys at temperatures from liquid nitrogen to about 800 K.

(iii) To study the crystallization behaviour of these alloys.

The subject matter of the thesis has been arranged in seven chapters.

The contents of the chapters are :-

Chapter 1

The first chapter introduces the amorphous alloys with a particular emphasis on the metal-metalloid systems. The scope and the objectives of the present investigation have been elaborated in this chapter.

Chapter 2

The second chapter contains a review of the present understanding on the amorphous transition metal-metalloid system in respect of its preparation techniques, magnetic properties, electrical transport properties, structure and annealing behaviour. The experimental results for certain specific systems like NiP, NiB and CoP alloys have been particularly emphasized in view of their direct relevance to the present investigation.

Chapter 3

This chapter describes the experimental procedure adopted for the preparation of amorphous Ni-P alloys films and the measurements carried out. The chemical analysis have been performed by gravimetric, and magnetic moment method. The micro-structure and the changes in the structure on heating have been determined by using hot stage transmission-electron-microscopy. The structural changes on annealing have been investigated by both, the selected area diffraction pattern (SAD) and X-ray diffraction technique. Vibrating Sample Magnetometer has been used to study the magnetic properties and the changes on annealing in the temperature range from 77 K to 800 K. The resistivity of the films and their change on annealing have been measured by four-probe method over a temperature range starting from liquid nitrogen temperature to 780 K.

Chapter 4

The effect of annealing on the structure of Ni-P alloys has been reported in this chapter. The structural changes, as observed by SAD and X-ray diffraction, indicate the state of the as-deposited samples. The samples are purely microcrystalline, a mixture of amorphous and microcrystalline, or amorphous depending upon the phosphorous content of the sample.

The precipitation of metastable phases and the crystallization of the amorphous samples have been observed by studying the X-ray diffraction and SAD at different intermediate temperatures during the process of crystallization.

Chapter 5

The magnetic behaviour of electroless Ni-P system has been investigated in the range of phosphorus from 5 to 23 atomic percent and the results have been presented in this chapter. The amorphous Ni-P alloys with phosphorous between 12 - 23 atomic percent shows a decrease in magnetic moment with an increase in phosphorus content and the sample becomes non-magnetic beyond 17 atomic percent. The Curie and Paramagnetic Curie temperatures of the samples have been estimated assuming weak ferromagnetism. The universal features of resistivity as reflected in Mooij Correlation have been explored. The effect of phosphorus content on TCR and room temperature resistivity has been reported here along with the thermal behaviour of resistivity of amorphous alloys.

Chapter 6

The Ni-P alloys may be classified in three categories on the basis of the annealing response. (a) Phosphorus less than 12 atomic percent (b) 12 - 21 atomic percent and (c) Phosphorus content greater than 21 atomic percent. The magnetic moment of the samples containing upto 12 atomic percent phosphorus decreases continuously with temperature, but the samples with 12 to 21 atomic percent show two peaks in magnetization. Beyond 21 atomic percent phosphorus only one peak in magnetization is observed on heating. Thus, the samples with 12 - 23 atomic percent phosphorus are amorphous showing crystallization behaviour through these peaks.

Annealing behaviour has also been investigated by resistivity and it is seen that the crystallization takes place through several metastable stages indicated by definite drops in resistivity. These stages have been identified and discussed. The irreversible changes have been confirmed by temperature cycling.

Chapter 7

The concluding remarks arrived at the end of this investigation are contained in chapter 7. The amorphous metal-metalloid system like Nickel-Phosphorus, though simple, yet, show many interesting features in the structure, magnetization and resistivity behaviour on annealing which can be profitably explored to know more about the nature of the amorphous phase and the complexities of crystallization.

A B S T R A C T

The nickel phosphorous alloys over the phosphorous composition range 5.4at.% to 23.5 at .% have been prepared using the electroless deposition technique. The technique consists in depositing a nickel phosphorous alloy on a substrate, suitably sensitized by SnCl_2 and PdCl_2 , from a bath containing nickel sulphate sodium citrate, ammonium sulphate and sodium hypophosphite through μ chemical reduction.

The structure of the as-deposited state and the effect of annealing on the as-deposited structure have been investigated using transmission-electron-microscopy, selected area diffraction, X-ray diffraction techniques in the temperature range of 300K to 670 K.

The magnetization and electrical resistivity behaviour and the effect of annealing on these properties have been investigated using Vibrating Sample Magnetometer and four probe resistivity measurements in the temperature range from 120 K to 800 K.

The electroless Ni-P alloys may be, from the structural point of view, classified into four regions:

- (i) Polycrystalline containing less than 11 at .% phosphorous.
- (ii) Microcrystalline containing 11-14 at.% phosphorous.

(iii) Mixed microcrystalline and amorphous having 14-18 at.% phosphorous and

(iv) Amorphous for more than 18 at.% phosphorous.

The alloys are observed to be weak itinerant ferromagnets with strong short range order. The magnetic moments of as-deposited state are found to be 4.40, 2.43, 1.58 & 0.60 emu/g for samples containing 13.0, 15.0, 16.4 and 17.3 at.% respectively. The T_c are found to be 398, 318 and 283 K and T_p 498, 469 and 432 K for samples containing 15, 16 and 16.4 at.% phosphorous respectively.

The Mooij correlation can be observed in the electrical resistivity behaviour. The resistivity is found to be 71 μohmcm for 11 at.% phosphorous sample and finally increases to a value of 187 $\mu\text{ohm cms}$ and the T C R, which is much less than that for the crystalline phase, decreases to a value of $12 \times 10^{-5}/\text{K}$ for 21.5 at.% phosphorous. ^{sample} The extrapolated value for T C R reduces to zero at 23.5 at.% phosphorous. In the temperature range of 140 K to 280 K, the resistivity is observed to be linear with T^2 and then becomes linear with T from 280 K to 400 K.

The polycrystalline and microcrystalline films containing less than 12 at.% phosphorous undergo a stress relaxation at around 450 K and subsequently, around 650K

the precipitation of Ni_3P reduces the resistivity markedly and enhances the magnetization. In the amorphous films containing more than 18 at.% phosphorous there is a very small reduction of resistivity at around 420 K and attributes to atomic relaxation. A continued heating shows a lowering of resistivity over a broad temperature range and a corresponding peaks in the magnetization. At the end of this temperature range there is a sharp drop in resistivity and another peak in magnetization to correspond with it. The former reaction taking place over a broad temperature range results in the precipitation of nickel and its higher phosphides. The extent of this reaction reduces with increasing phosphorous content and it becomes non-existent in an alloy containing about 23.5 at.% phosphorous. The alloys with intermediate phosphorous contents of 12 to 18 at.% show a superposition of the characteristic reactions taking place in the microcrystalline and amorphous regions.

L I S T O F P U B L I C A T I O N S

1. Study of the Crystallization Behaviour of Electroless Ni-P films by Electron and X-ray Diffraction, Z, Metallkde, 76, 492, 1985.
2. Electron Microscopy study of Chemically deposited Ni-P film, Bull. Mater.Sci.8, 433, 1986.
3. Electron-microscopy study of Chemically deposited amorphous Ni-P films, National Symposium on Thin Film Science and Technology (9-11) Bangalore, India, Jan.1985.
4. Transformation in Electroless Ni-P alloys- a resistivity study (under communication).
5. Magnetization Behaviour on annealing in electroless Ni-P alloys (under communication).
6. The Crystallization studies on the amorphous electroless metal-metalloid system: Ni-P (to be communicated)

C O N T E N T S

Chapter		Page
1	INTRODUCTION	1
2	THE AMORPHOUS TRANSITION METAL-METALLOID SYSTEM:A REVIEW	
2.1	THE AMORPHOUS METAL-METALLOID SYSTEM	6
2.2	THE PREPARATION TECHNIQUES	7
2.3	THE STRUCTURAL STUDIES;NICKEL PHOSPHOROUS	8
2.4	THE MAGNETIC STUDIES	12
2.5	THE ELECTRICAL RESISTIVITY STUDIES	18
2.6	ANNEALING AND CRYSTALLIZATION BEHAVIOUR STUDIES	21
3	EXPERIMENTAL PROCEDURES	27
3.1	THE ELECTROLESS DEPOSITION TECHNIQUE	27
	3.1.1 The General Considerations	
	3.1.2 Selection Of The Composition of Bath	
	3.1.3 The Substrate Preparation Procedure	
3.2	THE COMPOSITIONAL ANALYSIS	35
	3.2.1 Gravimetric Method	
	3.2.2 The Magnetic Moment Method	
3.3	THE STRUCTURAL MEASUREMENTS	36
3.4	MAGNETIC MEASUREMENTS	38
3.5	THE RESISTIVITY MEASUREMENTS	39
4	THE STRUCTURE OF ELECTROLESS DEPOSITED Ni-P ALLOYS: ANNEALING STUDIES	41
4.1	RESULTS: ELECTRON-MICROSCOPY AND X-RAY DIFFRACTION	43
	4.1.1 Polycrystalline Films	
	4.1.2 Apparently amorphous films	

4.1.3	Amorphous As-deposited Samples	
4.1.4	Films Containing Both Microcrystalline and Amorphous Regions.	
4.2	ANNEALING STUDIES: CHARACTERISTICS OF AS-DEPO- SITED STATE	45
4.3	DISCUSSION	47
4.4	SUMMARY	51
5	THE MAGNETIZATION AND ELECTRICAL RESISTIVITY BEHAVIOUR OF ELECTROLESS AMORPHOUS Ni-P	52
5.1	THE MAGNETIC PROPERTIES: RESULTS	52
5.1.1	The Compositional Dependence of Magnetization	
5.1.2	The Temperature Dependence Of Magnetiza- tion.	
5.2	DISCUSSION	57
5.3	ELECTRICAL RESISTIVITY: RESULTS	59
5.3.1	The Compositional Dependence of Resistivity.	
5.3.2	The Temperature Dependence of Resistivity	
5.4	DISCUSSION	63
5.5	SUMMARY	66
6	THE CRYSTALLIZATION BEHAVIOUR OF ELECTROLESS Ni-P SYSTEM	67
6.1	ANNEALING STUDIES USING HOT STAGE ELECTRON- MICROSCOPY AND X-RAY DIFFRACTION: RESULTS	68
6.1.1	Hot Stage Electron-Microscopy	
6.1.2	X-Ray Diffraction Studies	
6.2	ANNEALING STUDIES USING VSM: RESULTS	71
6.2.1	The Annealing Behaviour Of The Magneti- zation Of Polycrystalline Ni-P System	

6.2.2	The Annealing Behaviour Of The Magnetization Of Amorphous Ni-P System.	
6.3	RESISTIVITY CHANGES ON ANNEALING:RESULTS	81
6.3.1	The Annealing Behaviour Of The Resistivity of Polycrystalline And Microcrystalline Ni-P System	
6.3.2	The Annealing Behaviour Of The Resis- tivity Of Amorphous Ni-P System.	
6.4	DISCUSSION: THE CRYSTALLIZATION BEHAVIOUR	86
6.5	SUMMARY	94
7	CONCLUDING REMARKS	96
	REFERENCES	103

CHAPTER 1

INTRODUCTION

The magnetic amorphous metallic alloys, lacking crystalline order and having rather unique magnetic, electrical, mechanical and other properties resulting from their amorphous structure, are a subject of current interest both from a fundamental as well as the application point of view.

The present intense interest in amorphous alloys, or METGLASSES as they are more widely referred to, can be traced to the following factors :

(i) The invention, by Duwez in 1959, of a practical way to quench a metallic melt at rates as high as a million kelvin per second.

(ii) The prediction of the possibility of ferromagnetism in such alloys by Gubanov (1) in 1960 and the experimental confirmation of this somewhat improbable prediction by Mader and Nowick (2) five years later in 1965 on vacuum deposited Co-Au alloys.

(iii) The gradual realization that these alloys have unique properties some of which were earlier considered to be mutually exclusive, e.g., the amorphous alloys are strong like oxide glasses but unlike oxide glasses they can also be deformed plastically. Moreover the unexpected form of magnetism in the alloys have made them a good candidate for the replacement of Fe-Si laminations in power transformers.

Yet another feature of interest from application point of view is the absence of macroscopic magnetocrystalline anisotropy that amorphous ferromagnets have, as this results in a high initial permeability and a very low coercive force.

In the amorphous alloys, in contrast to crystalline alloys, one can vary the composition continuously in a single phase and hence can study a physical property as a function of composition and temperature, and at the same time just like crystalline alloys, they are known to display a complete range of electronic behaviour, i.e., conductors (even super conductors), semiconductors and insulators. It is, however, important to realize that through the change of temperature and composition, certain not so obvious changes such as structural relaxation, do occur in the amorphous phase and these may well influence the electrical, magnetic and crystallization behaviour etc. of the phase.

A broad question, which always so to say haunts the investigator while studying any amorphous system, is that in what ways does the lack of crystalline order affects the physical properties such as electrical resistivity, magnetization, mechanical characteristics etc. of the system. Then, of course, this question apart, one attempts to get answers to other related questions such as the factors that stabilize the amorphous phase—the crystallization behaviour, and to what extent does the above properties depend upon the method used for the preparation of the alloys.

The present work is an attempt to understand the crystallization behaviour of amorphous metal-metalloid system through the annealing studies on the structure, magnetization and electrical resistivity. Although many work exist on the structure, magnetic properties, resistivity behaviour, as well as some on the effect of annealing on these properties, few have been to study the crystallization behaviour. Here, annealing studies have been made on all these properties in an integrated way for the purpose of evolving a clear picture of the steps involved, the phases formed etc. during the crystallization.

The system that has been selected for this purpose of investigating the crystallization behaviour is a magnetic amorphous alloy, Nickel-Phosphorous, which is a transition metal-metalloid alloy and belongs to the former of the two important classes of magnetic amorphous alloys, the transition metal-metalloid alloys and the rare earth-transition metal alloys.

The study of Ni-P alloy because of its simplicity may be considered as a starting point for the understanding of the crystallization behaviour of more complex ternary and quaternary systems. Also there are other aspects that needs more investigation such as the nature of the as-deposited state, the way the preparation method influences the annealing behaviour.

The electroless deposition is the method of preparation that has been chosen to investigate the above aspects of the Ni-P system. The reasons for this choice

have been such as the simplicity of this method as compared to, say, the melt quenching. Also relatively speaking, compared to the electrodeposition methods, a few studies only have opted for films prepared by electroless technique. The modes of crystallization and the thermal stability of these alloys as probed through annealing studies do, to an extent, depend upon the techniques used in the alloy preparation. Many discrepancies in the results of an amorphous Ni-P system have been attributed by workers to concentration inhomogenieties in the amorphous samples and it has been pointed out that the degree and distribution of these inhomogenieties depend on the method of preparation.

A systematic investigation of structural, magnetic and electrical properties of electroless deposited $\text{Ni}_{100-x}\text{P}_x$ alloy in the composition range of x as five atomic percent to as high as twenty four atomic percent and over the temperature range of 120 K to 800 K has been undertaken in the following sequence.

First, since it is the structure that governs the behaviour of the physical properties, the structure of the as-deposited state is investigated by electron-microscopy, selected area diffraction and supplemented by X-ray diffraction and through the annealing of the as-deposited state. The result of this investigation is presented in chapter 4.

Next, the intrinsic properties of the amorphous phase such as magnetic moment, Curie and paramagnetic Curie temperature, resistivity and the temperature coefficient of resistivity (TCR), their compositional and temperature

dependence have been investigated using vibrating sample magnetometer (VSM) and four probe measurements. The results of this aspect form the subject matter of chapter 5.

Finally in chapter 6 a systematic study of crystallization has been undertaken through the annealing response of both the magnetization as well as the resistivity of the amorphous phase in the temperature range upto 800 K. The purpose of this study is to have an understanding of the crystallization behaviour of transition metal-metalloid (TM-M) class of magnetic amorphous alloys and in particular, Ni-P system. The study is concluded in chapter 7. In chapter 2 a review is presented of the work done by earlier workers on the structure, electrical and magnetic properties and the crystallization behaviour of the metal-metalloid system with a particular emphasis on Ni-P and Co-P alloys along with the principles of different methods of preparation of amorphous alloys. Chapter 3 gives the details of the experimental procedures used in the present investigation.

CHAPTER 2

THE AMORPHOUS TRANSITION METAL-
METALLOID SYSTEM : A REVIEW

The chapter presents a brief review of the work done by the earlier investigators on the annealing studies on the structure, magnetic and electrical resistivity of the amorphous transition metal-metalloid system. Although, broadly speaking, many review articles and books (3-8) are available, most deal with amorphous alloys prepared by rapid quenching from the melts. In this review, however, the emphasis is on electroless and electrodeposited transition metal-metalloid system Ni-P.

2.1 THE AMORPHOUS METAL-METALLOID SYSTEM

Though it is difficult to produce metals in the amorphous form, certain metallic alloys composition can be prepared in the amorphous form and are reasonably stable in this state. The amorphous magnetic alloys, the class to which NiP belongs, have been the subject of considerable investigation and consist of one or more transition metals Fe, Co, Ni alloyed with glass formers such as B, P, Si, Al along with Cr or Mo that are added to impart certain specific properties (9). The magnetic properties, hardness, strength as well as corrosion properties appear to be of particular interest for industrial applications. Some examples of the amorphous alloys are Au-Si, Pd-Si, Co-P, Fe-B, Ni-P, Fe-P-C, Fe-Ni-P-B; Mg-Zn, Cu-Mg; Zr-Cu, Zr-Ni, Ti-Ni.

2.2 THE PREPARATION TECHNIQUES

The important techniques of the preparation of the amorphous alloys are a) Splat quenching, b) Sputtering and evaporation, c) Ion implantation, d) Electrodeposition, and e) Electroless deposition. Mentioned below is only the physical idea of these methods very briefly.

One of the important way of making amorphous alloys is to quench the melt so rapidly that there is insufficient time for the crystallites to nucleate and grow (splat quenching). Yet another is to deposit the allow from vapor phase on to a cold substrate, so that the impinging atoms (3) have no time to arrange themselves in a crystalline lattice (vapor quenching) so that the solidification takes place so rapidly that the atoms are frozen in their liquid configuration. To achieve a high quenching rate one needs to maximize the contact area between melt and the cooling medium. The various techniques used for this purpose are splat quenching, melt spinning, atomization etc..

The sputtering technique is based upon atom by atom constitution of the product. This technique has been extensively used for the preparation of rare earth-transition metal films, which is an important class of amorphous alloys. This is due to high quenching rates inherent in sputtering methods $\sim 10^8$ K/sec. The sputtering is typically carried out in the presence of an inert gas e.g. Argon. Evaporation methods, in a way, are similar to sputtering methods.

The ion implantation technique consists in amorphizing a metal foil by ion implanting solute atom in it. This technique has been used to prepare some otherwise impossible amorphous alloys such as Cu-W or Pt-Au. This method allows some freedom from the compositional restrictions imposed by constitutional phase diagrams.

Many transition metal-metalloid amorphous alloy systems have been prepared by electrodeposition technique. It has been observed that the precise composition of the product depends strongly on the deposition conditions and bath composition during sample formation. In contrast sample fabrication by other methods such as melt quenching, sputtering, etc. results in a product having a composition very nearly that of the melt from which it is formed.

Typical baths used for amorphous Ni-P and CoP samples have been described (10,11). The baths are essentially the same as used by Brenner (12) to prepare first Ni-P amorphous alloy samples by electrodeposition. Similar baths have been used later on by many workers (13-15) to prepare amorphous samples.

The electroless deposition technique, being the method used in this work, is presented in chapter 3.

2.3 THE STRUCTURAL STUDIES: NICKEL PHOSPHOROUS

Brenner (12) was the first to prepare Ni-P alloys by electrodeposition and he claimed it to be an amorphous system but this aspect was not studied much until 1965. Goldstein (16) studied electroless deposited Ni-P alloys containing 12.5 to 17.4 at. % phosphorous using X-ray and electron-diffraction,

and found them to be a dense, amorphous, liquid like structure. It was claimed to be the first occurrence of an amorphous metallic solid in massive form. The as-deposited state of chemically reduced nickel is highly metastable. Graham et.al. (17) analyzed electron and X-ray diffraction patterns of as-deposited electroless Ni-P alloys (8 to 16 at. % phosphorous) and concluded that the structure of alloys is a supersaturated solid solution of P dissolved in fcc nickel with numerous stacking faults. They also detected a $\langle 111 \rangle$ fibre texture, the strength of which increased with annealing. To account for the precipitation hardening in these alloys they proposed a plane of coherency between the crystal structures of nickel and the precipitated Ni_3P . The findings of Graham et.al. (17) were later confirmed by Pai and Marton (18).

Albert et.al (19) also found on the basis of X-ray studies that the as-deposited films with phosphorous contents from 0.5 to 14 at. % had a strained single phase f.c.c. structure. Meada (20) studied electron diffraction patterns of electrodeposited films containing upto 7 at. % phosphorous and he also found fcc polycrystalline nickel with a $\langle 111 \rangle$ fibre texture. Grain size decreased rapidly with increasing phosphorous content and was only 50 to 60 A° in films containing 4 at. % phosphorous.

Randin et.al. (21) and Schlesinger and Marton (22) found electroless deposited Ni-P alloys to be a supersaturated solid solution in a metastable liquid like state and the solid solution of phosphorous in nickel as a metastable intermediate state between that of a mixture of nickel plus phosphorous and

the equilibrium system of Ni + Ni₃P. This intermediate state includes phosphorous atoms chemically bonded to nickel atoms as phosphide. Cargill (10) analyzed X-ray interference functions for electrodeposited Ni-P alloys of 19 and 26 at.% P and found that they had more short range order than observed in a liquid noble metal above its melting point. Reasonable agreement with X-ray data has been obtained by using models of dense random packing of hard spheres. Somewhat better agreement was obtained by using spheres of slightly different sizes.

While the most previous X-ray studies show the as-deposited high-phosphorous content films to be amorphous, the evidence from an electron microscopy study is to the contrary. Bagley and Turnbull (23) followed the mode of transformation to the equilibrium state and concluded that only a sample with a composition of nearly Ni₃P is initially amorphous. At slightly lower phosphorous content, isothermal annealing of the films resulted in crystallite coarsening, suggesting an original microcrystalline structure. The Ni-P samples with composition ranging from 12 to 17 at. % have been found to be microcrystalline by Berrada (24) while Ni₈₂P₁₈ sample is amorphous as shown by X-ray diffraction. X-ray diffraction patterns for microcrystalline Ni-P alloys show a mixture of fcc Ni+Ni₃P. The D.T.A. trace and high value of H_c, were also indicating that the sample containing from 12 to 17 at.% P are a mixture of two phases i.e. Ni and Ni₃P.

Bennett et.al. (25) studied Ni-P system containing 15 to 25 atomic % phosphorous prepared by both electrodeposition

and electroless deposition methods and assumed them to be amorphous. Alloys prepared by the two techniques give different knight shifts, suggesting different local structure. Linewidth measurements support a binary dense random packing of hard-spheres model in which phosphorous atoms have only Ni neighbours.

A. Cziraky et.al. (26) in the study of electroless deposited Ni-P alloys prepared samples by chloride as well as sulphate bath and also by electrodeposition method. The SAD pattern of the samples produced by chloride bath contains a diffuse ring at 2.03 \AA° . While with certain sulphate baths and electrodeposited samples SAD contains one more diffuse ring at 3.3 \AA° . Its position coincides with the first occurring line 220 of the Ni_5P_2 compound.

With the help of NMR studies, it was observed that the samples prepared by chemical reduction exhibit a much higher degree of inhomogeneity than the samples prepared by other methods. Yamasaki (27) studied electroless deposited Ni-P system with phosphorous contents 12.5 and above atomic percent examined by large angle X-ray scattering and concluded that the structure of this system is quite similar to that of the amorphous material obtained by other methods such as rapid quenching of liquid metal and electrodeposition. Cortiju and Schlesinger (28) studied electroless Ni-P films and concluded that it is a solid solution of phosphorous in crystalline fcc nickel structure. The smearing out of the diffraction pattern for low pH (high phosphorous contents) value can

initially be attributed to one or more of the following :

- (i) partial crystallinity
- (ii) small crystallite size
- (iii) internal strains.

Co-P and Ni-B

The Co-P and Ni-B systems are similar to Ni-P in many ways, they are, like Ni-P, prepared by electrodeposition and electroless techniques. Extensive structural studies have been carried out on these systems. Instead of attempting a review, only some of the important work is referred to here.

In Co-P the early work has been of Fisher and Chilton (29), Judge et.al. (30), Konbe and Kanematsu (31). The more recent and important work has been of Pan and Turnbull (32), Cargill and Cochran (33-36), Riveiro et.al. (37-38).

The structural studies on Ni-B system are of more recent origin. The first important one being of Gorbunova et.al. (39), Hedgecock et.al. (40) on electroless Ni-B system. Rapidly quenched Ni-B was studied by Takahashi et.al. (41) Kaul and Rosenberg (42) and Bakonyi and Panissod (43-44).

2.4 THE MAGNETIC STUDIES

Nickel-Phosphorous

It was Rhodes and Wohlfarth (45) who gave experimental data for Curie Weiss constant and saturation magnetization of a wide variety of ferromagnetic substances, and used this to calculate respective values for the numbers of magnetic carriers q_c and q_s . A plot of the ratio q_c/q_s as dependent on the Curie temperatures reveals two branches. For one, the

ratio $q_c/q_s \approx 1$ and for the other $q_c/q_s > 1$. The second branch corresponds to nickel and its alloys in addition to some other substances and their alloys and these were classified as weak itinerant ferromagnets. This criteria has been used to classify the nature of ferromagnetism in amorphous Ni-P alloys.

Albert (19) studied Ni-P films prepared by the techniques of electroless, electrodeposition and vacuum coating with phosphorous contents from 0 to 11 at. % and noted that the spontaneous magnetization of Ni-P films decreases linearly with increasing phosphorous contents until being non-magnetic at about 15 at. %. Simpson and Brambley (46) studied the variation of saturation magnetization with temperature of Ni₈₅P₁₅ alloy, in the as-deposited state and also in a crystalline metastable single phase condition. The Curie temperature and saturation magnetization were appreciably reduced, having values 390 K and 7 emu/gm respectively, as compared to pure nickel. The corresponding state curves were found to be below as compared to the crystalline phase.

Pan and Turnbull (47) studied magnetic properties of Ni-P alloys prepared by electrodeposition technique containing 12 - 23 atomic percent phosphorous with the help of Foner VSM in fields upto 8 K Oe between 70 and 370°K. Ferromagnetic Curie temperatures, T_c , determined by the 'method of thermodynamic parameters' were found to decrease from 212 to 75 K as phosphorous concentration increases from 12.41 to 16.8 at. %. Paramagnetic Curie temperatures, T_p , were deduced from the temperature dependence of initial susceptibilities χ_1 , above T_c . The difference $T_p - T_c$ were of the

order of 100 °K for all specimens and several times larger than for crystalline ferromagnetic materials. At high field the low temperature magnetization decreases with phosphorous concentration and ferromagnetism disappears at about 17 at. %, in close agreement with T_c measurement and at phosphorous composition 16 - 18 at. %, amorphous Ni-P alloys behave as weak itinerant ferromagnets and has a decreasing paramagnetic susceptibility beyond that composition.

Schneider and Weisner (48) studied the magnetic properties of rapidly quenched Ni-P alloys with 12 to 18 atomic percent phosphorous. The Curie temperature is estimated by extrapolating the M_s vs T curve at 8 K Oe to $M = 0$ and comes out to be (513 ± 10) K which is comparable with T_c of the metastable fcc single phase of $Ni_{85}P_{15}$ ($T_c = 530$) (46). The amorphous $Ni_{82}P_{18}$ shows no ferromagnetic order, it seems to be a simple paramagnet. The solubility limit of phosphorous in nickel is very small. Therefore the results are compared with those of Ni-Si alloys. The value of remanance to saturation magnetization $\frac{M_r}{M_s}$ increases by annealing to about 0.5, whereas the ratio $\frac{M_r}{M_s}$ of the quenched alloy (as-prepared) is very low. The increase in M_r/M_s is attributed to the removal of strain.

Berrada et.al. (24) made a detailed study of electro-deposited Ni-P alloys containing 15 to 25 atomic percent phosphorous. The experimental results show that the magnetism is not of the same nature below and above a critical conc. which determines two concentration ranges : the first one

(15 to 18 at. % phosphorous) presents the character of a weak homogeneous ferromagnetism, while inhomogeneties dominate the magnetic properties of the second one (18 to 25 at. % phosphorous), i.e., the amorphous alloys in this range are characterized by magnetic clusters, whose size increases with phosphorous concentration.

The saturation magnetization and the Curie temperatures deduced from Arrott plots decrease linearly with increasing phosphorous concentration in the range 15 to 18 at. % phosphorous. The Arrott plots are linear in wide temperature and magnetic field ranges. The slopes of straight lines are nearly temperature independent and the intercept of these lines with M^2 axis varies linearly with $(T/T_c)^2$ above and below the Curie temperature. These results show that the alloys are nearly homogeneous weak ferromagnets.

For larger phosphorous concentration (greater than 18 at. %) results are quite different, as Arrott plots are no more linear and the magnetization results from two contributions $M = \chi H + M_c(H, T)$: (i) a non magnetic part $\chi(T)H$, slowly temperature dependent and decreasing with increasing phosphorous concentration and (ii) a magnetic contribution $M_c(H, T)$ which saturates at low temperatures for fields H_s decreasing with increasing concentration of phosphorous; this contribution is not a unique function of H/T .

In this concentration range, the phosphorous atoms are well distributed in the alloy, and the fluctuations of the moment on atoms contributing to the total magnetism are

rather negligible. Thus Ni-P system remains magnetic in the whole conc. range 15 to 25 at. % phosphorous, although a critical concentration separates (18 at. % phosphorous) two different magnetic behaviours. In the range 18 to 25 at. % phosphorous coercivity measurements also confirm the existence of inhomogenities.

Pure nickel phosphorous film has been deposited (Tamura and Endo (49)) onto the glass substrate cooled by liquid nitrogen. The Curie temperature T_c and spontaneous magnetization σ_s in the amorphous state show a marked decrease compared with crystalline state. The ratio of T_c and σ_s between amorphous and crystalline state are respectively about 0.85 and 0.60. The decrease of T_c and σ_s are due to its amorphous structure and not caused by its impurities.

In crystalline materials the inverse paramagnetic susceptibility χ^{-1} depends linearly on temperature (Curie - Weiss Law), if one excludes temperatures very near to T_c . The amorphous materials exhibit a strong upward curvature of $\chi^{-1}(T)$ (50) in a very wide temperature range. Bakonyi (51) made a detailed study of the disappearance of the spontaneous magnetization in nickel-metalloid alloys with increasing metalloid (B, C, Si or P) content. These elements form a continuous series of homogeneous solid solutions with nickel in the form fcc - Ni(M) upto a critical concentration of metalloid. He (51) proposed a new scheme on the band structure changes upon alloying in these systems which is capable of explaining all the existing experimental observations. Alloying nickel with metalloids has two effects

(i) the d-band is gradually filled up when the solute concentration increases and (ii) at the same time the exchange splitting of the d-bands decreases. Since both the effects work parallel, we could call this scheme as a band desplitting and filling (BD + F) model. This picture does not require the density of states to remain unchanged with respect to those of pure nickel although there are several indications that changes are not substantial upto concentrations necessary for completely suppressing the ferromagnetism of nickel. Bakonyi et.al.(15) also made a detailed study of melt quenched and electrodeposited Ni-P amorphous alloys in the concentration range of phosphorous from 18 to 22 at. %, below room temperature. All the alloys investigated contain magnetic inhomogeneities, the amount and nature of which depend on impurities and on the details of sample preparation and it could be established that Ni-P alloys with phosphorous content greater than 18 at. % exhibit Pauli paramagnetism and Pauli susceptibility was found to decrease rapidly with phosphorous content. They also found a similarity of the electronic structure and short range order in amorphous Ni-P alloys and crystalline Ni_3P compound.

The magnetic properties of electrodeposited amorphous Co-P system has been very widely studied (11,29-33, 52). One of the, such, important study is of PAN and Turnbull (32) who investigated system having phosphorous concentration in the range 18 to 33 at. % and found that the ratio of remanance to saturation magnetization, i.e., σ_r/σ_s were several hundred times lower for amorphous than for polycrystalline, the

magnetic moment. decreases with increasing phosphorous content and more rapidly at phosphorous concentration greater than 23 at. %. T_c also decreases with increasing phosphorous content and would vanish at a content well below 33 at. % .

2.5 THE ELECTRICAL RESISTIVITY STUDIES

Nickel-Phosphorous

The early study of the electrical resistivity of Ni-P alloys has been by Schlisinger and Marton (22). In this study the resistivity of the chemically as-deposited films was found to be orders of magnitude higher than that of corresponding bulk material. During heating, the resistivity of fresh films is found to undergo a drastic reduction. Boucher (53) studied electrical resistivity of Ni-Pd-P alloys prepared by rapid quenching from the melt between temperature range 4.2 K and 300 K and in some cases upto 450 K. For a given phosphorous content of either 20 or 25 at. %, the resistivity and its temperature coefficient at room temperature are practically independent of the ratio of Ni to Pd, the resistivity varies with phosphorous content. The temperature coefficient of resistivity decreases with increasing phosphorous content and becomes negative around 24 at. % phosphorous. Around this composition, the alloys have a very small TCR which varies within $\pm 2 \times 10^{-5} / K$ from specimen to specimen. Pai and Marton (18) studied electroless Ni-P alloys containing upto 16 at. % phosphorous. When the as-deposited films are heated in vacuum, the resistivity was observed to change drastically, accompanied by structural transformation of the film from a single phase fcc

structure to a two phase structure of fcc nickel and tetragonal Ni_3P . The mechanism responsible for the changes in resistivity can be described by two different thermally activated processes. One is the annihilation of grain boundaries, which decreases the resistivity, and the other process is the formation of Ni_3P which tends to increase the resistivity. It was observed that a large proportion of Ni_3P is formed only above 573 K. The activation energy of the process was found to be both temperature and film thickness dependent.

Based on the model of resistivity and Mathiessen's rule, the observed resistivity in the present case may be expressed as

$$\rho = \rho_1 + \rho_2 + \rho_3$$

where ρ_1 is largely the grain boundary part, ρ_2 is the Ni_3P part and ρ_3 is the phonon part of the total resistivity ρ . ρ_3 in our case is small and can be neglected.

In the temperature range 300 K - 700 K, errors between calculated values of ρ and the observed ones are less than 6%. Above 700 K, the deviation is much larger, which is believed to be due to following reason : When the crystal size of nickel is sufficiently large i.e., at 775 K, complete conduction path will appear, formed solely by nickel. Under this condition the entire current will be almost conducted through nickel only, inspite of the presence of Ni_3P , and with the result, the resistivity decreases drastically. The model suggested here may be applicable to other cases also. Cote (14) made electrical resistivity measurements

between 4 K and 300 K on glassy Ni-P alloys prepared by electrodeposition method, which are used to show that liquid transition metal theory is applicable to the metallic glasses and explains his results for Ni-P and Beeby's "sinking band" (54) model is far better approximation than the rigid band model for Ni-P.

In view of the amorphous structure of the metallic glasses, liquid metal theory is thought to provide a basis for understanding the electronic properties of these glasses.

The transport property measurements combined with structure factor determination by X-ray measurements (14) are found to be consistent with a liquid like structure for Ni-P alloys. The high temperature contribution to the resistivity may be explained in the framework of the extended Ziman theory (55) as was discussed by Meisel and Cote (56) and Cote and Meisel (57); as a result they obtained for amorphous alloys the analogue of the Bloch-Gruneisen function for crystalline alloys : the resistivity shows a quadratic temperature dependence at low temperatures and a linear one at high temperatures.

Cote (14) has shown that the room temperature resistivity of electrodeposited Ni-P alloys increases from 104 to 175 $\mu\Omega\text{cm}$ while TCR undergoes a gradual transition from $1.8 \times 10^{-4}/\text{K}$ to $-0.4 \times 10^{-4}/\text{K}$ over the composition range from 15 to 25 at. % phosphorous. The transition occurs at 23.00 at. % phosphorous which is remarkably close to similar transition at 24 at. % phosphorous seen by Boucher (53) for

Ni-Pd-P alloy. Berrada (13) reported investigation on Ni-P electrodeposited films from 15 to 25 at. % phosphorous in the temperature range of 1 K to 100 K. They have seen a resistivity minima between 5 K and 10 K and a quadratic temperature dependence above resistivity minima. Residual resistivity is significantly higher $\rho(0) \approx 100 \mu\Omega \text{ cm}$ than for crystallized nickel alloys in similar ranges and increases with phosphorous. For temperature greater than 100 K resistivity depends linearly on temperature and upto 100 K, they observed a quadratic temperature dependence of resistivity.

2.6 ANNEALING AND CRYSTALIZATION BEHAVIOUR STUDIES

Nickel-Phosphorous

Randin et. al. (58) studied electroless Ni-P films from 7 at. % to about 20 at. % phosphorous with the help of DTA study in the range of temperature from 300 K to about 800 K. It was observed that for samples containing 11.5 at. % to 14.15 at. % $\frac{P}{\Lambda}$ a diffuse peak of low intensity covers the entire temperature interval from 473 K to 573 K and a second peak at 583 K with small intensity and markedly broadened towards the high temperature side of the scale.

At low phosphorous concentration, e.g., at 7.3 at. %, the broadening of the latter peak is more pronounced.

At phosphorous contents larger than 17.4 at. %, one single sharp peak appears at 583 K.

So there are two reaction areas one below 573 K and other above 573 K. The intensity of the first peak is maximum at 14.15 at. % which vanishes after 17.4 at. %. The energy corresponding to second reaction area is proportional to phosphorous content. It has been concluded that the last products formed after crystallization are Ni and Ni₃P and no other phosphide. Albert (19) also found after annealing at 850 K a stable configuration Ni₃P + Ni of his Ni-P films containing upto 11 at. % phosphorous. The same conclusion was also derived by Bagley and Turnbull (59) for his electrodeposited films containing phosphorous from 12.5 to 25 at. % after annealing at above 673 K for half an hour. He also performed DSC measurements and obtained two exothermic transformations at 553 ± 2 K and second at 683 ± 5 K for his Ni-P sample containing 25 at. % phosphorous. But the sample containing 12.5 at. % phosphorous had only one reaction at 667 ± 2 K.

X-ray diffraction pattern of their 24.96 at. % phosphorous sample, heated for 2 minute at 598 K was too complex to be indexed but did not correspond to Ni₃P.

Maeda (20), studied electrodeposited Ni-P films containing only upto about 7 at. % phosphorous, found that the equilibrium phase obtained at 673 K contains not only Ni₃P but also higher phosphides like Ni₅P₄ and Ni₇P₃.

Pai and Marton (18) prepared ^{their} ~~his~~ Ni-P films by electroless deposition method and made a detailed structural study. Heat treatment of the sample ^{at} ~~of~~ 373 K causes no appreciable change. Further heating gives a peak, centred

at the Ni [111] position. When the sample is heated to 673 K or above, some well resolved peaks appear corresponding to fcc Ni and tetragonal Ni₃P. No evidence of Ni₃P appears in the diffraction spectrum of Ni-P films heated below 573 K. The Ni₃P crystals are believed to be dispersed in the matrix of nickel crystals and form a crystal mixture of Ni and Ni₃P. Simpson and Brambley (46) made observations on his electroless Ni₈₅P₁₅ samples, for crystallization behaviour through DTA, which showed two peaks, one at 537 K, corresponding to amorphous to a metastable single phase transition and the second peak at 659 K. The second peak corresponds to a transition from a metastable fcc single phase to the equilibrium two phase alloy (Ni+Ni₃P). On the basis of unchanged constant value of magnetization in the temperature range 523 K to 568 K, they concluded that the sample continues to remain in the metastable fcc single phase.

Schneider and Wiesner (48) studied rapidly quenched Ni-P samples containing phosphorous from 12 to 18 at. %. They observed two sharp exothermic peaks at 476 K and 609 K. He however observed no peak in 16 at. % phosphorous sample in DTA, which he attributes to microcrystalline nature of his rapidly quenched samples.

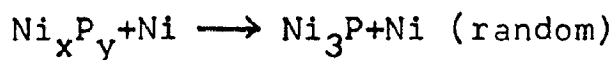
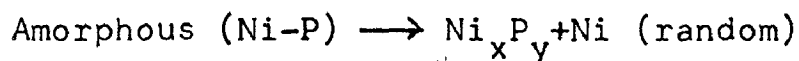
Based on these three DTA studies (46,48,58) one may conclude the following :

One peak is always observed in the region 310°C to 380 °C (583 K to 653 K). Intensity of this peak increases as the phosphorous content increases. This peak may be

attributed to the transformation of the sample to an equilibrium mixture of Ni + Ni₃P. A second peak at a lower temperature is observed only in samples with intermediate phosphorous range, i.e. from 11.5 to 17.5 at. %. This is usually low intensity and diffuse in nature. This peak may be attributed to a transition from amorphous to a metastable single crystalline phase. Thus both the samples containing less than 11.5 at. % phosphorous and those containing more than 17.5% P do not show this peak, one may conclude that in both these cases (less than 11.5 and greater than 17.5 at. %) transformation to intermediate phase does not take place i.e., samples with greater than 17.5 at. % phosphorous remain amorphous upto say 310 °C (583 K) and then transform to an equilibrium mixture of Ni + Ni₃P, while samples with less than 11.5 at. % remain a single metastable crystalline phase (a supersaturated solid solution of phosphorous dissolved in crystalline nickel). With increase of temperature, the crystallites grow and finally equilibrium transformation, to Ni + Ni₃P, takes place at about 310 °C (583 K). Only in the case of samples with phosphorous in the range 11.5 at. % to 17.5 at. %, that the initial as-deposited phase may contain a mixture of regions both amorphous and microcrystalline (60) and transform to an intermediate complex phase containing Ni_x+ Ni_xP_y (61) in the temperature range (473 - 573 K), before the sample finally goes to the equilibrium mixture of Ni + Ni₃P at above 310 °C (583 K).

Makhsosm (61) made a detailed electron microscopy study of electrodeposited Ni-P samples containing 7,12,20

and 22 at. % phosphorous to understand their crystallization behaviour. Heating a low phosphorous content film causes the crystalline array to decompose to an equilibrium mixture of Ni and Ni₃P. The heating of a high phosphorous content film causes several complex transformations following two reactions :



where Ni_xP_y is a newly discovered^{ve} phase with a variable composition. Further electron beam heating gives the second transformation to equilibrium mixture. The microstructure resulting from the above transformations depends on the variation in composition of the as-deposited specimens, rates of heating and temperature gradients. The mode of phase transformation is distinctly different in the microcrystalline and amorphous regions. Crystallization in amorphous regions occurs by nucleation and growth (23) of Ni_xP_y and Ni. Crystallization in microcrystalline regions occurs by nucleation and growth of Ni₃P phase and grain coarsening of Ni phase. No distinct crystallization front is observed as in amorphous regions.

Cziraky, et.al. (26) studied both electroless and electrodeposited Ni-P samples. They have used a chloride (c) bath and a sulphate (S) bath for electroless deposition. The DSC on C type samples (i.e. samples prepared from a chloride bath) for the substrate side and solution side exhibited markedly different crystallization processes. In C-type sample, the onset of crystallization process occurs at unusually low temperature (473 K). TEM

shows occurrence of nickel precipitates at 473 K. The S-type sample shows a much more systematic behaviour. The first stage of crystallization can be considered as the development of Ni-rich but still amorphous regions. SAD after second crystallization step demonstrates the presence of $\text{Ni}_7\text{P}_3 + \text{Ni}$ and $\text{Ni}_5\text{P}_2 + \text{Ni}$ phases. The diffraction pattern of Ni_5P_2 phase looked similar to that of the hexagonal Ni_xP_y phase identified by Makhsoos et.al. (61). During this crystallization step, Ni_xP_y is converted into Ni_3P . It is mentioned that after crystallization only $\text{Ni}_7\text{P}_3 + \text{Ni}$ could be identified as final phases in the samples where third crystallization step is absent. (this was found in both C and S type samples and rapidly quenched samples). The transformation temperatures are almost independent of the phosphorous concentration. The second phase crystallization occurs at 613 K and third a very small peak at about 683 K for samples with phosphorous 16.4 to 19.3 at. %.

CHAPTER 3

EXPERIMENTAL PROCEDURES

This chapter presents the details of the electroless deposition technique, the different methods such as gravimetric and magnetic moment method used for the elemental analysis and the various measurement techniques used for producing structural, magnetic and resistivity data in the study of Ni-P system.

The magnetization behaviour is investigated using Vibrating-Sample-Magnetometer model 155 (EG and G PARC USA) with a model 151 temperature oven, model 153 cryostat and model 152 temperature controller.

The structural studies have been performed using PHILIPS Transmission-Electron-Microscope model EM 400 T/ST with a heating holder attachment PW 6592 and X-ray diffractometer model 1140/90 (PHILIPS, Holland).

The resistivity measurements are carried out using a standard four-probe method with provisions for low temperature upto 120 K.

3.1 THE ELECTROLESS DEPOSITION TECHNIQUE

Electroless deposition is the technique used for the preparation of samples for this work. Electroless nickel plating was first developed by Brenner and Riddell in 1946 and later many workers such as Goldstein et.al. (16), Graham et.al. (17), Randin et.al. (58), Simpson and Brambley (46) and very recently, Cziraky et.al. (26) used this technique for the study of the system Ni-P.

3.1.1 The General Considerations

Electroless Ni-P plating is carried out by immersing the objects with prepared surface in the solution heated to 363 - 368 K (90 - 95°C). The main components of the solution are nickel salt, hypophosphite, and organic compounds which prevent an increase in the concentration of hydrogen ions formed during the reaction and increase the rate of deposition and some bath stabilizer is also added.

The reduction of the metal from its salts by hypophosphite is a complex process which takes place only on surfaces which catalyze the reaction. The rate of electroless plating depends to a considerable extent on the temperature of the plating solution.

There is a change in composition of the solution which occurs during the process. The most important change is a decrease in the concentration of the nickel salt and of hypophosphite, so the components need to be replaced periodically for thick deposits, otherwise the rate of deposition will go on decreasing with change in composition of the deposit. However, the maintenance of a constant composition is very difficult due to the increase in the concentration of the hypophosphite oxidation products.

It has been observed that the reduction of nickel salts by hypophosphite starts spontaneously only on the surfaces of certain metals, such as nickel, cobalt, iron, palladium and aluminium. Other metals can also be plated by immersing the metal in the solution and bringing its surface in contact

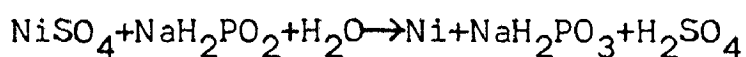
with nickel or another metal more electronegative than nickel, e.g., aluminium or iron.

The reduction of nickel is noticeable at 325 - 335 K and the rate of deposition increases with increasing temperature, and in solutions heated to 363 K (90°C), it reaches values comparable to electroplating. It was found that the rate of reduction with a low hypophosphite concentration does not depend substantially with increase of nickel salt concentration. But the highest rate of deposition of nickel-phosphorous is obtained at 30 g/ℓ nickel salt concentration.

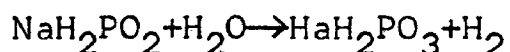
The salts of organic acids considerably affects the deposition rate. These salts are used to maintain pH at the optimum value, but it has been observed by some workers that these salts have specific influence on the process and on the rate of reduction of the nickel-phosphorous. As by the experiments performed by Gorbunova and Nikiforova (63), the optimum concentration of the buffer additive depends also on the hypophosphite concentration in the solution. In the present study 85 g/ℓ sodium citrate provides a fairly good rate of deposition (850 A°/min).

The action of hypophosphite in the chemical reduction of metals can be compared to the action of the electric current in electroplating processes. A "by product" of electroless process is hydrogen which is always evolved during the reduction of nickel-phosphorous.

According to the eqn. of main reaction :



1.8 gm of hypophosphite is needed for the reduction of 1 g of nickel, but the actual consumption of hypophosphite is attributed to the side reaction accompanying the reduction of the nickel, which causes evolution of hydrogen according to the reaction :



In addition some phosphorous is used up in the reduction of phosphorous to the elemental state.

The influence of the small amounts of impurities can have considerable influence on the course of the reaction. Foreign elements may find their way into the solution as impurities in the main reagents. In addition, substances formed in the oxidation-reduction reactions might also affect the course of the process.

Although increase in the hypophosphite concentration improve the rate of deposition of the sample, large amounts of reducing agents are not used as they cause the process to take place in the bulk of the solution.

High concentrations of nickel salts cause deterioration in the quality of deposits. To maintain the process at a constant rate, it is essential that hypophosphite and nickel salt be added periodically. Moreover ammonia may be added regularly to the bath to neutralize the acid formed in the reduction process, and to compensate for the losses of ammonia through evaporation.

From the above general discussion one can conclude that for electroless plating the constituents of the bath

required are as follows :

- (i) Plating Agent : For Ni-P plating, nickel sulphate or nickel chloride is the plating agent.
- (ii) Complexing Agent:(a) Sodium citrate (b) Ammonium sulphate with sulphate bath and ammonium chloride with chloride bath.
- (iii) Reducing Agent : For nickel-phosphorous plating, sodium hypophosphite is the reducing agent.

3.1.2 Selection Of The Composition Of Bath

Many baths for the deposition of Ni-P system have been developed and tried. Alkaline and acidic baths have been used for introducing some desirable properties. Sulphate and chloride baths used for the deposition of Ni-P amorphous samples have their own merits and demerits and the selection of the constituents of the bath depends on its efficiency, quality of the bath and nature of the deposit required.

The results with sulphate bath are reported to be very systematic, whereas with chloride bath, the results are arbitrary (26). The deposits on aluminium substrates exhibited higher magnetization than on brass substrates. According to Gorbunova and Nikiforova (64), the reduction of nickel salts in acidic solutions has a non-uniform composition and is basically a mixture of various phosphides. The Ni-P deposits are, therefore, nonmagnetic, while the deposits from alkaline (citrate) baths show magnetic properties.

The deposition of Ni-P is considerably higher in ammonical bath as compared to acid bath and becomes much

faster when palladium chloride is added to the solution. In the presence of 0.0005 gm palladium per one gm of nickel, the phosphorous content of the deposit changed from 2.3 to 3.7 % .

Alkaline bath has one more advantage as compared to acid bath, that it is easy to replace the solution, in addition to good quality of the deposit.

Keeping all the above considerations in view alkaline sulphate bath has been used in this work. The presence of complex forming agents (citrate and ammonia salts) in the alkaline solutions facilitate replacement and permit prolonged operating times.

The bath composition and operating conditions used in the sample preparation are as follows :

$\text{NiSO}_4 \cdot 7\text{H}_2\text{O}$	27 g/l
$\text{Na}_3\text{C}_6\text{H}_5\text{O}_7 \cdot 2\text{H}_2\text{O}$	85 g/l
$(\text{NH}_4)_2\text{SO}_4$	47 g/l
NaH_2PO_2	(15-40)g/l
pH value	8.5-9
Temperature of the bath	363 ± 2 K

No stirring

Both glass slides and aluminium foils were used as substrate for the deposition. The pH value is maintained throughout the deposition time by adding ammonia periodically. Before

immersing in the bath the glass substrates have to be first sensitized in a 1% SnCl_2 solution for 1 minute and then activated by immersing in a 0.1% PdCl_2 solution for about 30 seconds, followed each time by a rinse in deionized water. For aluminium substrates above procedure is not necessary, however immersing in PdCl_2 solution is desirable.

The bath used in our study is essentially the same as used by Simpson and Brambley (46) but with constituents adjusted to get an optimum rate of deposition of about $850 \text{ \AA}^0/\text{minute}$. All the chemicals used were of ANALAR grade or equivalent.

A 45 second deposit on a glass substrate corresponding to a thickness of about 650 \AA^0 was found suitable for transmission-electron-microscopy.

For the purpose of X-ray, VSM, resistivity and the elemental analysis, a deposit of the alloy has been prepared within about 1 hr. time, producing thicknesses from about $5 \mu\text{m}$ to $10 \mu\text{m}$ depending upon the amount of sodium hypophosphite in the bath. The substrate used is aluminium foil for this purpose.

3.1.3 The Substrate Preparation Procedure

The samples for TEM study are deposited on glass substrates of size $25 \text{ mm} \times 70 \text{ mm} \times 2 \text{ mm}$, which were physically removed and are picked up with the help of a porcep made of nonmagnetic material for loading on to the grid of TEM. Proper cleaning of glass substrate is very essential for

uniform adherence of the deposit~~e~~, which is done in steps as given below :

1. Teepol liquid detergent wash: Glass slides were rubbed with cotton dipped in liquid detergent and are washed in running water.
2. The glass substrates are put in the chromic acid for 12 hours which is initially heated and are washed thoroughly in deionised water.
3. The slides are passed through a hot solution of 10% NaOH and are washed again thoroughly in deionised hot water.
4. The glass slides are given an etching treatment and again rinsed in deionized water.
5. The glass substrates are now dried in the atmosphere of isopropyl alcohol.

For other purpose as mentioned above aluminium foils (99.95% pure) of size 0.3 mm thick and 3 cm wide strips have been used. Cleaning of the aluminium substrates is done by following the steps given below :

- a. degreasing with the organic solvent
- b. drying with hot air
- c. rubbing with Vim powder
- d. washing with running water
- e. etching in 1:1 nitric acid
- f. finally washing in deionised water and are dried under compressed air.

After deposition, aluminium foils are dissolved in hot NaOH solution, by removing edges of the deposited film from

all sides in order that NaOH may come in direct contact with aluminium and can attack it. By this process one gets two samples deposited under the same conditions one on each side of the aluminium substrate. Thick films in the form of foils, 25 mm x 80 mm x (5 - 10 μm) are obtained for the purpose of X-ray diffraction, compositional analysis, resistivity measurement and magnetization studies. Outer edges of the samples are removed and only inner sample of the size approximately (2 x 6) cm^2 is taken for studies. The samples in the form of foils have been assumed to have the same composition as those of thin films deposited on glass for transmission electron microscopy study, as the same bath conditions were maintained throughout the period of deposition. However, compositional analysis indicates that the composition of the especially thick samples deposited under same bath conditions differ in composition as much as 5%.

3.2 THE COMPOSITIONAL ANALYSIS

The following methods are used for the elemental analysis of Ni-P deposits.

1. Gravimetric method.
2. Magnetic Moment Method.

3.2.1 Gravimetric Method

Dimethyl-glyoxime method has been employed for the analysis of nickel. The accuracy of the method is $\pm 1\%$.

The nickel is precipitated by the addition of an alcoholic solution of dimethyleglyoxime to a hot faintly acid nickel salt solution and then rendering the solution ammonical

by adding slight excess of aqueous ammonia. The bright red precipitate is filtered, washed with cold water, and is dried at 383 - 393 K temperature and has been weighed as nickel dimethyl-glyoximate. The phosphorous amount is estimated to be the difference of the total amount of the sample taken.

The satisfactory analysis for phosphorous in the samples for TEM study is not possible with an accuracy of less than 5.0%, as the amount of the sample is very small. This is because of the thickness requirement for TEM study, which should not exceed approximately 1000 Å.

3.2.3 The Magnetic Moment Method

Following Bagley and Turnbull (23) a magnetic moment method has been used to analyze the concentration of nickel and phosphorous in the as-deposited samples. The method consists in heating the as-deposited Ni-P sample to a temperature more than 675 K for about half an hour. By this process Ni-P sample is transformed into an equilibrium mixture of Ni and Ni₃P. The amount of nickel present in the equilibrium mixture in the annealed sample is measured by VSM (Ni₃P is paramagnetic) and thereby the amount of phosphorous and nickel present in the as-deposited sample can be estimated (Table 3.1).

3.3 THE STRUCTURAL MEASUREMENTS

The structural study of the samples has been carried out using transmission-electron-microscope and X-ray diffractometer.

The transmission-Electron-Microscope used is model EM 400 T/ST with a heating holder attachment PW 6592.

The general form of the holder is similar to that of the other holders for the goniometer stage. In this holder the specimen is clamped into a small furnace element, which is insulated from the holder by zirconium oxide spheres. A small heating element is fitted into the body of the furnace which is protected by a cover. A thermocouple is insulated on to the furnace and the connections for this and the heater are carried through the four-channel ceramic tube. A temperature control and measuring unit is attached with this heating holder which contains the current supply for the heater and also the circuitry necessary to measure the voltage generated by the thermocouple. Thus unlike other workers (Makhsoos et.al., (61)), we had the advantage of precise information of the sample temperature at every stage of this study.

The operating voltage has been kept fixed at 100 KV. The electron-micrographs have been taken at magnifications from 20,000 to 80,000 and for selected area diffraction patterns the camera lengths generally used are 140 mm, 200 mm, 290 mm and 410 mm.

The X-ray diffraction study is carried out using X-ray Diffractometer model 1140/90 PHILIPS, equipped with a scintillation counter. Filtered MoK α radiations (Zr filter) have been used. The scanning speeds used are 1 $^\circ$ and 2 $^\circ$ per minute. Cu K α radiations have also been used for certain samples for cross checking of angular positions of maxima of the X-ray intensity.

3.4 MAGNETIC MEASUREMENTS

Magnetic moment measurements (e m u/gm) are carried out on a Foner type Vibrating Sample Magnetometer model 155 of Princeton Applied Research Corporation.

The specifications are as follows :

Sensitivity - Apparatus has 5 calibration ranges to be used as ± 0.01 , $\pm .1$, ± 1.0 , ± 10 and ± 100 e m u full scale.

The minimum detection limit - 0.00001 e m u.

Absolute Accuracy - Less than 2%

Reproducibility - Better than 1%

Maximum sample size - 2.5 mm diameter.

With model 155 VSM, model 151 temperature oven is used which allows sample temperatures to be set anywhere in the range of ambient to 1050 K. Model 153 cryostat and model 152 temperature controller are also available with this 155 model in the laboratory for the present study.

A constant magnetic field of 5 KOe has been applied for all the measurements in this study.

The continuous measurements of the magnetic moment with temperature in the range of 77K to 800 K, have been made with Omniscribe 2-Channel Recorder model 521.2-14. It is a 2-channel chart recorder with voltage sensitivity range between 0.001V/25 cm to 10V/25 cms in different steps.

A Chromel-Alumel thermocouple for the temperature measurements has been used.

The semi-micro METTLER balance model- H 54 R, with a resolution of 0.00001 gm, has been used for weighing the samples.

3.5 THE RESISTIVITY MEASUREMENTS

A standard four-probe technique has been used for the resistivity measurements. For this purpose the sample strips of the typical dimensions (10 mm x 1 mm x 5-10 μm) are cut from deposited foils.

The sample has been weighed on Mettler balance model H 54 R with an accuracy of ± 0.00001 gm. The thickness of the sample is obtained through weighing a sample of known area and using density values as given by Cargill (10) (table 3.2) for different phosphorous composition of amorphous Ni-P samples.

The electrical resistivity has been measured using the setup shown in figure 3.1 in the temperature range of 300 K to 800 K. A very fine copper wire is used for making contacts with the samples, using silver paste.

A constant current source and 3 and a half digit multimeter have been used for the measurement of current, the voltage is measured with a microvoltmeter and temperature with a, Chromal-Alumal thermocouple. A sheet of mica is used as a sample holder. The sample holder assembly is kept in a quartz tube, which is evacuated. This resistivity measurement set-up is fabricated by the candidate. The electrical connections and the thermocouple connections are carried out through a vacuum seal. The sample holder assembly has been fixed on a steel tube of small bore which also serves the purpose of

carrying nitrogen vapors. A brass tube is also fitted with the vacuum coupling, which connects experimental quartz tube to the rotary pump for evacuation. A heating coil is wrapped around the quartz tube for heating the sample to temperatures upto 800 K. Yet another heating coil is wrapped over the steel tube to change the liquid nitrogen to vapors and also used for raising the temperatures, when necessary, from a lower temperature. A photograph of the complete set-up is also shown in figure 3.2.

The resistance measurements are estimated to be accurate within $\pm 0.1\%$ and the overall accuracy in the measurements of resistivity is only $\pm 10\%$. This is because of the uncertainties in sample geometry.

L I S T O F T A B L E S

- 3.1 Values of magnetic moment (emu/g) for different concentration of phosphorous in the Ni-P sample.
- 3.2 Density values of amorphous Ni-P samples with different phosphorous contents.

L I S T O F F I G U R E S

- 3.1 Diagram of the Resistivity set-up fabricated in the laboratory by the candidate.
- 3.2 A photograph of Resistivity set-up.

TABLE 3.1

Magnetic Moment of annealed samples (e m u/g)	Phosphorous content in the sample (at. %)
40.29	7.32
38.45	8.20
36.67	9.07
34.83	9.94
33.78	10.45
33.60	10.54
33.00	11.64
31.15	10.79
29.31	12.49
28.06	13.07
27.47	13.32
25.62	14.15
24.10	14.80
23.92	14.89
23.78	14.97
21.94	15.79
20.10	16.59
18.26	17.40
16.41	18.19
14.57	19.00
12.73	19.76
10.89	20.54
9.05	21.31
7.20	22.07
6.28	22.45
5.36	22.89
3.52	23.58
1.68	24.32
0.00	25.00

TABLE 3.2 RESULTS OF DENSITY MEASUREMENTS FOR THE Ni-P
SAMPLES (Cargill)

Sample (at. % Ni)	(g/cm ³) as deposited
73.8	7.727
76.0	7.791
77.2	7.801
78.9	7.930
81.4	7.999
84.8	8.163
88.8	8.315

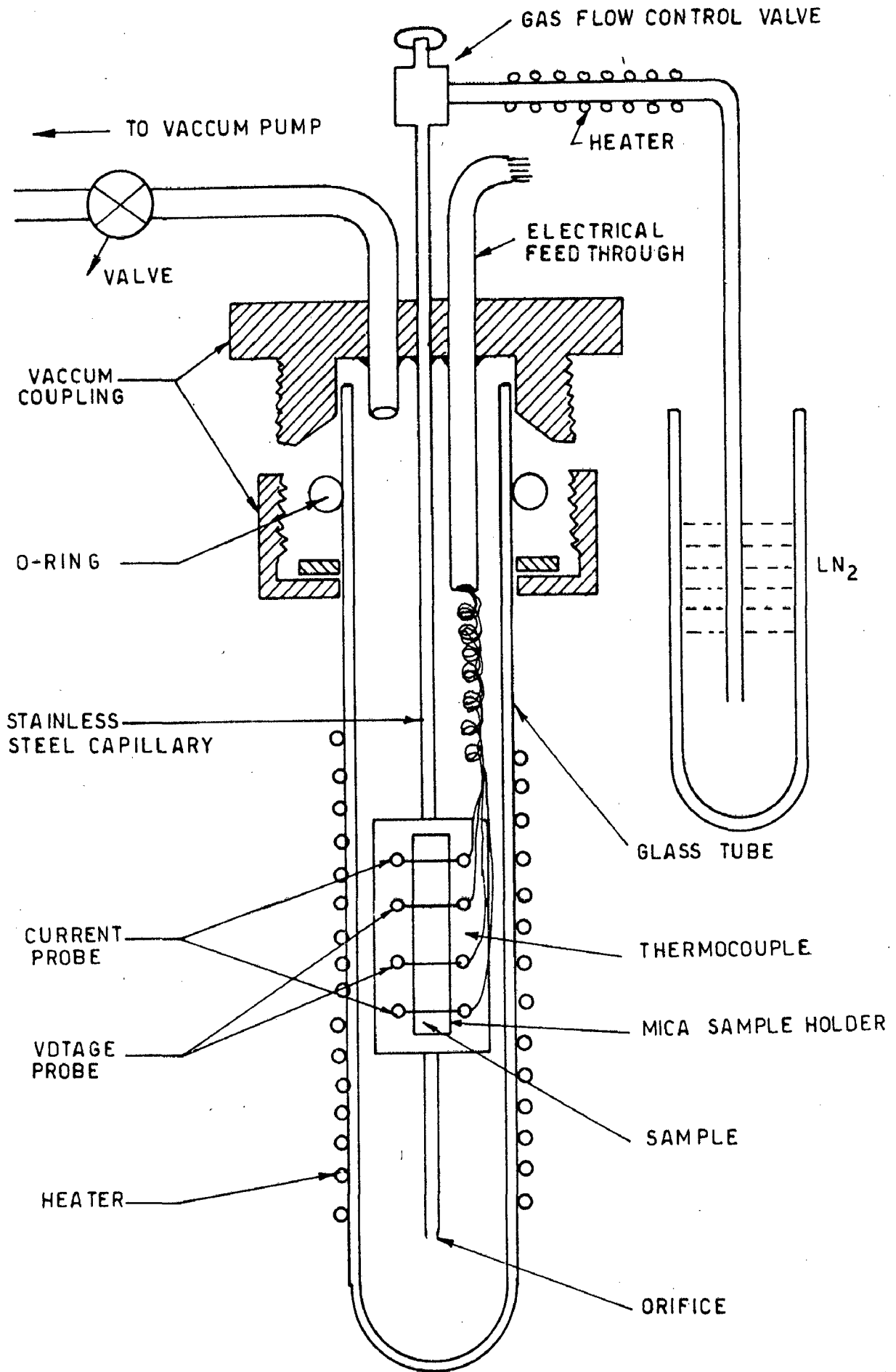


FIGURE - 3.1

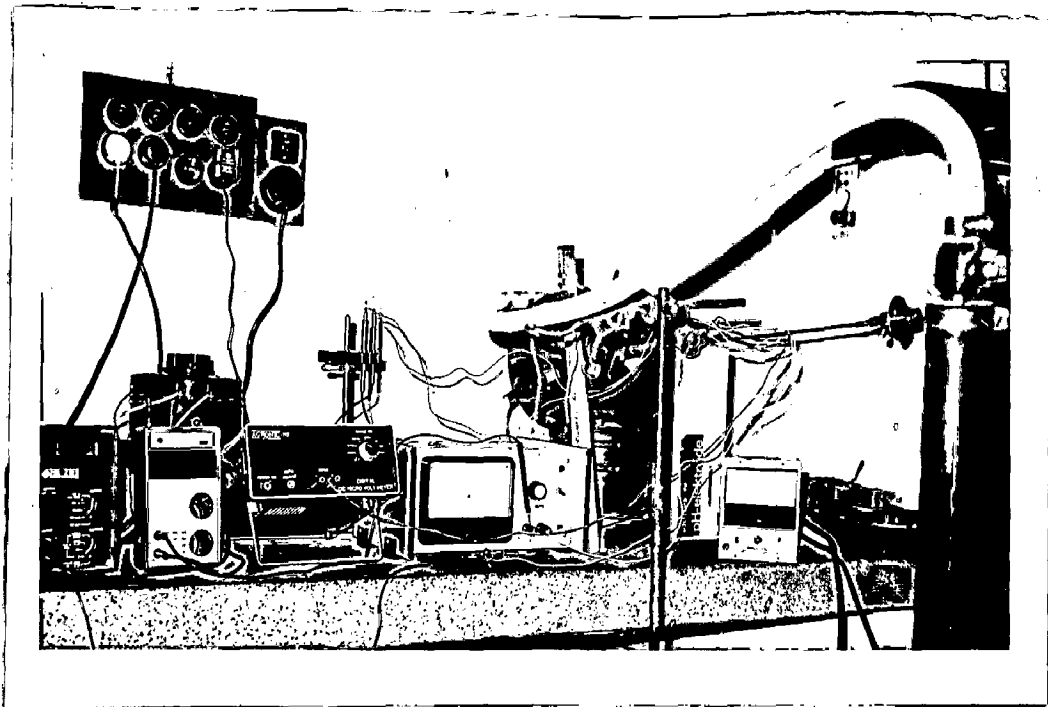


FIGURE 3.2

CHAPTER 4

THE STRUCTURE OF ELECTROLESS DEPOSITED
Ni-P ALLOYS: ANNEALING STUDIES

The early studies, apart from the Brenner's work (12) who was the first to deposit amorphous Ni-P, on the structure of electrodeposited Ni-P has been of Albert et.al (19), Meada (20), Bagley and Turnbull (23), Cargill III (10) and more recent studies are of Makhsoos et.al. (61) and Bakonyi et.al (62). On the structure of electroless Ni-P alloys relatively less studies have appeared. The earliest study has been that of Goldstein et.al. (16) and after some years Graham et.al (17). The most significant study on the structure and other aspects as well, of electroless Ni-P system has been of Simpson and Brambley (46) and A. Cziraki et.al. (26) (Bakonyi's group). The work by these and other authors has been reviewed in chapter 2.

Both for electroless as well as for electrodeposited Ni-P films, in the case of low phosphorous (upto about 12 at. %), it has been established by these workers that the alloy in the as-deposited state is a metastable polycrystalline phase, whereas in the case of high-phosphorous (more than 12 at. %) it is not clear, whether the system in the as-deposited state is truly amorphous or just 'looks amorphous'.

There can be two obvious approaches to resolve whether the as-deposited state of Ni-P films with high-phosphorous contents is amorphous or microcrystalline with a very small grain size. A direct approach is the use of high resolution

dark field transmission electron microscopy studies and the observation of crystallites in the untransformed region. However, this approach fails to distinguish between amorphous and microcrystalline states if the crystallite size is less than about 30 \AA (Makhsoos et.al., 61). In the indirect approach the crystallization behaviour is studied. If the as-deposited state of the film is amorphous, then crystallization will take place by nucleation and growth, while a microcrystalline state will transform to the equilibrium state through a simple crystallite coarsening mechanism. However, in the case of unusually large nucleation rates, it may be difficult to distinguish between the two cases, unless one undertakes a detailed annealing study as the crystallite growth depends both on heating rate and annealing temperature.

In the present chapter we have examined the thin films of electroless deposited Ni-P alloys with different P-contents. The thin films were subjected to electron-microscopy while heating on the stage of the microscope. The transmission-electron-micrographs and selected area diffraction patterns (SAD) of the films with different phosphorous contents were analyzed to determine the nature of the as-deposited electroless films. In the present study the sample temperature was monitored throughout the study on the stage of the microscope. Thick electroless as-deposited films were also subjected to X-ray diffraction to verify further the results of electron-microscopy. The details of the techniques used are reviewed in chapter 3.

4.1 RESULTS: ELECTRON MICROSCOPY AND X-RAY DIFFRACTION

The electron microscopy of thin as-deposited electroless films were carried out at ambient temperature to characterize its microstructure and selected area diffraction (SAD) pattern and the results are reported in 4.1.1 for polycrystalline films, in 4.1.2 for microcrystalline and in 4.1.3 for amorphous films. These results have been supplemented with the X-ray diffraction patterns of thick as-deposited films obtained from the baths correspondingly used for thin films.

In section 4.2 the effects of heating the thin films in the hot stage of electron-microscope have been reported as the induced mode of change which is indicative of the nature of the deposits.

The samples prepared with 20 g/l sodium hypophosphite in the bath were found to contain phosphorous ranging from 11 to 14 at. % on analysis and are referred as sample I. The samples deposited with a bath containing sodium hypophosphite 30 and 40 g/l were observed to contain phosphorous ranging from 14 to 18 and 18 to 21 at. %, respectively and will be referred to as sample II and III.

4.1.1 Polycrystalline Films

Fig. 4.1 (a) shows the electron micrograph of as-deposited polycrystalline film containing 8 - 11 at. % phosphorous, obtained from a bath containing 15 g/l NaH_2PO_2 . The microstructure contains fine crystallites deposited in the island formation. In the case of crystalline deposits each

island has different orientation leading to individual grains. The selected area diffraction pattern of this film is shown in figure 4.1 (b) where one observes Debye rings indicating that the film is crystalline and electron beam is incident on many crystallites whose sizes are small. The lattice parameter of this deposit is a little different from the bulk crystalline nickel.

4.1.2 Apparently Amorphous Films

Fig. 4.2 (a) shows electron micrograph of as-deposited film of sample I, and figure 4.2 (b) is the corresponding selected area diffraction (SAD) pattern, which shows two diffuse rings and a very feeble third diffuse ring. Figure 4.2 (c) shows the X-ray diffraction pattern of the same sample I containing only one peak corresponding to the position of (111) peak of nickel which is quite broad. However, the broadening may be due to microcrystallinity or due to the amorphous nature of the sample. The diffraction pattern also contains two likely weak peaks between $2\theta = 21.0$ and 23° . The main peak occurs at $2\theta = 20.1^\circ$ and the width at half maximum, $\Delta 2\theta = 1.2^\circ$.

4.1.3 Amorphous As-deposited Samples

Fig. 4.3 (a), (b) and (c) shows micrograph, SAD and X-ray diffraction pattern respectively of the sample containing (18 - 21) at. % P (sample III), deposited from a bath containing 40 g/l NaH_2PO_2 . SAD shows only one diffuse ring and a very weak outer ring which can not be seen in the photograph. Micrograph shows no crystallites in the as-deposited state but the indication of island growth still persists. The X-ray diffraction

pattern shows only one broad halo at $2\theta = 20.2$ with a width at half maximum $\Delta 2\theta = 3^\circ$.

4.1.4 Films Containing Both Microcrystalline And Amorphous Regions

These films have been deposited from a bath containing 30 g/l of NaH_2PO_2 , sample II, having P contents in the range 14 to 18 at. %. Under electron microscope the samples appear inhomogeneous, containing regions with microstructures characteristic of microcrystalline state in some places and of amorphous state in other places. The selected area diffraction pattern of these regions further confirmed these observations. The SAD and micrographs are, however, not shown as these appear similar to sample I or sample III. The X-ray diffraction of these samples has been shown in figure 4.4, where one observes a broad peak at $2\theta = 20.4^\circ$ with a width at half maximum $\Delta 2\theta = 2.5^\circ$, characteristic of amorphous state superimposed over a relatively sharper peak with smaller intensity on a lower 2θ side characterizing the microcrystalline state.

4.2 ANNEALING STUDIES: CHARACTERISATION OF AS-DEPOSITED STATE

The annealing studies as reported in this section have been carried out primarily to distinguish further the nature of the as-deposited films which "looks amorphous" i.e., the microcrystalline and truly amorphous films. In figure 4.5 (a) The micrograph of a sample I heated at 623 K for 2 minutes shows a grain structure similar to the crystalline deposits as shown in figure 4.1 (a). Figure 4.5 (b)(i) and 4.5 (b)(ii)

are SAD's of the same sample heated to and held for 2 minutes at 440 K and 623 K. These SAD patterns show a continuous sharpening of rings, with the increase in crystallite size as the temperature increases; when the crystallites grow beyond the spot size of electron beam SAD shows a spot pattern. Figure 4.6 (a) and 4.6 (b) are the electron micrographs of the sample II heated at 423 K and 613 K for 2 minutes. It has already been reported earlier in section 4.1 that these samples are inhomogeneous and the area under examination is truly amorphous as indicated by its SAD of as-deposited state. It has been evident that the grain structure has not developed at 423 K, only some island marks exist due to thickness difference. But the same sample when heated to 613 K the transformation to crystalline structure has started and grains typical of polycrystalline deposits have started appearing. The SAD of the sample heated ^{at} 613 K is shown in figure 4.6 (c). This SAD pattern consists of a superposition of broad diffuse rings on the spot pattern. A similar pattern is also observed for the sample III containing (18 - 21) at. % phosphorous when heated to 618 K and held for 2 minutes as can be seen from figure 4.7 (a). A relatively no sharpening of diffraction rings was observed even though the samples were heated upto 613 K for 2 minutes. When the samples were heated to 643 K, the spot patterns are obtained as shown in figure 4.6 (d) for sample type II and figure 4.7 (b) for sample type III containing phosphorous in the range (18 - 21) at. %. However, certain regions of sample II (14 - 18) at. % phosphorous show SAD after heating at 628 K for 2 minutes having sharp rings together with spot

pattern as shown in figure 4.6 (e). X-ray diffraction analysis of the two types of samples—microcrystalline and amorphous were carried out after heating the samples for 30 minutes. It can be seen from the diffraction patterns for different samples that upto 473 K the line broadening in amorphous samples are much higher compared to that in microcrystalline samples as shown in figure 4.8. But after heating at 573 K for 30 minutes both these samples have become crystalline with line width of the same order of magnitude.

4.3 DISCUSSION

The phosphorous content of Ni-P deposits obtained chemically from a bath containing 15 g/l NaH_2PO_2 and having pH value around 9 will be below 12 at. % as it has been confirmed from the compositions of thick deposits of varying thickness. The electron-micrograph and SAD of these deposits show crystalline nature of the films as it has been observed by earlier workers like Graham et.al. (17), Maeda (20) and Albert et.al. (19). However, these deposits are metastable and contain phosphorous in the solution more than the solubility limit. The lattice parameter of these deposits are more than that observed in bulk pure nickel and it is a function of phosphorous content in the samples. The exact determination of phosphorous content in the thin film examined under electron-microscope could not be carried out because phosphorous content changes with time during deposition due to change in pH (± 1) and gravimetric analysis could be carried only for thick films. Due to this limitation the variation of lattice parameter of metastable deposits with

phosphorous content could not be reported. The crystallinity of the film is evident also from the fine grain structure showing extremely small crystallites. In several regions the films are often observed to have uneven thickness irrespective of the nature of deposits.

The deposits obtained by chemical deposition are often uneven as shown in electron-micrographs in figure 4.2 (a) and 4.3 (a). The unevenness appears to result from the details of deposition process where the atoms arriving at the substrate form islands and covers it by the lateral growth of these islands.

The SAD of the samples I show broad diffuse rings similar to SAD obtained from samples containing greater than 18 at. % phosphorous but the extent of broadening observed in the latter samples are more than those obtained from the former ones. Also, the high phosphorous deposits have just one broad diffuse ring of reasonable intensity as shown in figure 4.3 (b) along with a very feeble diffuse ring but the deposits with 11 - 14 at. % phosphorous have two clearly observable diffuse rings along with a feeble one as shown in figure 4.2 (b). The sample II has some regions showing diffuse rings in SAD like figure 4.2 (b) and others similar to that shown in figure 4.3 (b).

The X-ray diffraction pattern from the thick samples belonging to different composition classes are quite revealing. The samples I show X-ray diffraction peaks which are quite sharp when compared with those obtained from samples III as shown respectively in figure 4.2 (c) and 4.3 (c). The samples

in the intermediate phosphorous range have shown broad X-ray diffraction peak along with the relatively sharp ones similar to that observed in figure 4.2 (c) but with a reduced intensity.

From the discussion of the evidences from electron microscopy, SAD and X-ray diffraction, it appears that the samples I is in a state which is distinctly different from the state of deposits of samples type III. The samples of intermediate phosphorous content is in a mixed state resulting from phosphorous segregation. The regions of lower phosphorous is in a state similar to deposits containing 11 - 14 at. % phosphorous and the regions of high phosphorous are in a state akin to samples containing more than 18 atomic percent of phosphorous. The degree of diffuseness and the number of rings in SAD indicate that the samples type I are microcrystalline and those with phosphorous beyond 18 at. % are in truly amorphous state. The samples with intermediate phosphorous contents have both microcrystalline and amorphous regions.

The annealing studies have been carried out following Bagley and Turnbull (23) to confirm our findings further regarding the state of the deposits with various phosphorous content.

The diffuse rings in SAD of the sample I shown in figure 4.2 (b) become progressively sharp on heating, as evident from figure 4.5b(ii), SAD of the same sample with 11 - 14 at. % phosphorous heated to 623 K for 2 minutes in TEM. The reduction in broadening may be attributed to the lowering of defect density and growth of grains. The grain growth is a diffusion dependent process and, in principle, it takes place at all

temperatures depending on the magnitude of diffusion coefficient. Thus, one observes continuous reduction in broadening as the sample is progressively heated. The state of this sample is therefore microcrystalline and it coarsens to crystalline state at elevated temperatures by grain growth. Bagley and Turnbull (23) has characterized flash evaporated high phosphorous content films following a similar line of argument.

The diffuse rings in SAD pattern of figure 4.3 (b) remains quite diffuse on heating as shown in figure 4.6 (c), the SAD of the same sample III heated to 623 K for 2 minutes in TEM. In addition there is a spot pattern characteristic of crystalline nickel superimposed over it. The co-existence of crystalline phase as well as the one characterised by diffuse rings indicate that there is a definite transformation process going on presumably the crystallization of the amorphous state. It is inferred that this is a further confirmation of deposits having phosphorous in excess of 18 atomic percent, being truly amorphous.

The broadening of X-ray peaks after heating the samples for half an hour at different temperatures as shown in figure 4.8 has shown that the microcrystalline state has a much less line broadening as compared to that in the amorphous state. The reduction in the broadening of amorphous state with temperature upto 473 K may be attributed to a relaxation in the amorphous state. But again the line width from amorphous sample is much longer at 473 K, when compared to that obtained in

179288
Central Library University of Roorkee
ROORKEE



microcrystalline sample. Also, there is a small difference in line width obtained at 473 K and 573 K which is indicative of grain growth even at 473 K. Our results are also similar to Makshsoos et. al. (61) conclusions for electrodeposited Ni-P system that 7 and 12 at. % phosphorous films are microcrystalline and 18 and 22 at. % samples are amorphous.

4.4 SUMMARY

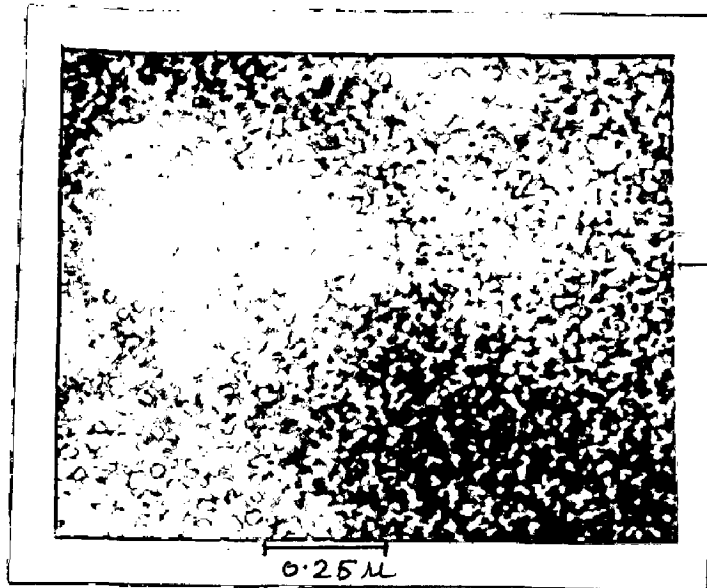
An examination of the structure of electroless deposited Ni-P films containing 8 to 21 atomic percent phosphorous has been carried out using transmission-electron-microscopy, selected area electron diffraction and X-ray diffraction techniques.

A further observation of the films while heating has been performed to distinguish the mechanism, development of grain structure-- only growth characterising a microcrystalline film or nucleation and growth manifested in amorphous films.

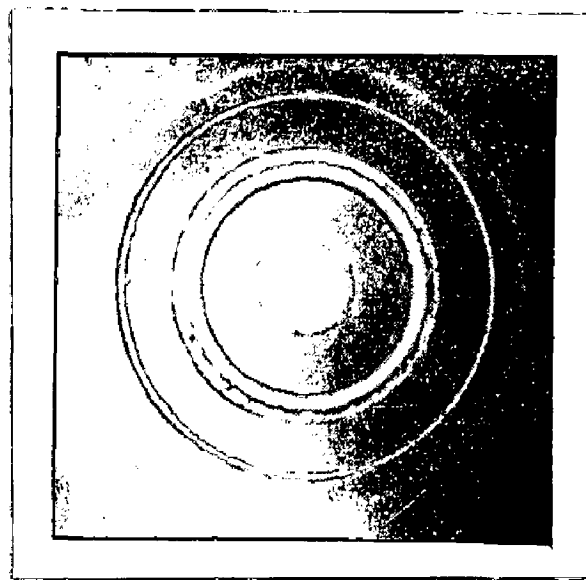
The results indicate that the alloys are crystalline for a phosphorous content of less than 11 at. % , microcrystalline for a phosphorous content of 11 to 14 at. % , mixed-microcrystalline and amorphous, for phosphorous content of 14 to 18 at. % and amorphous for a phosphorous content exceeding 18 at. % .

L I S T O F F I G U R E S

- 4.1(a) Electron micrograph of as-deposited polycrystalline Ni-P sample containing (8-11) at.% phosphorous.
- (b) SAD of the region shown in fig.4.1(a)
- 4.2(a) Electron-micrograph of as-deposited state of sample I
- (b) SAD of the region shown in fig.4.2(a)
- (c) X-Ray diffraction pattern of the Ni-P sample I containing 12 at.% in the as-deposited state.
- 4.3(a) Micrograph of a electroless Ni-P sample III in the as-deposited state.
- (b) SAD of the region shown in fig.4.3(a).
- (c) X-Ray diffraction pattern of as-deposited Ni-P sample III.
- 4.4 X-Ray diffraction pattern of as-deposited Ni-P sample II
- 4.5(a) Micrograph of sample I heated at 623 K for 2 minutes.
- (b)(i) SAD of sample I heated at 440 K for 2 minutes
- (ii) SAD of the region shown in fig.4.5(a).
- 4.6(a) Electron-micrograph of sample II heated at 423 K for 2 minutes.
- (b) Electron-micrograph of sample II heated at 613K for 2 minutes.
- (c) SAD of sample II heated at 613 K for 2 minutes.
- (d) SAD of sample II heated at 643 K for 2 minutes.
- (e) SAD of sample II heated at 628 K for 2 minutes.
- 4.7(a) SAD of sampleIII heated at 618 K for 2 minutes
- (b) SAD of sample III heated at 643 K for 2 minutes.
- 4.8 The variation of Full width at half maximum($\Delta 2\theta$) with with temperature for amorphous and microcrystalline Ni-P samples.



(a)



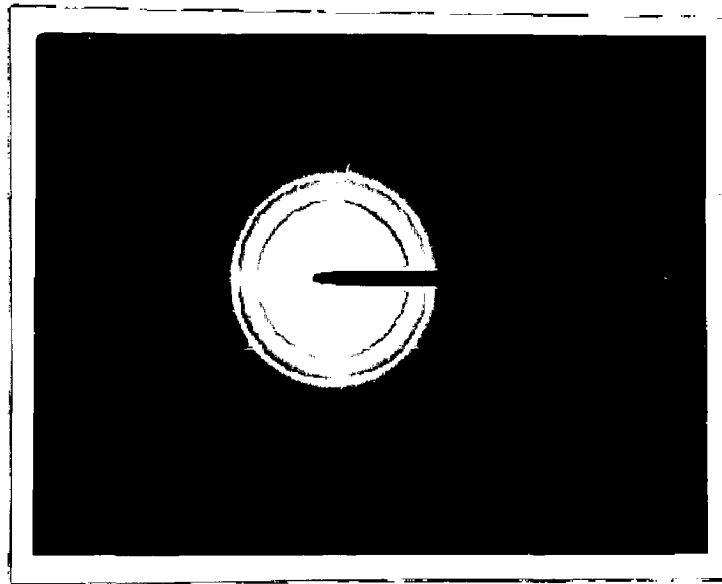
(b)

FIG.4.1(a) ELECTRON-MICROGRAPH OF AS-DEPOSITED
POLYCRYSTALLINE Ni-P SAMPLE CONTAINING
(8-11) AT. % PHOSPHOROUS

(b) SAD OF THE REGION SHOWN IN FIG.4.1(a)



(a)



(b)

FIG. 4.2(a) ELECTRON MICROGRAPH OF AS-DEPOSITED STATE OF SAMPLE I

(b) SAD OF THE REGION SHOWN IN FIG. 4.2(a)

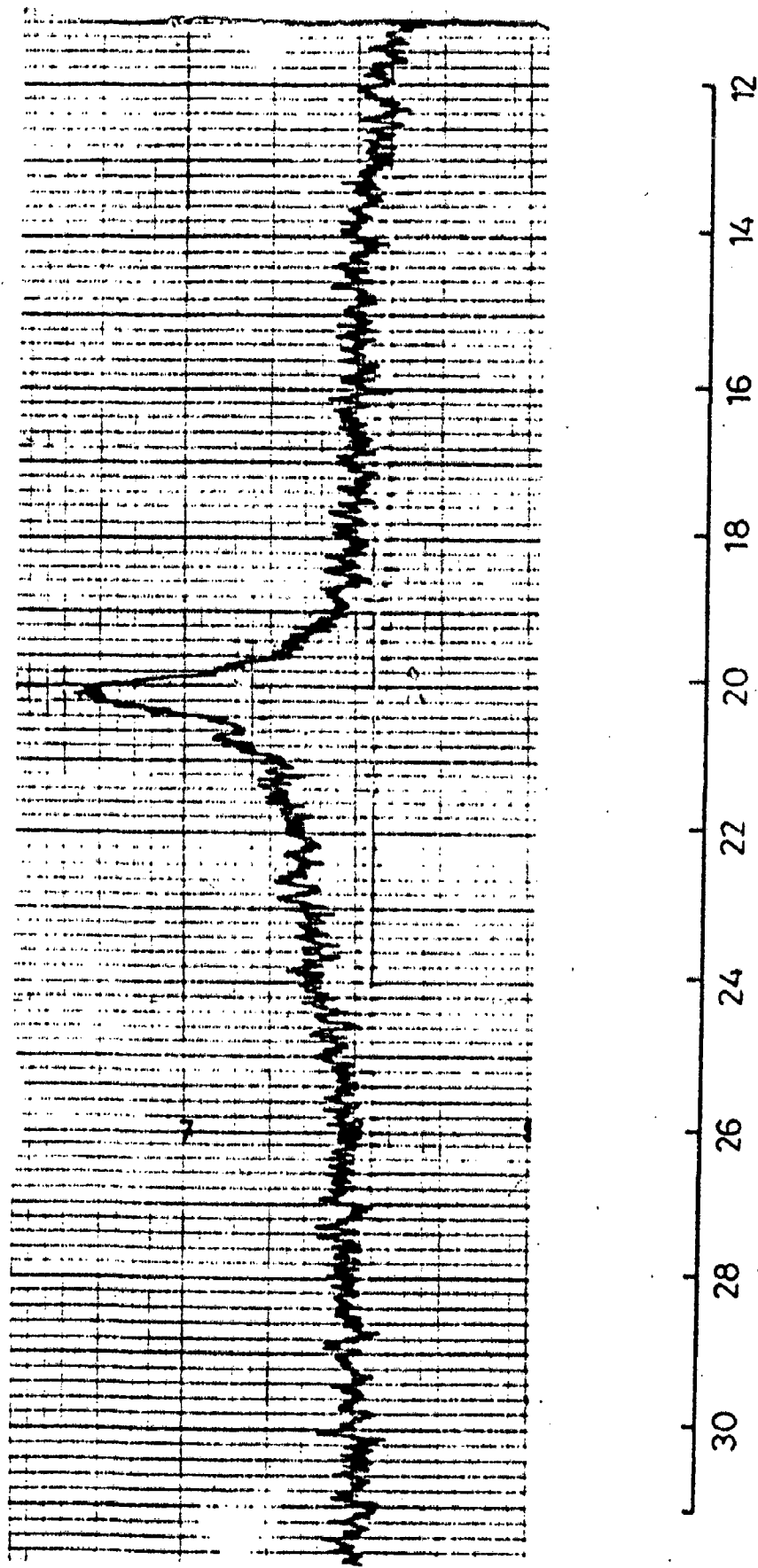
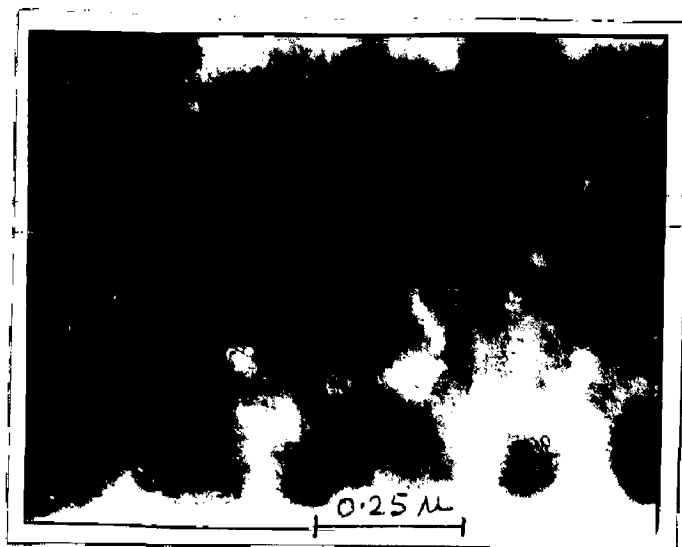
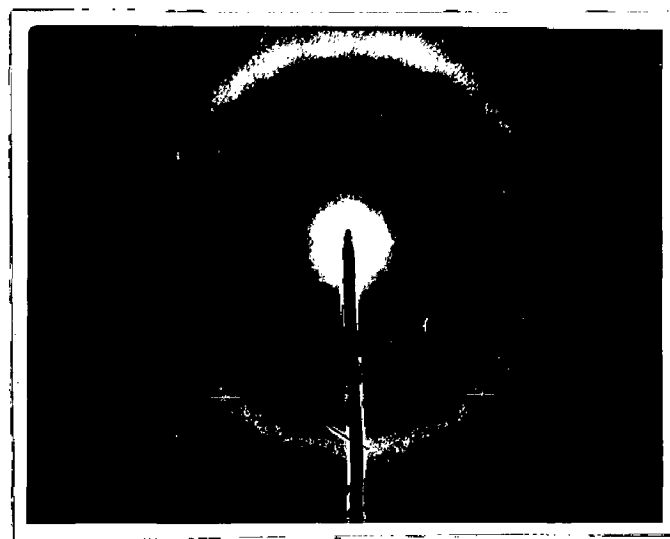


FIG. 4.2 (c) X-RAY DIFFRACTION PATTERN OF Ni-P SAMPLE I CONTAINING 12 AT. % IN THE AS-DEPOSITED STATE.



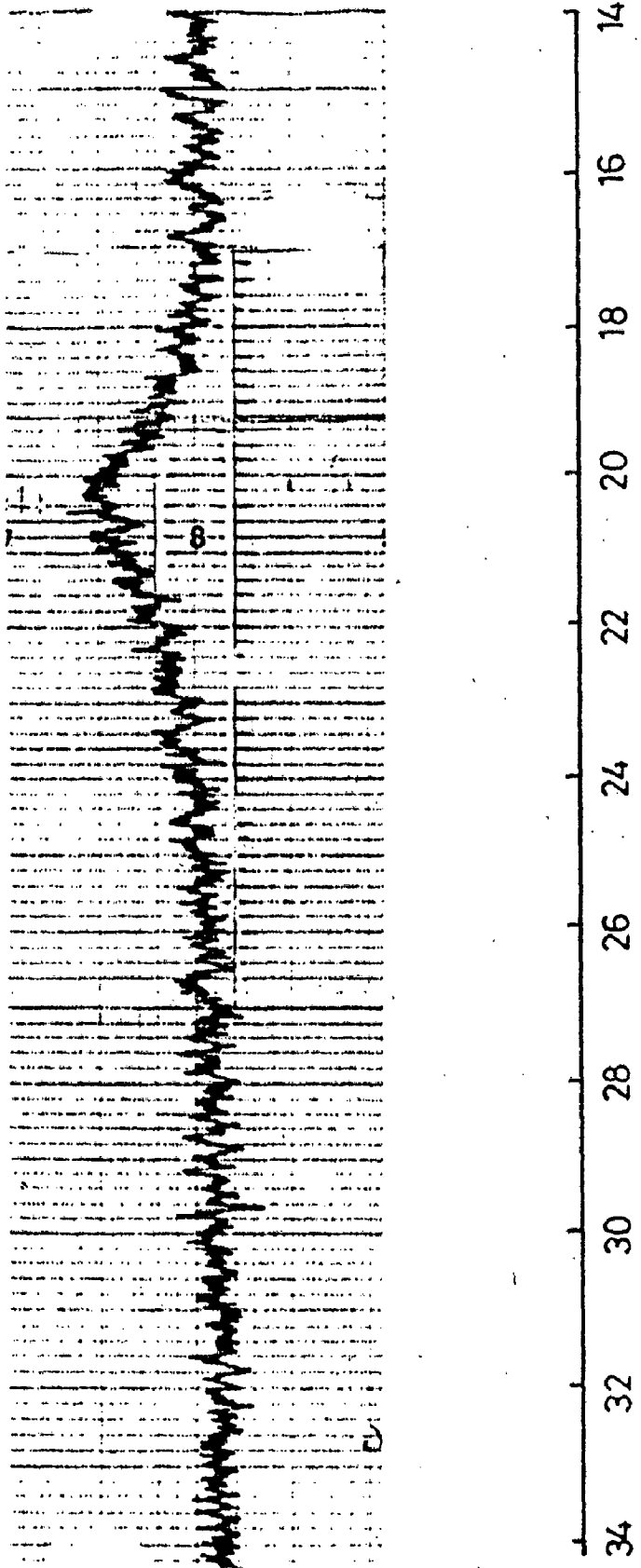
(a)



(b)

FIG.4.3(a) MICROGRAPH OF A ELECTROLESS Ni-P SAMPLE
CONTAINING (18-21) AT.% PHOSPHOROUS (SAMPLE III)
IN THE AS-DEPOSITED STATE

(b) SAD OF THE REGION SHOWN IN FIG.4.3(a)



• FIG. 4.3 (c) X-RAY DIFFRACTION PATTERN OF AS-DEPOSITED Ni-P SAMPLE III
CONTAINING 20 AT. % P.

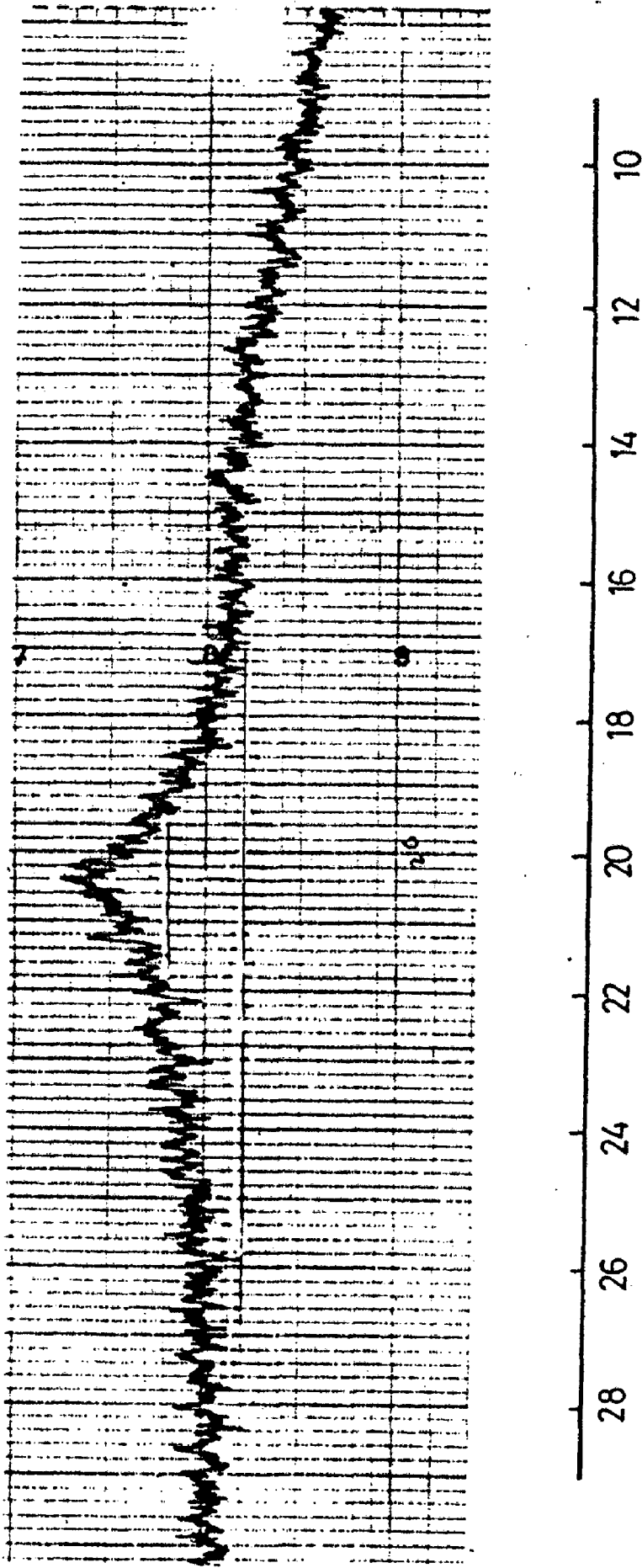
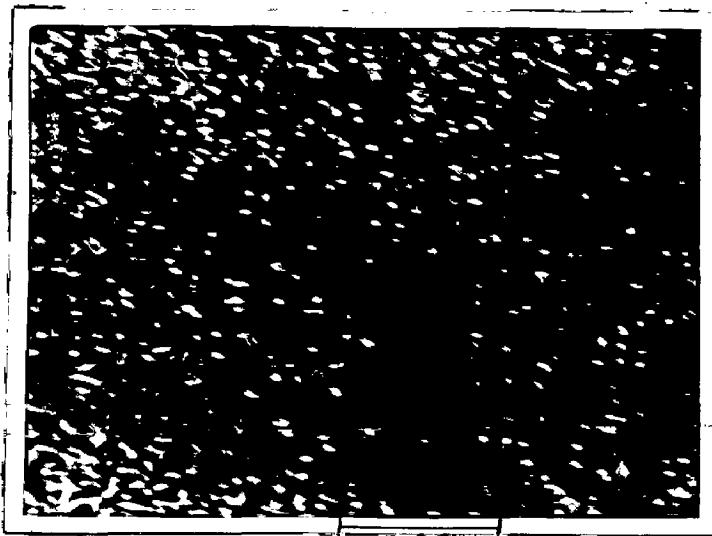
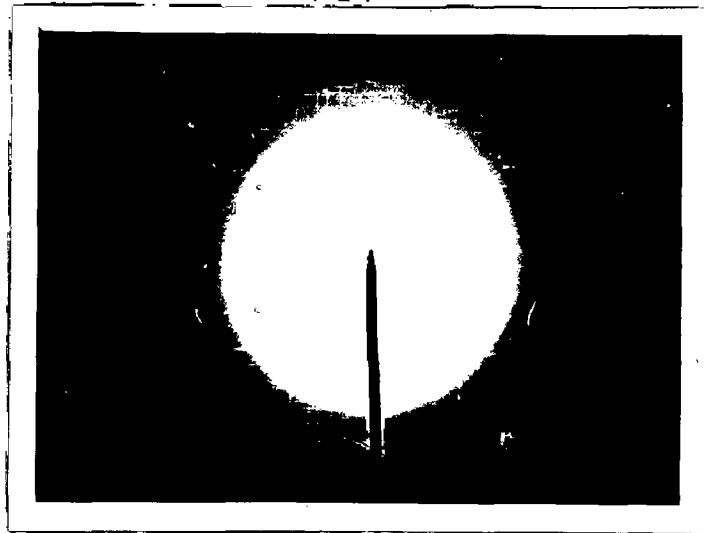


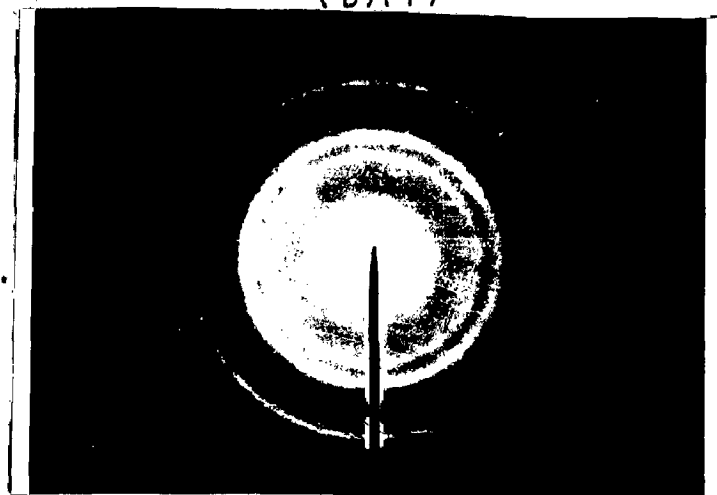
FIG. 4.4 X-RAY DIFFRACTION PATTERN OF AS-DEPOSITED Ni-P SAMPLE II
CONTAINING 17 AT.% P.



(a)



(b)(i)



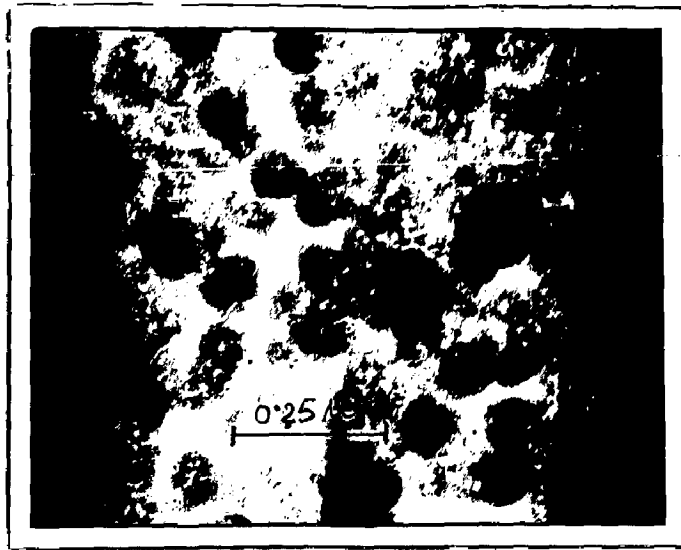
(b)(ii)

FIG.4.5(a) MICROGRAPH OF SAMPLE I, HEATED AT 623 K FOR 2 MINUTES

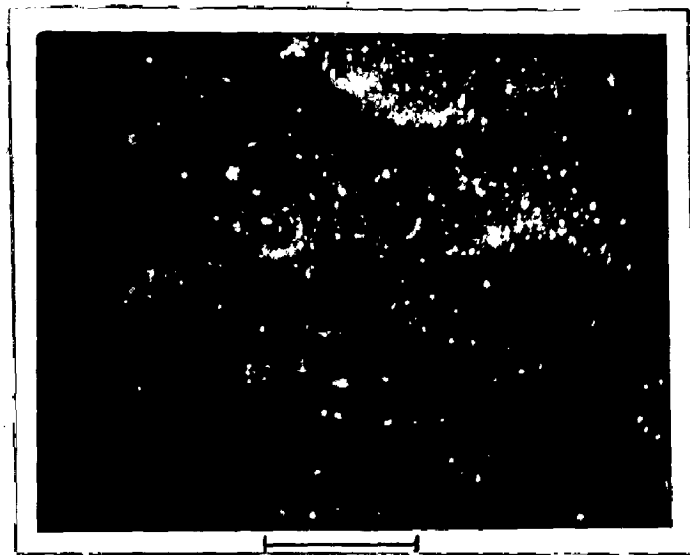
(b)

(i) SAD OF SAMPLE I HEATED AT 440K FOR 2 MINUTES

(ii) SAD OF THE REGION SHOWN IN FIG 4.5(a)



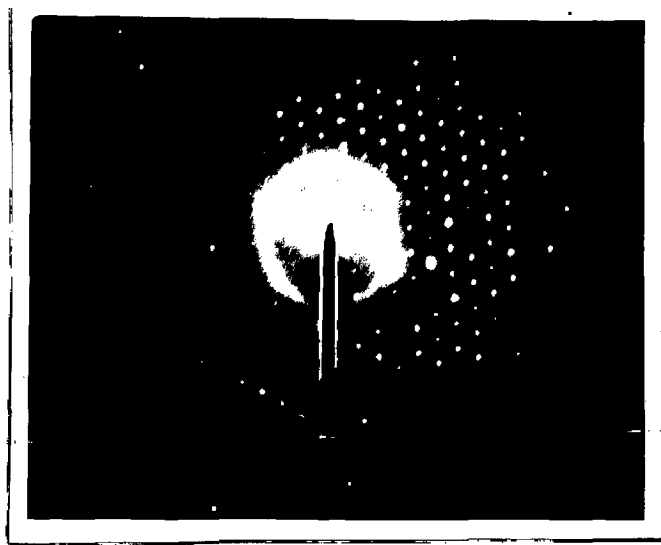
(a)



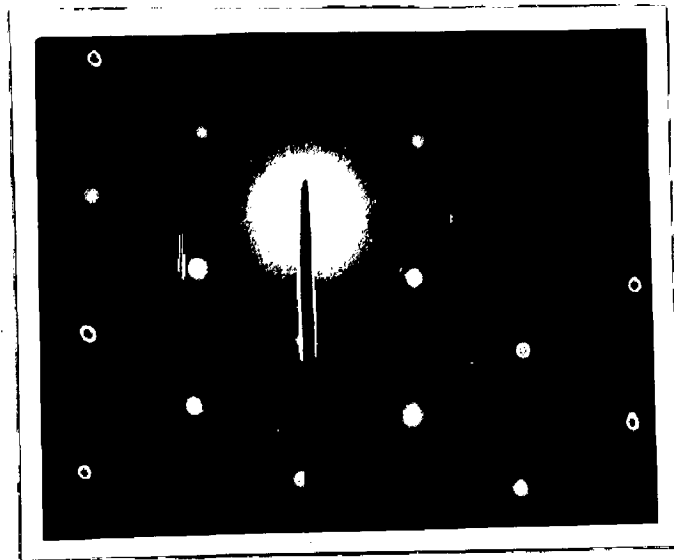
(b)

FIG. 4.6 (a) ELECTRON MICROGRAPH OF SAMPLE II HEATED AT 423 K FOR 2 MINUTES

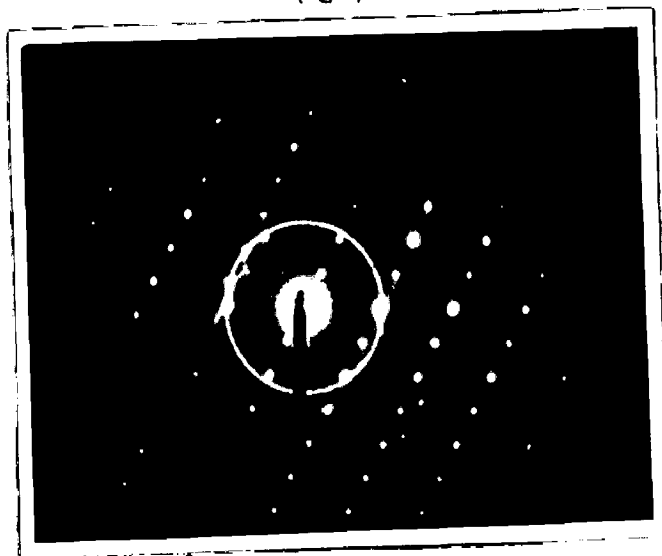
(b) ELECTRON MICROGRAPH OF SAMPLE II HEATED AT 613 K FOR 2 MINUTES



(c)

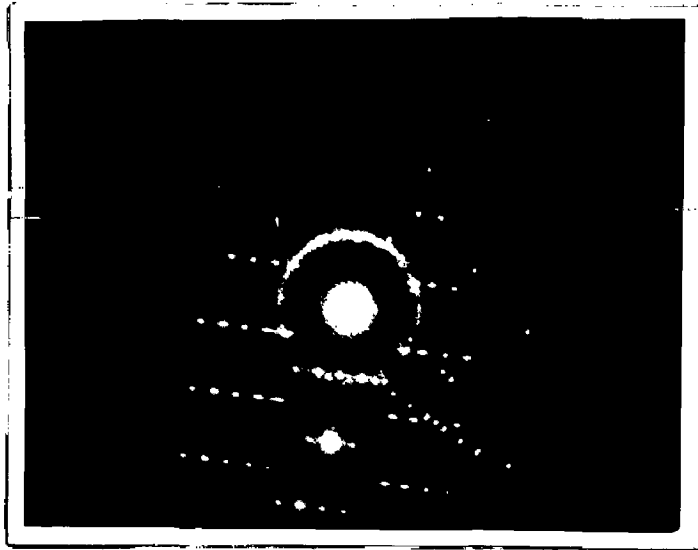


(d)

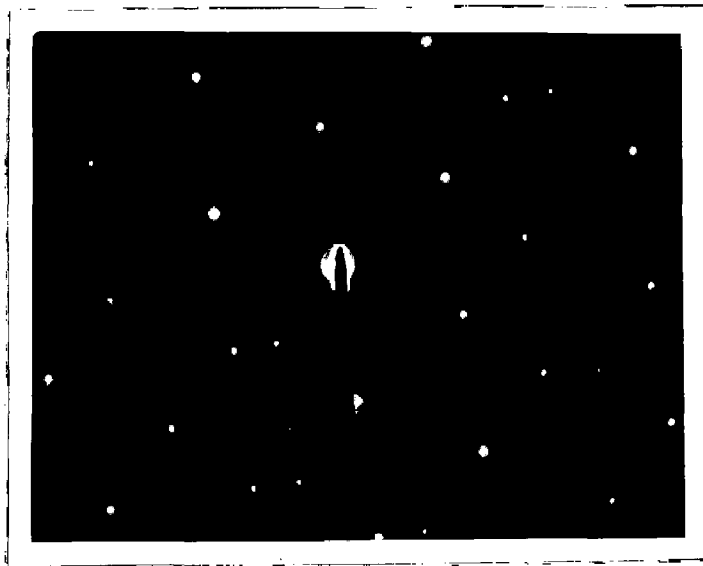


(e)

FIG. 4.6(c) SAD OF SAMPLE II HEATED AT 613K FOR 2 MINUTES
(d) SAD OF SAMPLE II HEATED AT 643K FOR 2 MINUTES
(e) SAD OF SAMPLE II HEATED AT 628K FOR 2 MINUTES



(a)



(b)

FIG. 4.7(a) SAD OF SAMPLE III HEATED AT 618K FOR 2 MINUTES

(b) SAD OF SAMPLE III HEATED AT 643K FOR 2 MINUTES

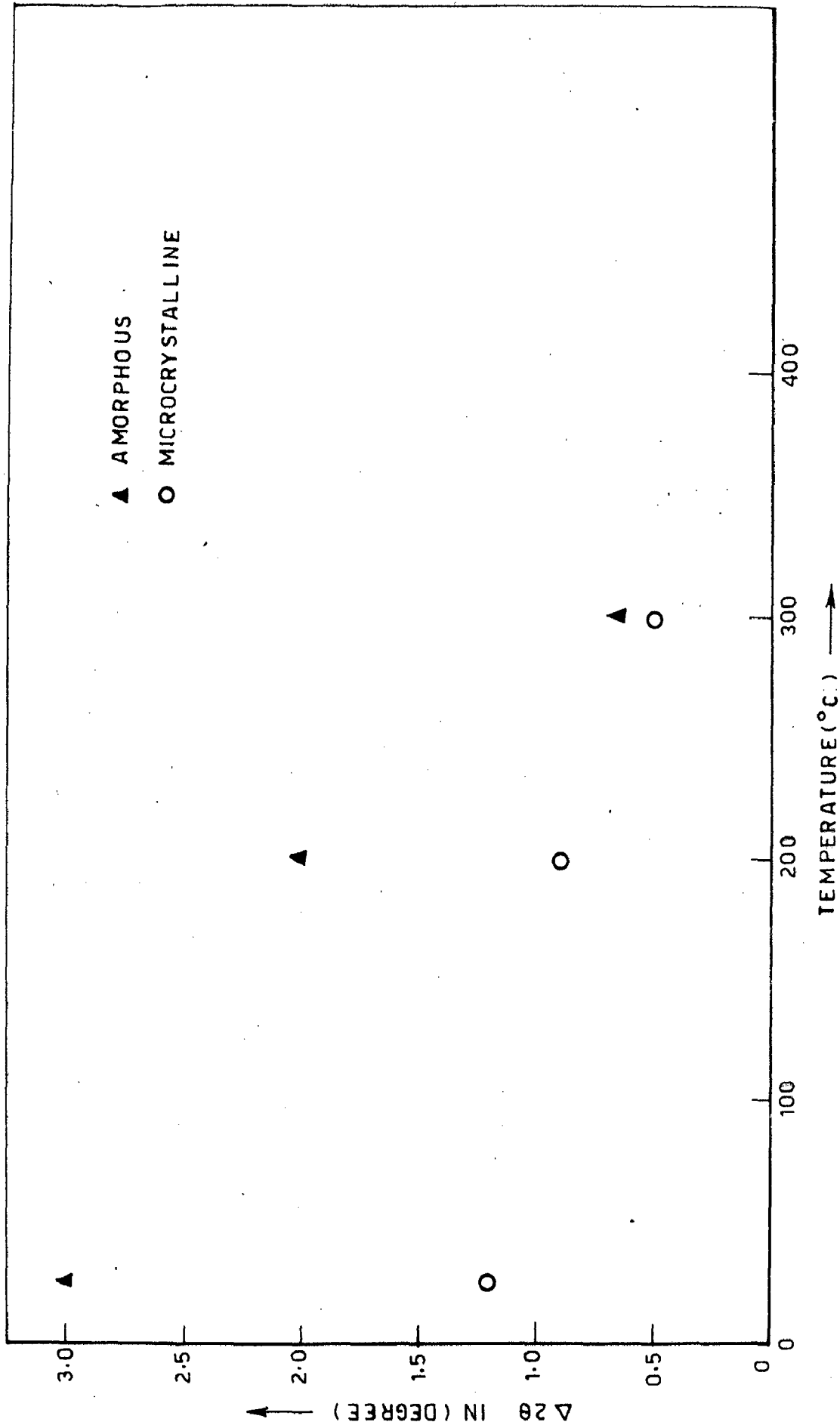


FIG. 4.8 - THE VARIATION OF FULL WIDTH AT HALF MAXIMUM ($\Delta 2\theta$) WITH TEMPERATURE FOR AMORPHOUS AND MICROCRYSTALLINE Ni-P SAMPLE

CHAPTER 5

THE MAGNETIZATION AND ELECTRICAL RESISTIVITY
BEHAVIOUR OF ELECTROLESS AMORPHOUS Ni-P

This chapter contains results of investigations on the magnetic and electrical resistivity behaviour of the electroless Ni-P system over the composition range 5 at. % to 23.5 at. % phosphorus. The magnetic moment, Curie and paramagnetic Curie temperatures and their compositional dependence for the amorphous phase is investigated and the nature of ferromagnetism of these alloys as a weak itinerant ferromagnet is discussed. The results of compositional and temperature dependence of the electrical resistivity and the temperature coefficient of resistivity are presented. The resistivity data are observed to show a correlation in their behaviour as pointed out by Mooij (65).

5.1 THE MAGNETIC PROPERTIES : RESULTS

The magnetic behaviour of amorphous Ni-P system has been investigated by many workers such as Pan and Turnbull (47), Simpson and Brambley (46), Schneider and Wiesner (48), Berrada et.al. (13) and Bakonyi et.al. (15,51) and has been reviewed in chapter 2.

In this section the results of the magnetic measurements on amorphous Ni-P system in the composition range of 5.4 at. % to 23.5 at. % phosphorus using Vibrating Sample Magnetometer in the temperature range of 77 K to 400 K is presented. The details of the method of measurement using Vibrating Sample Magnetometer have been discussed in chapter 3.

5.1.1 The Compositional Dependence Of The Magnetization

Fig. 5.1 shows the variation of magnetic moment of electroless Ni-P samples with phosphorus concentration ranging from 5.4 at. % to 12 at. % . It can be seen from the figure, that the magnetic moment of as-deposited films decreases with increasing concentration of phosphorus in the system. This behaviour is similar to the previous findings for the polycrystalline Ni-P films of Albert et.al. (19) and Maeda (20). The data of Albert et.al and Maeda have also been plotted in figure 5.1 for a comparison.

The magnetic moment data for electroless Ni-P samples is lower, throughout the phosphorus range studied, as compared to the data of Maeda on electrodeposited samples containing upto 7 at. % phosphorus and Albert et.al. on the samples prepared by electroless, electrodeposition and vacuum deposition containing phosphorus upto 9.0 at. % .

The extrapolated value of magnetization for zero phosphorus content composition is about 44 emu/g, while the magnetization value of pure crystalline nickel is 55 emu/g. The curve cuts the zero magnetization axis at 14.0 at. % phosphorus for electrodeposited films.

Fig. 5.2 shows the variation of the as-deposited magnetic moment of Ni-P alloy containing 12.0 to 23.5 at. % phosphorus. The magnetic moment, measured at 300 K, decreases with increasing phosphorus content from 12 to 17 at. % smoothly, similar to the previous observations (Pan and Turnbull (32) and Berrada et.al. (13)) for electrodeposited films. At 17 at. % phosphorus, the magnetic moment reduces to a small value of

0.62 emu/g at 300 K. This amount of magnetization which is essentially the paramagnetic contribution, decreases further as we increase the phosphorus concentration beyond 17 at. % and finally becomes zero at about 23.5 at. % .

Fig. 5.2 also shows the data of Pan and Turnbull for the electrodeposited samples having phosphorus content from 12 to 23 at. % , Berrada et.al. for the electrodeposited Ni-P alloys in the concentration range (15 - 25) at. % phosphorus and Simpson and Brambley (46) for the electroless deposited samples containing 15 at. % phosphorus. It is observed that the magnetic moment curve obtained in the present investigation is lower throughout the composition range studied, though the nature of variation is similar. The extrapolated magnetic moment corresponding to zero phosphorus for the amorphous nickel is about 18.5 emu/g. whereas Pan and Turnbull obtained a value of 40 emu/g. But Tamura and Endo (49) observed a magnetization of 33 emu/g in amorphous nickel.

In figure 5.3 the variation of magnetic moment with the phosphorus concentration in the system for the entire composition range from 5.4 at. % to 23.5 at. % phosphorus has been plotted. It is clear that the magnetic moment decreases more rapidly with phosphorus upto 12 at. % whereas it decreases at a much smaller rate in the amorphous region of more than 12 at. % phosphorus.

Following the theory of Yamauchi and Mizoguchi (66) as discussed in chapter 2, the magnetic moment σ of an amorphous alloy having the composition $M_{1-x}G_x$ is given by

$$\sigma = \frac{m(1-x) - n x}{(1-x)}$$

where M represents 3d transition-metal, which is nickel in our case, G represents metalloid element i.e., phosphorus, and n is the electrons transferred from metalloid phosphorus atom to fill the m holes of the down-spin nickel atom. The magnetic moments of the samples under investigation have been calculated in amorphous region using the above formula with $m = 0.6$ and $n = 3$ following Yamauchi and Mizoguchi and this data are also shown in figure 5.3. These calculations give a much higher value of magnetic moment than those obtained experimentally. However, one should point out that the above expression uses 0.6 holes/ atom in the down-spin nickel atom, which is the case for f.c.c. crystalline nickel corresponding to 57 emu/g, while extrapolated value, for amorphous nickel from our data is much lower and is only 18.5 emu/g.

5.1.2 The Temperature Dependence Of Magnetization

The temperature dependence of magnetization for the Ni-P samples containing 15.0, 16.0, 16.4 and 17.3 at. % phosphorus in the temperature range 77 K to 400 K are shown in figure 5.4. The Curie temperatures of these alloys have been estimated by extrapolating the corresponding curves to zero magnetization. As can be seen from the figure, the values T_c comes out to be 398, 318 and 283 K for the samples having phosphorus content of 15, 16 and 16.4 at. % respectively. The sample containing 17.3 at. % phosphorus exhibits a small value of magnetization, even at a field of 5 KOe and temperature 77 K and is essentially paramagnetic. The extrapolated values of magnetization to zero K are estimated to be 3.95, 2.75, 1.90

and 0.92 emu/gm for the samples containing 15.0, 16.0, 16.4 and 17.3 at. % phosphorus respectively.

Simpson and Brambley (46), for their electroless Ni-P samples containing 15 at. % phosphorus, estimated a Curie temperature of 390 K by extrapolation, our value is 398 K. Pan and Turnbull (47) studied Ni-P alloys prepared by electro-deposition technique and obtained a much lower Curie temperature of only 190 K for a sample containing 15 at. % phosphorus. However, they employed an elaborate and accurate method of thermodynamic parameters. The high values of T_c obtained by extrapolation of the present data may be due to partial crystallization of our samples as pointed out by Pan and Turnbull. Schneider and Wiesner (48) also made experimental study of rapidly quenched Ni-P alloys and estimated Curie temperature of Ni-P samples containing 15 at. % phosphorus, to be (513 ± 10) K which is even higher than the value estimated in the present investigation for a sample of the same composition.

In figure 5.5 the temperature variation of susceptibility and $(\text{susceptibility})^{-1}$ for the sample containing 16.4 at. % phosphorus in paramagnetic region have been shown. By extrapolating the linear portion of the inverse susceptibility curve to the temperature axis, the paramagnetic Curie temperature for the sample comes out to be 432 K. The paramagnetic Curie temperatures for the samples containing 15 and 16.00 at. % phosphorus employing the same technique (not shown in the figure) are estimated to be 498 K and 469 K respectively. The values of T_p obtained by Pan and Turnbull are much lower.

Fig. 5.6 shows the dependence of the Curie temperatures and paramagnetic Curie temperatures of the amorphous samples on composition for the phosphorus contents ranging from 12 to 17 at. %. The Curie temperature as well as paramagnetic Curie temperatures decrease with increasing phosphorus contents.

Fig. 5.7 shows the corresponding state curves for two amorphous Ni-P samples containing 15 and 16.4 at. % phosphorus and that of pure crystalline nickel for comparison. The extrapolated magnetization values, characterizing the amorphous state, corresponding to a given temperature, has been plotted when the samples are observed to crystallize below the Curie temperature. Both the amorphous samples, as expected, show similar corresponding state curves and these are less flat compared to the curve for pure nickel. In other words the normalized magnetization reduces initially at a relatively faster rate with reduced temperature in the amorphous state as compared to that in crystalline nickel. The curves for amorphous alloys fall below that of the crystalline nickel. Harris et al. (67,68) have explained this lowering by a random distribution of local anisotropy field but Handrich (69,70) attributes it to a distribution of exchange integral arising out of structural fluctuations in the amorphous alloys.

5.2 DISCUSSION

The results show that the electroless deposited amorphous Ni-P system displays rather weak ferromagnetism. In electrodeposited Ni-P system (47) and in general for metallic glasses it is usual that, though poor conductors, yet their 3d

electrons are just as itinerant as in a crystalline transition metal alloys.

Following the criteria of Rhodes and Wohlfarth (45) discussed in chapter 2, the estimate of (q_c/q_s) comes out to be 7 (where q_c is the number of carriers per atom deduced from Curie-Weiss constant and q_s is the number of carriers deduced from saturation magnetic moment at zero K for 16.4 atomic percent phosphorus sample confirming the itinerant nature of the weak ferromagnetism for the electroless samples. Also, T_c has been estimated for this sample using the relation of Edwards and Wohlfarth (71) for weak ferromagnet,

$$\sigma(H,T)^2 = \sigma(0,0)^2 \left[1 - (T/T_c)^2 + 2\chi_0 \frac{H}{\sigma(H,T)} \right]$$

where, $\sigma(H,T)$ is the magnetization at field H and temperature T, $\sigma(0,0)$ is the extrapolated value of magnetization at zero field and 0 K temperature, χ_0 is the susceptibility at 0 K and taken to be 0.7×10^{-4} emu/g/Oe. The value of T_c calculated in this way is 134 K, and it is quite low as compared to an estimate of 283 K for this sample from the magnetization versus temperature graph (Fig. 5.2). But it is close to the value of T_c of 125 K obtained by Pan and Turnbull (47) and that of about 140 K of Berrada et.al. (24). The simple extrapolation of the initial portion of the magnetization versus temperature curve to get T_c , as done in this work, yields a higher value of T_c due to high value of susceptibility that contributes to the observed magnetization near T_c and the partial crystallization which exists at this composition for the Ni-P system as discussed in chapter 4. The situation is further complicated by the strong tendency of nickel atoms to

precipitate and segregate and its contribution in the vicinity of ferro to paramagnetic transition as pointed out by Bakonyi et.al. (15). The paramagnetic Curie temperatures for these samples are higher than the corresponding Curie temperatures by about 100 K or more. Such large differences between para and ferromagnetic Curie temperatures are unusual in crystalline ferromagnetic materials and this, broadly speaking, points out to the fact that in amorphous ferromagnets the short range magnetic order is strong relative to long range order.

Berrada et.al. (13) conclude that electrodeposited Ni-P alloys in the phosphorus concentration range 15 to 18 at. % are nearly weak homogeneous ferromagnets but beyond 18 at. % phosphorus alloys the nickel-rich inhomogeneities become important. The present investigation shows that there are extreme inhomogeneities in electroless Ni-P sample, leading to the co-existence of microcrystalline and amorphous state in the composition range between 14 to 18 at. % phosphorous. As a result these samples are in a mixed magnetic state leading to a high observed T_c . The weak ferromagnetism of nickel phosphorous metalloid alloys, immediately before the disappearance of the ferromagnetism, has recently also been pointed out in a series of papers by the group of Bakonyi et.al. (43,44,51) and confirmed by the theory of Malozemoff et.al (72).

5.3 ELECTRICAL RESISTIVITY:RESULTS

The most important early investigation of the electrical resistivity of electrodeposited amorphous Ni-P system has been

reported by Cote (14) and Cote and Meisel (57). It was Pai and Marton (18) who first reported resistivity and structural measurements on electroless Ni-P films. The other investigations are of Berrada et.al. (13) on electrodeposited and recently on both electrodeposited and chemically deposited Ni-P alloys by Bakonyi's group (62). The resistivity behaviour of amorphous metallic alloys in general can be understood by Ziman's theory extended by Evans et.al. (73) and Nagal and Tauc (74) and applied to Ni-P alloys by Cote and Meisel (57). The work is briefly reviewed in chapter 2.

This section presents the results of electrical resistivity measurements using the d.c. four probe method on electroless Ni-P system from 11.0 at. % to 21.5 at. % phosphorus in the temperature range of 120 K to 400 K. The measurements at temperatures higher than 400 K relate to the crystallization behaviour of the system and are presented in chapter 6. The details of the measurement set-up are presented in chapter 3.

The results are, broadly speaking, similar to that for electrodeposited Ni-P system although the present data are in somewhat restricted range of phosphorus composition as well as temperature. The system is observed to show a correlation between resistivity ρ and the temperature coefficient of resistivity (TCR) as first reported by Mooij (65), and a quadratic temperature and then a linear temperature dependence of the resistivity in the temperature range studied.

5.3.1 The Compositional Dependence Of Resistivity And TCR

The variation in resistivity and the TCR at 300 K with the phosphorus composition for the electroless Ni-P system in

their as-deposited state is shown in figure 5.8 and figure 5.9 respectively. Table 5.1 gives our values of ρ and TCR at 300 K for different phosphorus composition. In the graphs also included are the data of Cote (14) on electrodeposited Ni-P system and of Boucher (53) on quenched $(\text{Ni}_{50}\text{Pd}_{50})_{100-x}\text{P}_x$ alloys for a comparison.

In figure 5.8, the resistivity can be seen to increase from a value of $71 \mu\Omega\text{cm}$ at 11.0 at. % phosphorus to a value of $187 \mu\Omega\text{cm}$ at 21.5 at. % phosphorus and thus follows the trend of the data of Cote as well as Boucher of first a slower increase and then a rapid one at about 19 at. % phosphorus. Our values are somewhat lower than of Cote. It is usual that, due to increased disorder the resistivity of amorphous system has a much higher value compared to corresponding crystalline alloys and that it also shows the feature of increase in resistivity with the increasing metalloid concentration (75). As can be seen from table 5.1, in the microcrystalline region of (11-14) at. % phosphorus the resistivity values are lower than $100 \mu\text{ ohm cm}$ but it attains a value of $101 \mu\text{ ohm cm}$ at 15.4 at. % phosphorus, which is a composition at which both amorphous as well as microcrystalline regions are present in the structure (chapter 4).

The temperature coefficient of resistivity (TCR) is also seen to gradually decrease to a value of $12 \times 10^{-5}/\text{K}$ at 21.5 at. % phosphorus. The values of TCR obtained in the present study are higher than that given by Cote on electrodeposited samples. Although the samples of suitable size have not been available for resistivity measurements beyond 21.5 at. %

phosphorus, extrapolating the present data, TCR is expected to become negative beyond 23.5 at. % phosphorus, whereas Cote gives a value 23.0 at. % phosphorus for this transition. The much higher value of $55 \times 10^{-5}/K$ for samples with phosphorus less than 14 at.% points again to their microcrystalline nature. The effective valence $C_1Z_1 + C_2Z_2$ for the transition from the graph is 1.56, where C is the concentration and Z is the valence of the alloy components; nickel is assumed to have a valency Z_2 as 0.5 electrons per atom and phosphorus has a valency Z_1 as 5 electron per atom.

Mooij (65) analyzed the transport data of a large number of crystalline as well as disordered alloys of transition metals and observed the correlation that the temperature dependence of the resistivity is lost as ρ approaches $200 \mu \text{ ohm cm}$ irrespective of whether the origin of the temperature dependence is disorder or electron phonon scattering and that apart from these saturation effects, the temperature coefficient of resistivity becomes negative for alloys with ρ of about $150 \mu \text{ ohm cms}$. In figure 5.10, the variation of the TCR with resistivity ρ has been shown at different compositions and temperatures. Although the present data does not extend upto negative values of the TCR, and there are no samples with $130 \mu \text{ ohm cm}$ to $180 \mu \Omega \text{ cm}$ resistivity values in this study, one can clearly observe that samples with higher resistivity values have lower temperature coefficients.

5.3.2 The Temperature Dependence Of Resistivity

Fig. 5.11 and figure 5.12 show the results of resistivity variation with the temperature in the range of 120 K to 400 K for phosphorus composition from 11.0 at. % to 21.5 at. % .

In figure 5.11, the resistivities of Ni-P samples of 11.0 at. % and 20.6 at. % phosphorus is plotted in the range of 120 K to 280 K with T^2 and figure 5.12 is the plot of resistivity with T for the samples with phosphorus content 11, 13.8, 15.4, 18.8, 19.7 and 20.6 at. % in the temperature range of 280 K to 400 K. It can be seen that the plots are approximately linear with T^2 in the range from 140 K to 280 K and with T in the range from 280 K to 400 K. In the figure 5.12, one also notices a decreasing slope with temperature with increasing phosphorus content, as expected, since there is an overall decrease of TCR with increasing phosphorus. Rapp and coworkers (76) observed for the metglass 2826 and 2826 B such a proportionality of ρ with T^2 beyond the region of resistivity minima. Such a behaviour was also observed by Maitrepierre (77) in the study of amorphous Ni-Pd-P alloys prepared by rapid quenching in the low temperature range. Hasegawa (78) studied amorphous alloy of composition $(\text{Fe}_{100-x}\text{Ni}_x)_{75}\text{P}_{15}\text{C}_{10}$ with x changing from 0 to 50 and found that in the low temperature range, a T^2 dependence followed by a linear T dependence, observed above a temperature T_0 in the range of 150 K to 240 K. Cote and Meisel (57) applied Evans modification of Ziman liquid metal theory to amorphous and disordered crystalline alloys to explain this behaviour i.e., quadratic temperature dependence at low and linear temperature dependence of resistivity at higher temperature.

5.4 DISCUSSION

Our results of electrical resistivity measurements on electroless amorphous Ni-P system below its crystallization temperature may be discussed in the light of broad features shown by amorphous transition metal-metalloid.

The features are :-

- (i) Due to increased disorder, they show a rather large resistivity in the range of 100 μ ohm cm to 200 μ ohm cm. Our samples in the composition range of 15 at. % phosphorus attain a value of 100 μ ohm cm (less than 14 at. % phosphorus is the microcrystalline region) and the sample with 21.5 at. % phosphorus exhibits a value of about 185 μ ohm cm.
- (ii) The resistivity increases with the increasing metalloid concentration. An almost doubling of the magnitude of resistivity has been observed with an increasing metalloid content, phosphorus.
- (iii) The temperature coefficient of resistivity is smaller compared to the crystalline alloy of the same composition. The value of TCR obtained for 21 at. % phosphorus sample is $12 \times 10^{-5}/K$ ~~μ ohm~~ with that for the crystalline phase $4 \times 10^{-3}/K$ as can be seen from cooling curves, discussed in chapter 6.
- (iv) A transition may occur from a positive TCR to a negative value as the concentration of phosphorous increases. In this investigation a decrease of TCR from $52 \times 10^{-5}/K$ to $12 \times 10^{-5}/K$ has been observed as the phosphorus concentration is raised from 11.0 at. % to 21.5 at. % and by extrapolation it is expected to become negative beyond 23.5 at. % of phosphorus.

- (v) One observes a correlation between ρ and TCR (Mooij's correlation) and a limiting resistivity at high temperature. This limiting resistivity is believed to result when electron mean free path equals the inter-atomic distances as the disorder cannot reduce the mean free path any further. Mooij correlation has also been observed in noble and alkali metals alloys that have relatively low resistivity. The plot of ρ with TCR confirms the Mooij observation for electroless Ni-P samples as well.
- (vi) A positive TCR for alloying a monovalent with a multivalent element is expected upto effective conduction electron concentration of about 1.5 and a negative TCR from 1.5 to 2. In the present study the transition is observed to occur at 1.56.
- (vii) Following Cote and Meisel^{one} expects a quadratic temperature dependence followed by a linear temperature dependence of the resistivity. The present data, though only on two samples for lower temperature range, shows T^2 dependence in the temperature range 140 K to 280 K and a T dependence in the range from 280 K to 400 K. At a still lower temperature range a resistivity minima (13) is observed. However, the present investigation does not extend to that range of temperature.

5.5 SUMMARY

The magnetic and electrical resistivity behaviour of the electroless Ni-P system over the compositional range 5 at. % to 23.5 at. % phosphorous and a temperature range of 77 K to 400 K has been investigated.

The samples are found to be weak itinerant ferromagnet with strong short range order. The magnetic moment is observed to decrease with increasing phosphorous, first more rapidly and then less and to go to zero (by extrapolation) at 17.5 at. %. The Curie and paramagnetic Curie temperature also decrease with increasing phosphorous. The normalized magnetization is found to decrease at a relatively faster rate with reduced temperature in the amorphous state as compared to crystalline phase.

The resistivity is found to increase from an initial value of $71 \mu\Omega\text{cm}$ to $187 \mu\Omega\text{cm}$ at 21.5 at. %.

The TCR is seen to decrease to a value of $12 \times 10^{-5}/\text{K}$ with increasing phosphorous and 23.5 at. % is the extrapolated value at which TCR is to become negative with the effective value of valence as 1.56.

As pointed out by Mooij higher resistivity samples are found to have linear TCR. In the temperature range 140 K to 280 K the resistivity variation is observed to be linear with T^2 and linear with T in the temperature range 280 K to 400 K.

L I S T O F T A B L E

- 5.1 The variation of resistivity and TCR with phosphorous in Ni-P samples.

L I S T O F F I G U R E S

- 5.1 The variation of as-deposited magnetic moment of Ni-P alloy with phosphorous content less than 12 at.%.
5.2 The variation of as-deposited magnetic moment of Ni-P alloy containing 12 to 23.5 at.% P.
5.3 The variation of magnetisation of Ni-P system with phosphorous ranging from 5.4-23.5 at.%.
5.4 The magnetization vs. temperature in the temperature range of (77K-400K) containing 15, 16, 16.4, 17.3 at.% P.
5.5 The variation of χ and χ^{-1} with temperature containing 16.4 at.% phosphorous.
5.6 The compositional variation of Curie temperature T_c for 12, 15, 16 and 16.4 at.% P. and paramagnetic Curie temperature T_p for 15, 16, 16.4 at.% P.
5.7 The corresponding state curves for electroless amorphous Ni-P sample containing 15 and 16.4 at.% phosphorous.
5.8 The variation of resistivity with Ni-P sample containing 11 to 21.5 at.% phosphorous.
5.9 Variation of TCR at room temperature with phosphorous contents and with effective conduction electron concentration $C_1Z_1 + C_2Z_2$.
5.10 Variation of TCR with phosphorous contents in the electroless Ni-P sample at different temperatures upto 400 K.

- 5.11 Variation of resistivity vs (temperature)² of Ni-P sample containing 11 and 20.6 at.% P in the temperature range 120-300K.
- 5.12 Variation of resistivity with temperature range 280-400 K containing 20.6 and 11 at.% P and with temperature range 300-400 K containing 19.7, 18.8, 15.4 and 13.8 at.% P.

TABLE 5.1

ELECTRICAL RESISTIVITY (ρ) AND THE TEMPERATURE COEFFICIENT OF RESISTIVITY (α) OF ELECTROLESS Ni-P SYSTEM

Alloy Composition	300 K ($\mu\Omega\text{cms} \pm 20$)	$\alpha = \left(\frac{\partial \rho}{\partial T}\right)_{T=300\text{ K}} \times \frac{1}{\rho_T}$ (10^{-5} K^{-1})
Ni _{.89} P _{.11}	71	53
Ni _{.86} P _{.14}	79	58
Ni _{.85} P _{.15}	101	31
Ni _{.81} P _{.19}	109	22
Ni _{.80} P _{.20}	120	19
Ni _{.79} P _{.21}	128	12
Ni _{.78} P _{.22}	187	12

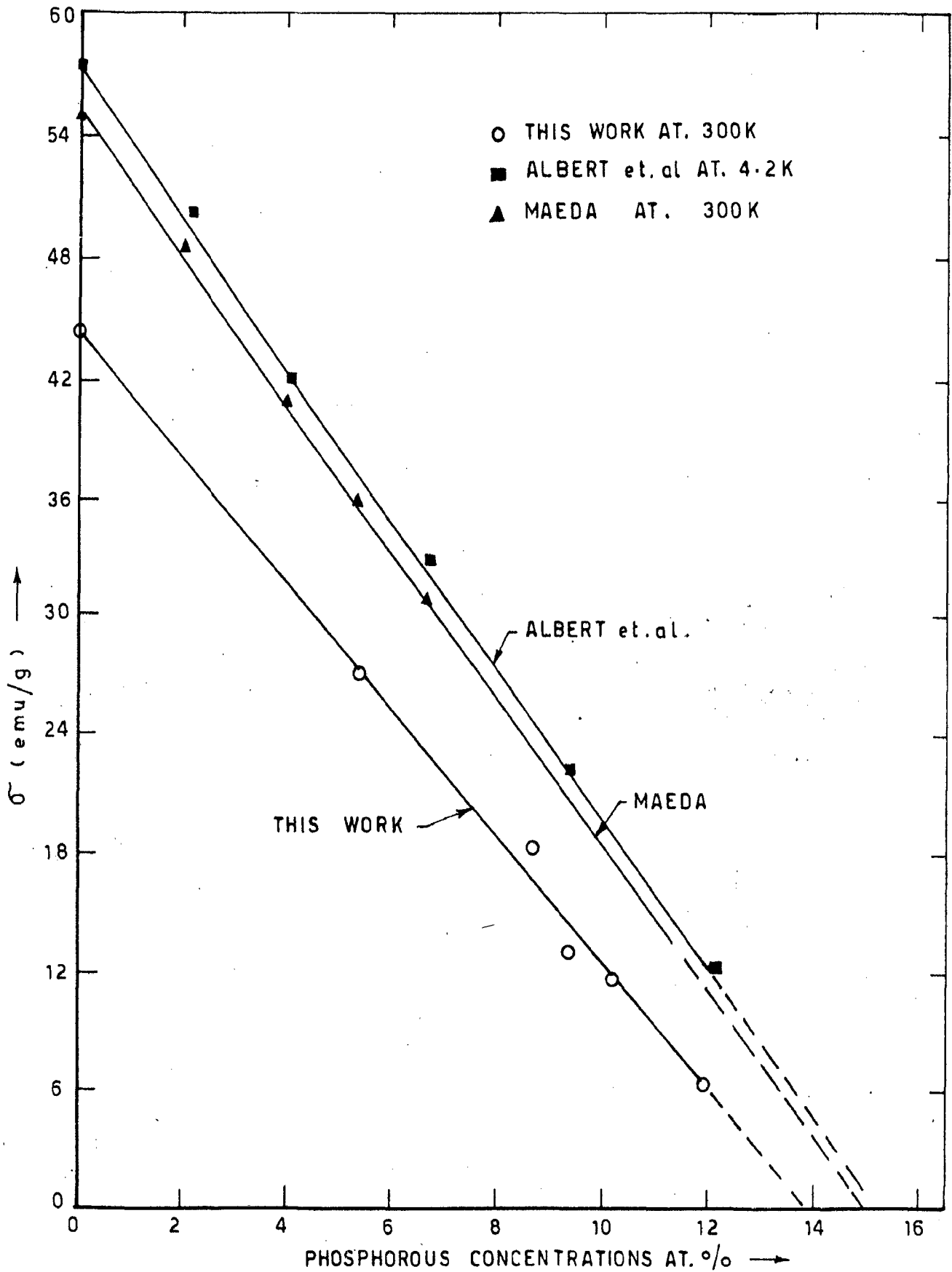


FIG. 5.1 THE VARIATION OF THE AS-DEPOSITED MAGNETIC MOMENT OF Ni-P ALLOY WITH PHOSPHOROUS CONTENT LESS THAN 12 AT.%. MAGNETIC MOMENT CAN BE SEEN TO DECREASE WITH THE INCREASING PHOSPHOROUS

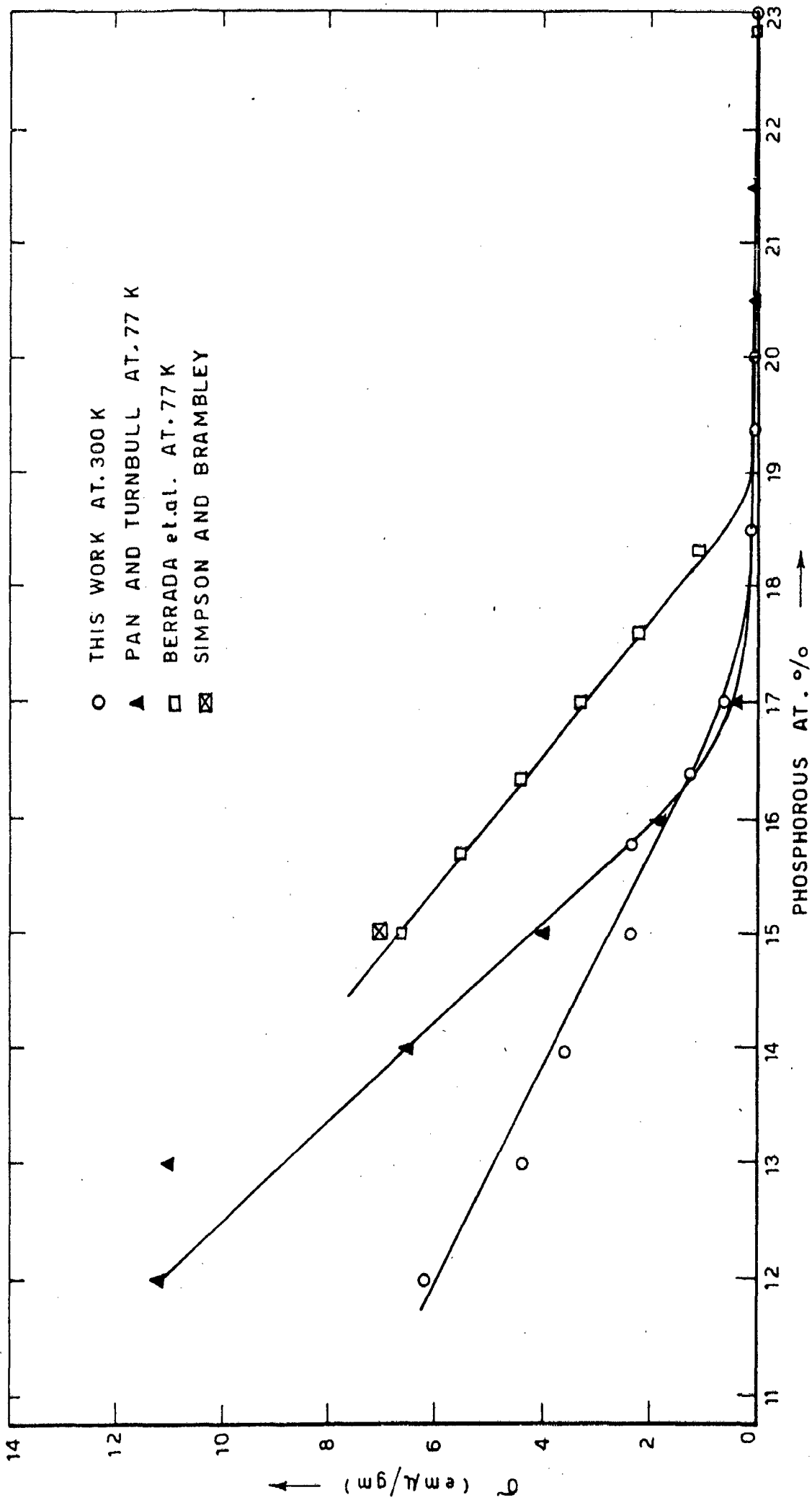


FIG. 5.2 - THE VARIATION OF THE AS-DEPOSITED MAGNETIC MOMENT OF Ni-P ALLOY CONTAINING 12 TO 23.5 AT. % P. THE EXTRAPOLATED VALUE CORRESPONDING TO AMORPHOUS Ni IS 18.5 e.m.u./g AND CORRESPONDING TO ZERO MAGNETIZATION THE PHOSPHOROUS CONCENTRATION IS ABOUT 23 AT. %

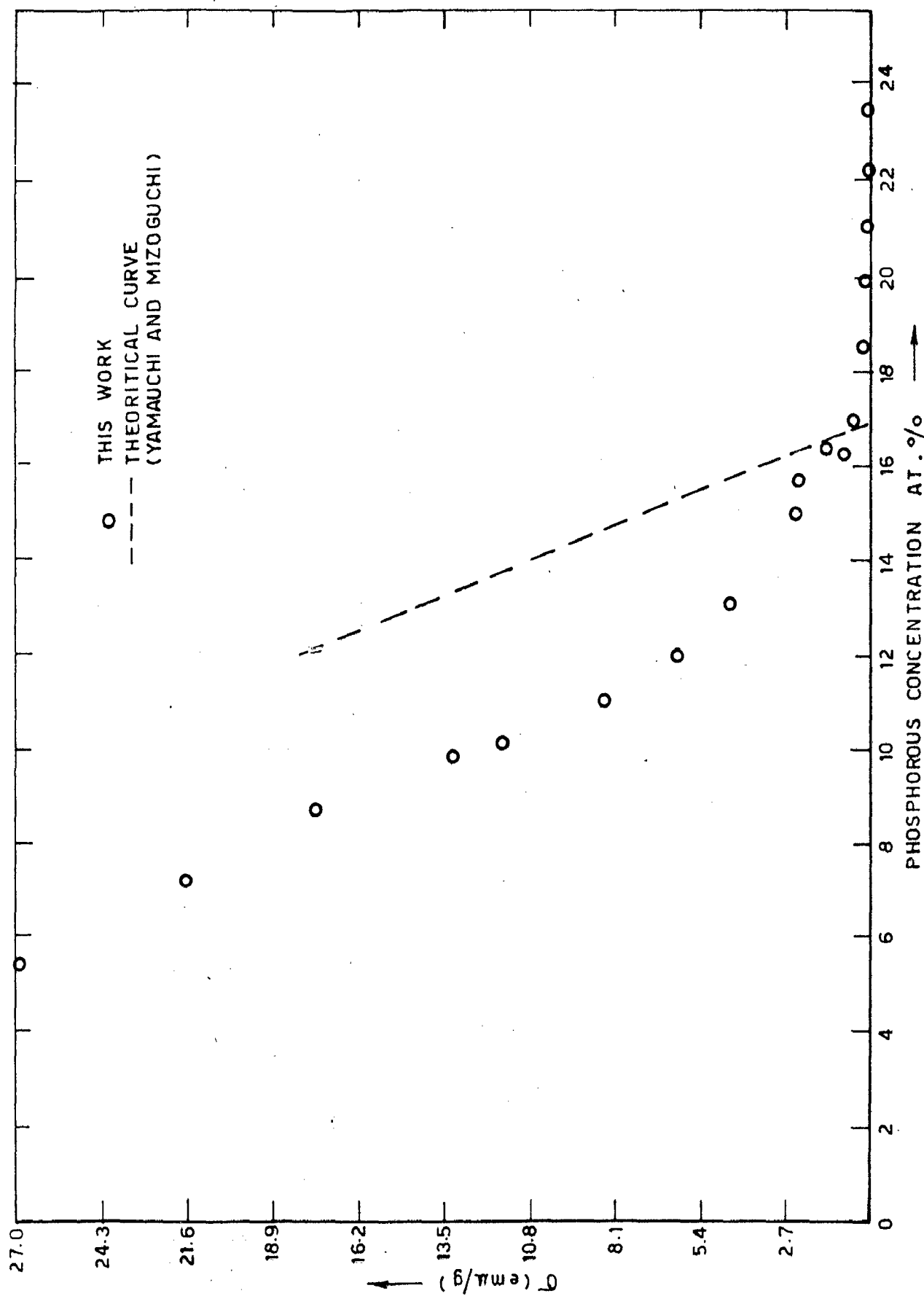


FIG. 5.3 - THE VARIATION OF MAGNETISATION OF Ni-P SYSTEM WITH THE COMPOSITION IN THE ENTIRE PHOSPHOROUS RANGE FROM 5.4 AT.% TO 23.5 AT.%. THE VARIATIONS AS PREDICTED BY THE CALCULATIONS OF YAMAUCHI AND MIZOGUCHI IS ALSO SHOWN IN THE GRAPH

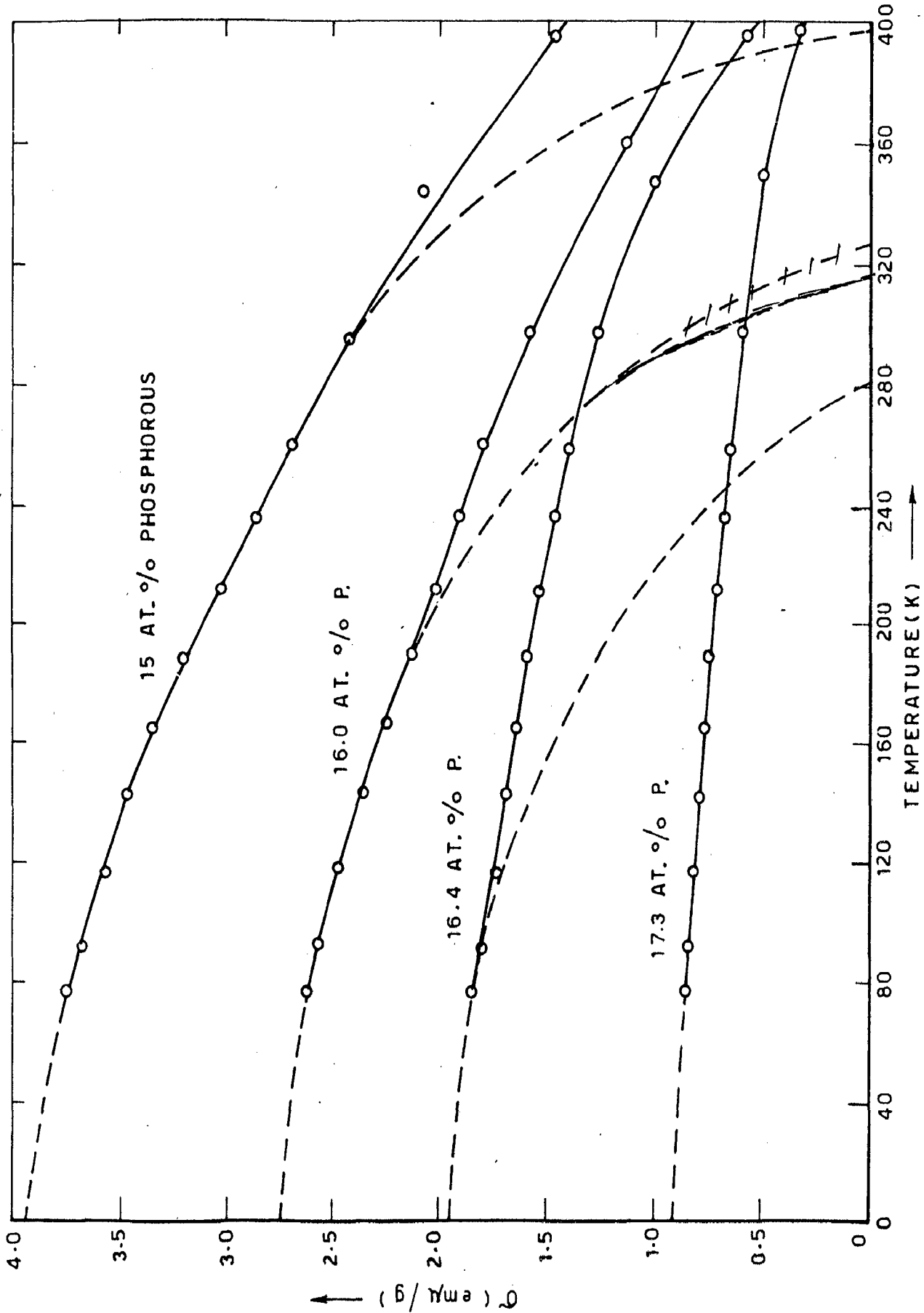


FIG. 5.4 - THE MAGNETIZATION VS TEMPERATURE BEHAVIOUR OF Ni-P SAMPLES IN THE TEMPERATURE RANGE (77K - 400K) CONTAINING 15,16,16.4 AND 17.3 AT. % PHOSPHOROUS

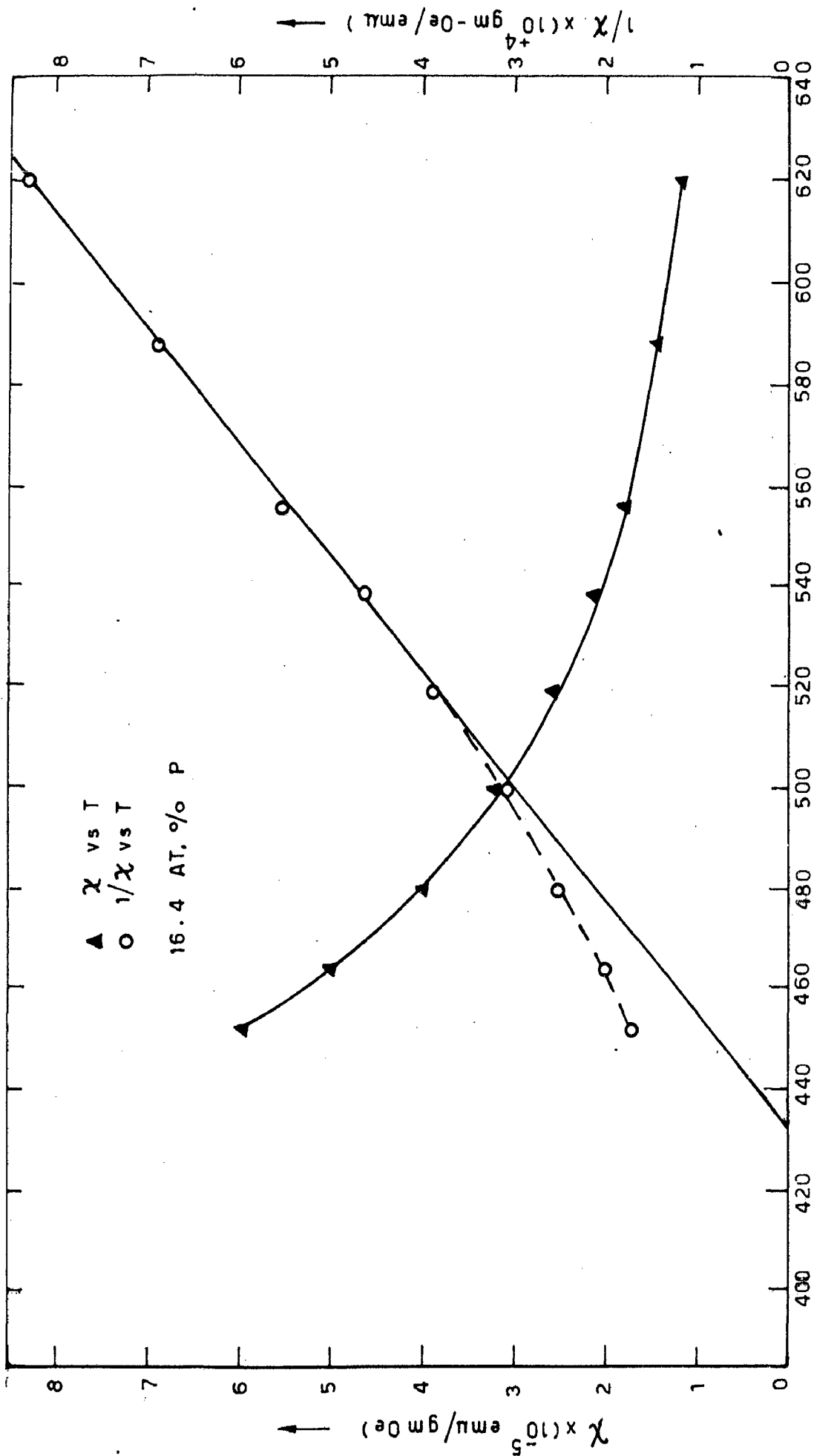


FIG. 5.5 - THE VARIATION OF χ , THE SUSCEPTIBILITY AND χ^{-1} , THE INVERSE OF SUSCEPTIBILITY WITH TEMPERATURE IN THE PARAMAGNETIC REGION FOR THE SAMPLE CONTAINING 16.4 AT. % PHOSPHOROUS. THE PARAMAGNETIC CURIE TEMPERATURE, T_p IS ESTIMATED BY EXTRAPOLATING THE LINEAR PORTION OF THE CURVE TO THE TEMPERATURE AXIS. T_p FOR THIS SAMPLE IS ESTIMATED TO BE 432 K

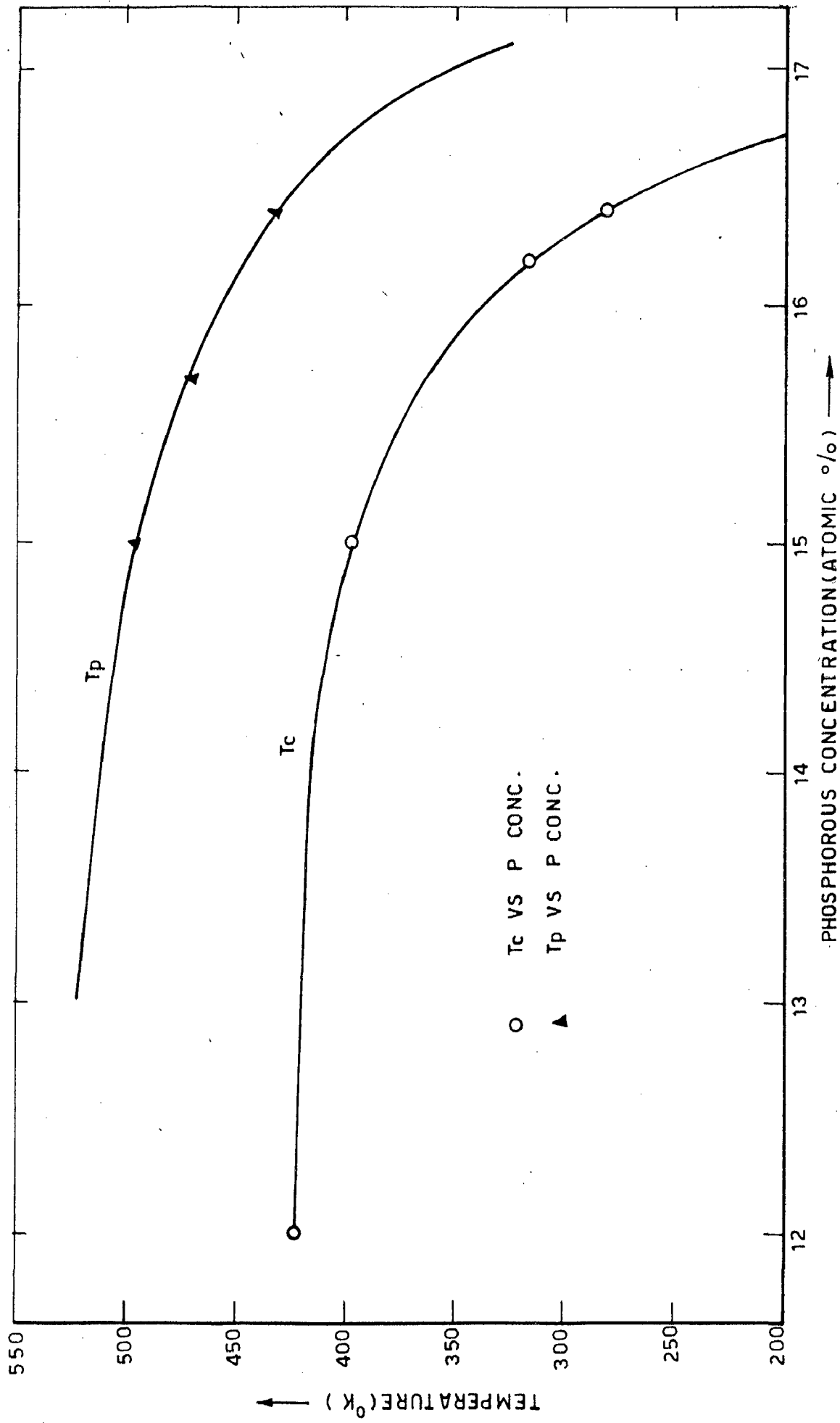


FIG. 5.6 - THE COMPOSITIONAL VARIATION OF CURIE TEMPERATURES T_c , FOR THE SAMPLES CONTAINING 12, 15, 16 AND 16.4 AT. % PHOSPHOROUS AND PARAMAGNETIC CURIE TEMPERATURES T_p FOR THE SAMPLES CONTAINING 15, 16 AND 16.4 AT. % P

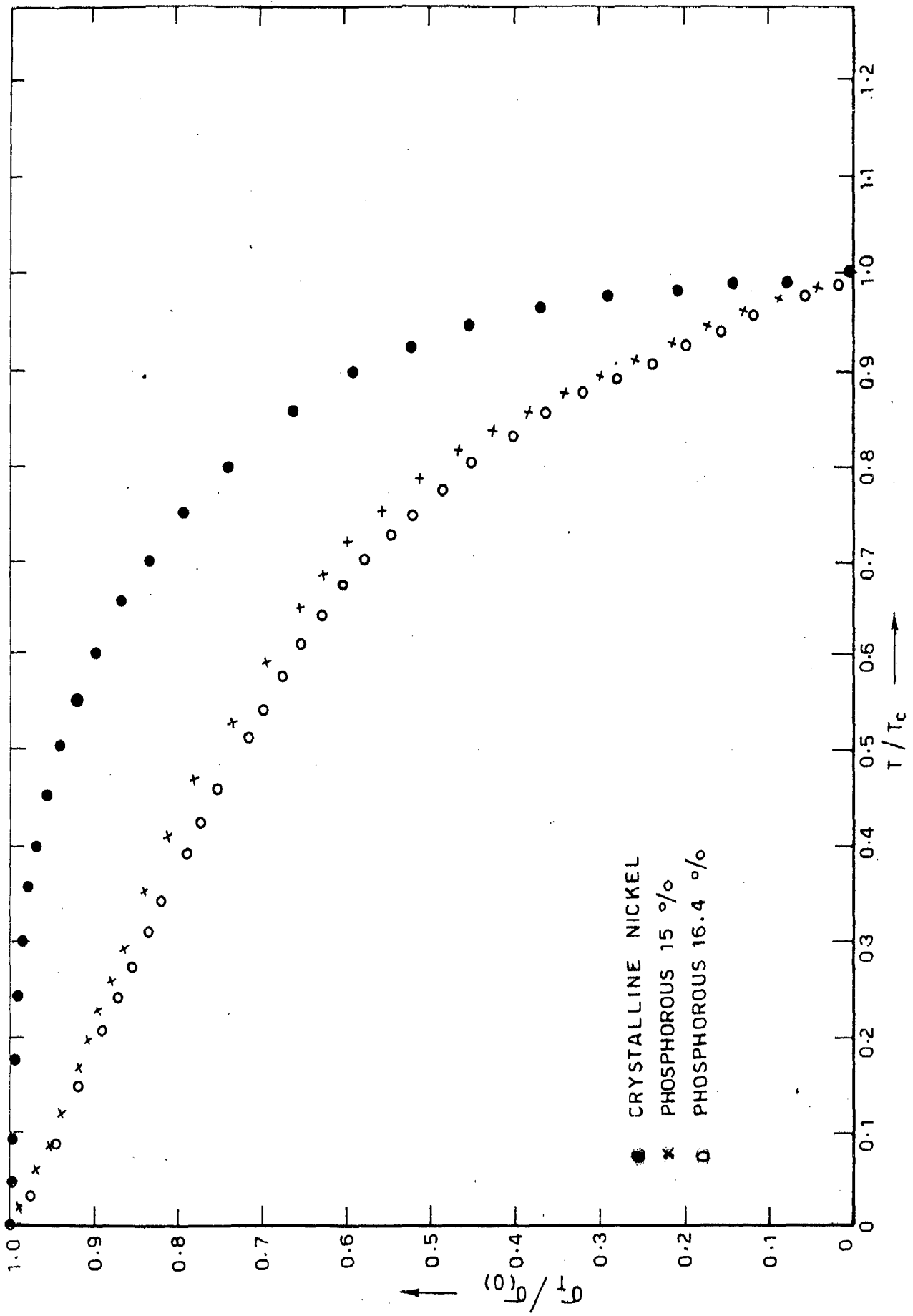


FIG. 5.7 - THE CORRESPONDING STATE CURVES FOR ELECTROLESS AMORPHOUS Ni-P SAMPLES CONTAINING 15 AND 16.4 AT.% PHOSPHOROUS. THE CURVE FOR PURE CRYSTALLINE NICKEL SAMPLE IS ALSO SHOWN

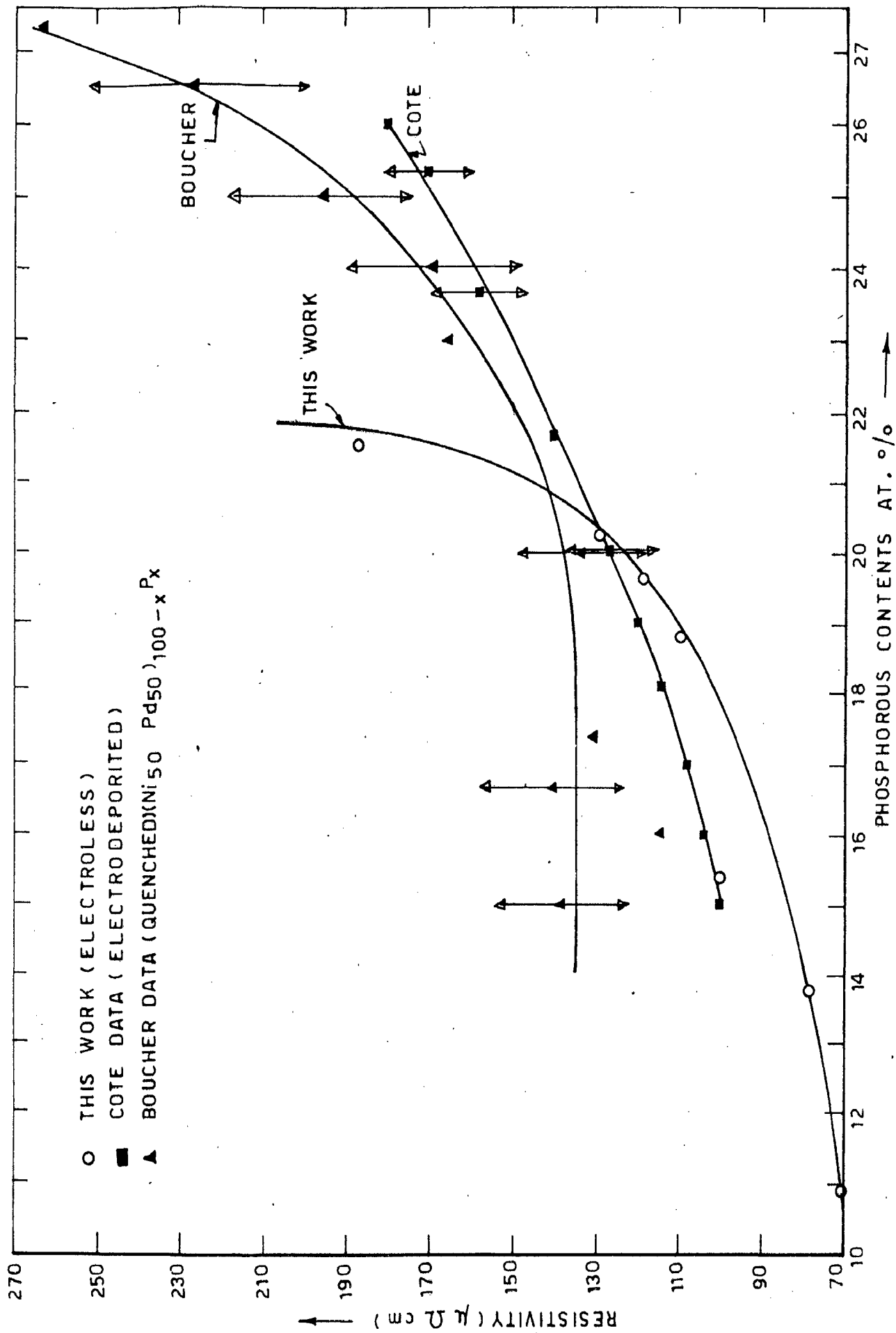


FIG. 5.8 - THE VARIATION OF RESISTIVITY WITH COMPOSITION OF Ni-P SAMPLES CONTAINING 11 TO 21.5 AT.% PHOSPHOROUS. THE FIGURE ALSO INCLUDES THE DATA OF COTE FOR ELECTRODEPOSITED Ni-P SAMPLES AND BOUCHER'S DATA ON QUENCHED $(\text{Ni}_{50}\text{-Pd}_{50})_{100-x}\text{P}_x$

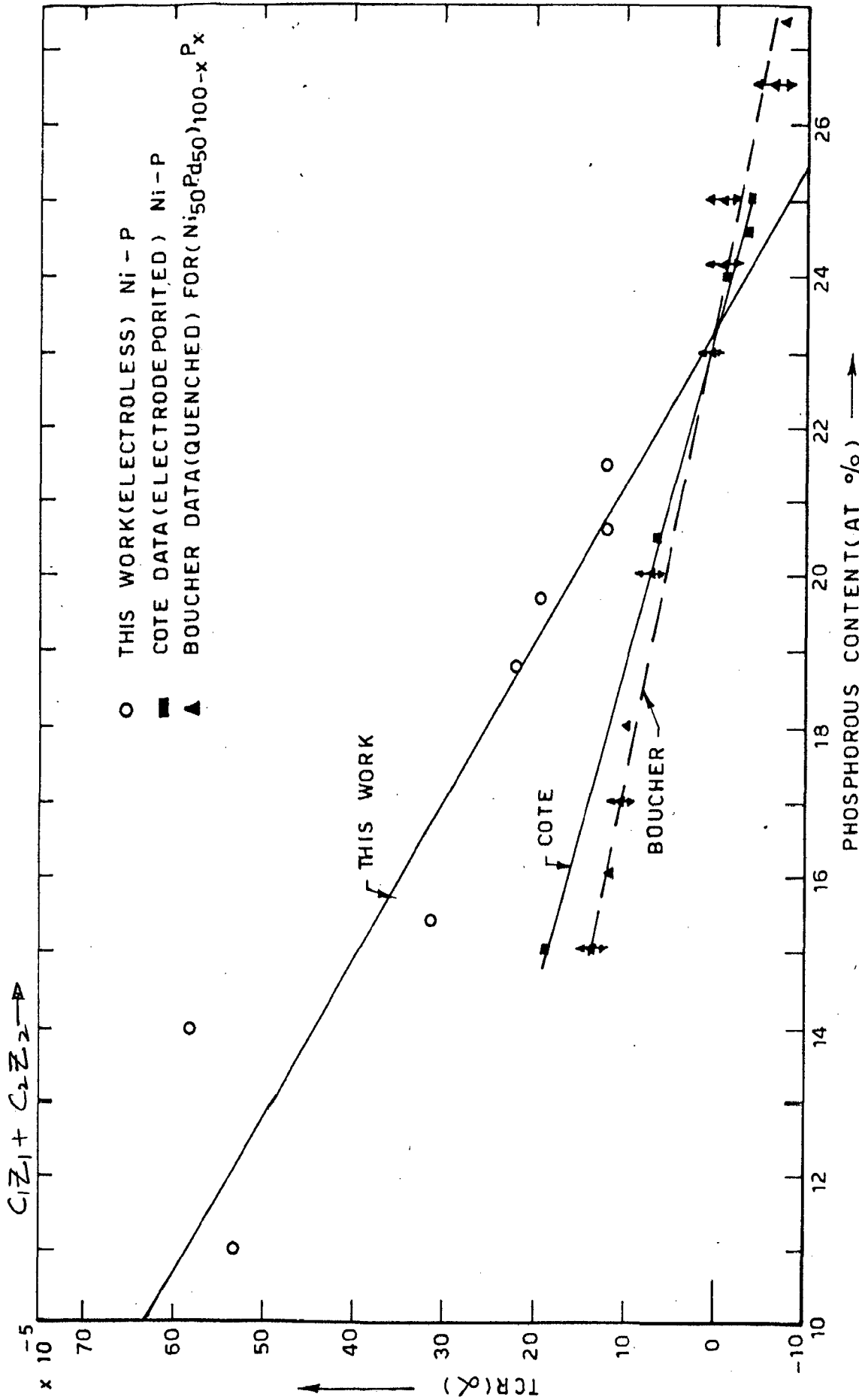


FIG. 5.9 - VARIATION OF TEMPERATURE COEFFICIENT OF RESISTIVITY (α) AT ROOM TEMPERATURE (300 K) WITH PHOSPHOROUS CONTENT AND WITH EFFECTIVE CONDUCTION ELECTRON CONCENTRATION $C_1Z_1 + C_2Z_2$. THE FIGURE ALSO INCLUDES THE DATA OF COTE ON ELECTRODEPOSITED AND BOUCHER et. al. ON QUENCHED (Ni₅₀ Pd₅₀)_{100-x} P_x ALLOYS

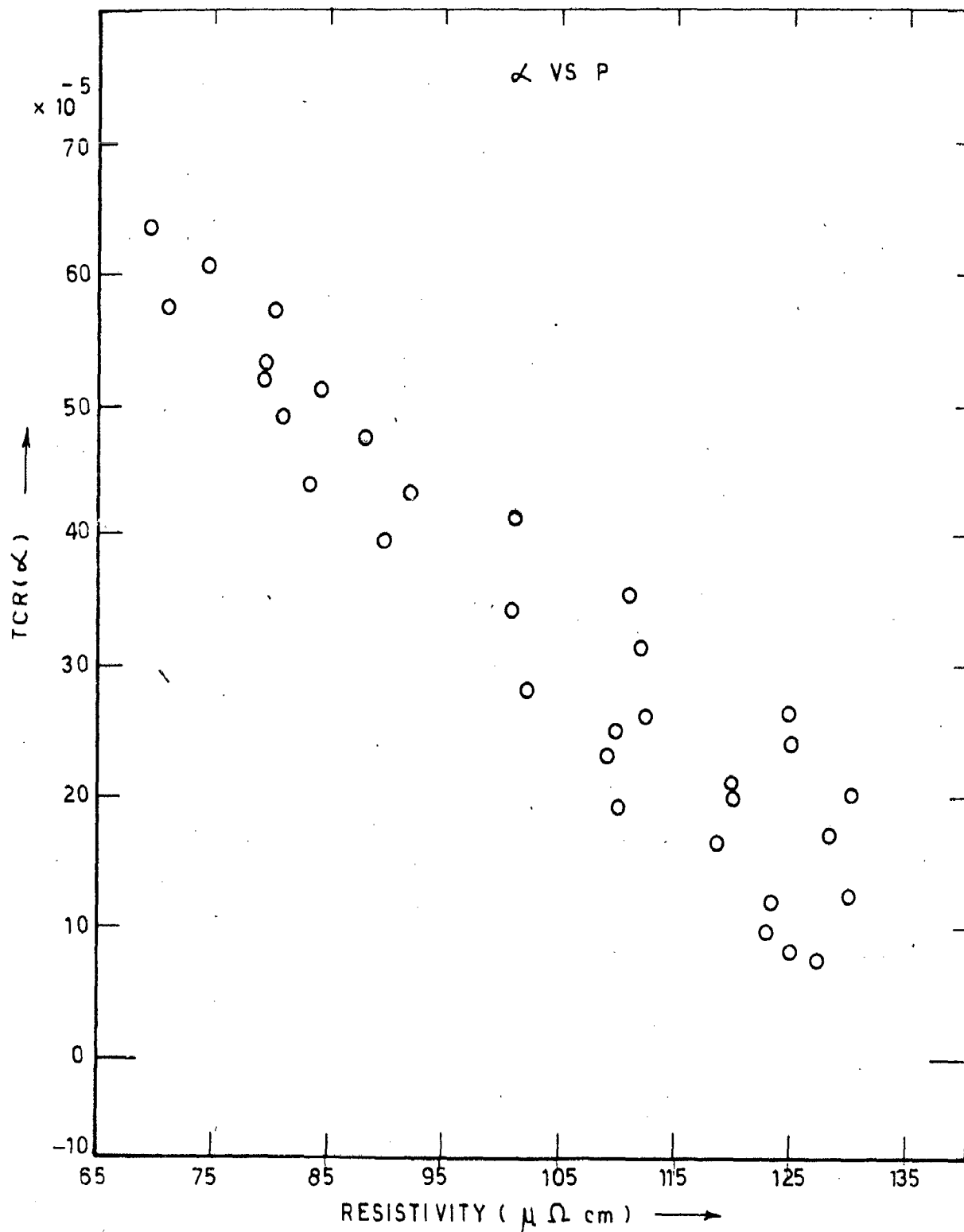


FIG. 5.10 - THE VARIATION OF TEMPERATURE COEFFICIENT OF RESISTIVITY WITH PHOSPHOROUS CONTENT IN THE ELECTROLESS Ni-P SAMPLE. THE SAMPLES WITH HIGHER RESISTIVITY CAN BE SEEN TO HAVE SMALLER VALUES OF THE TEMPERATURE COEFFICIENT AS OBSERVED BY MOOIJ

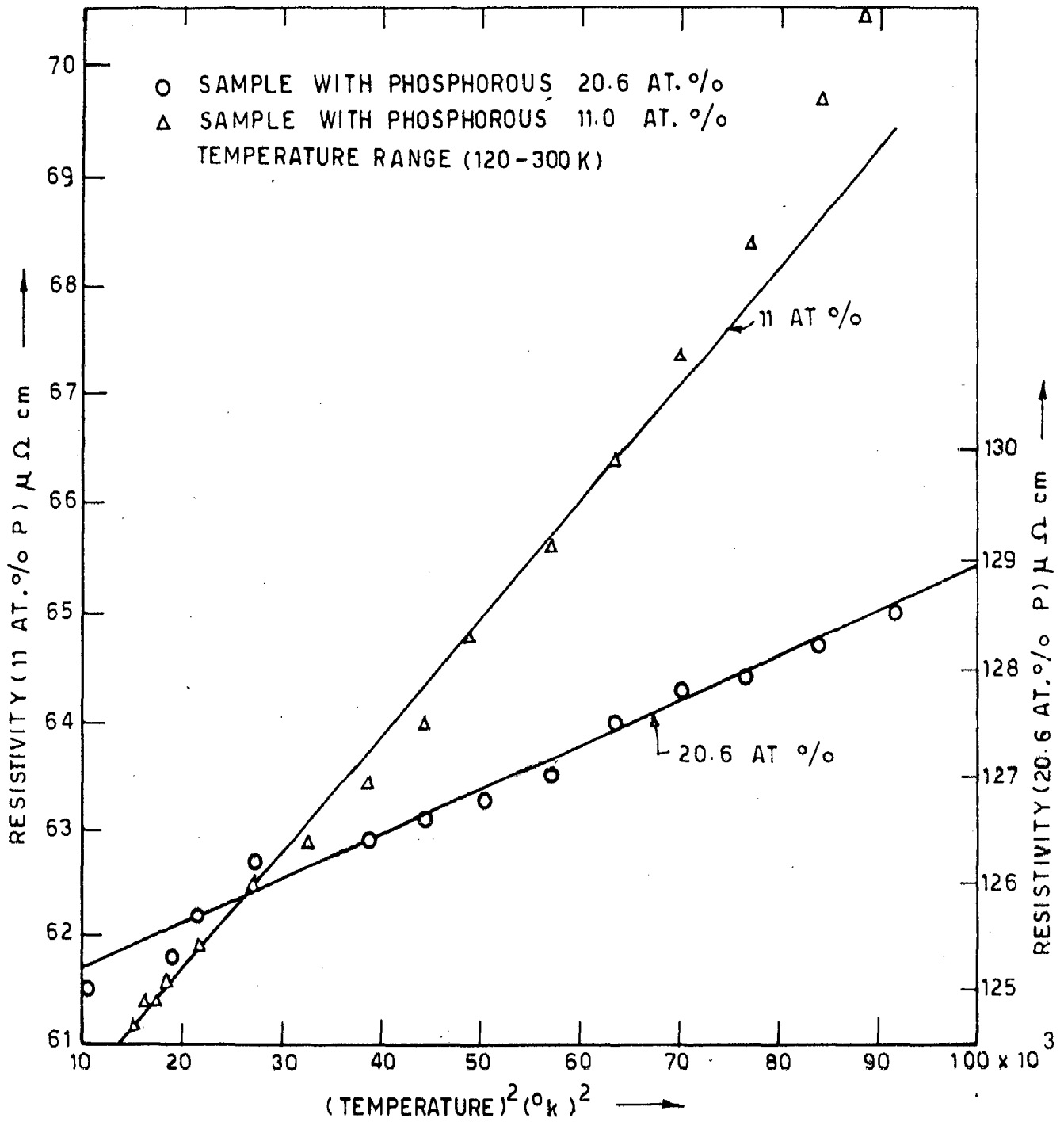


FIG. 5.11 - THE VARIATION OF RESISTIVITY VS (TEMPERATURE)² OF THE Ni-P SAMPLES CONTAINING 11 AT.% AND 20.6 AT.% PHOSPHOROUS IN THE TEMPERATURE RANGE (120-300 K) THE RESISTIVITY VS (TEMPERATURE)² VARIATION IS LINIER FOR THIS TEMPERATURE RANGE

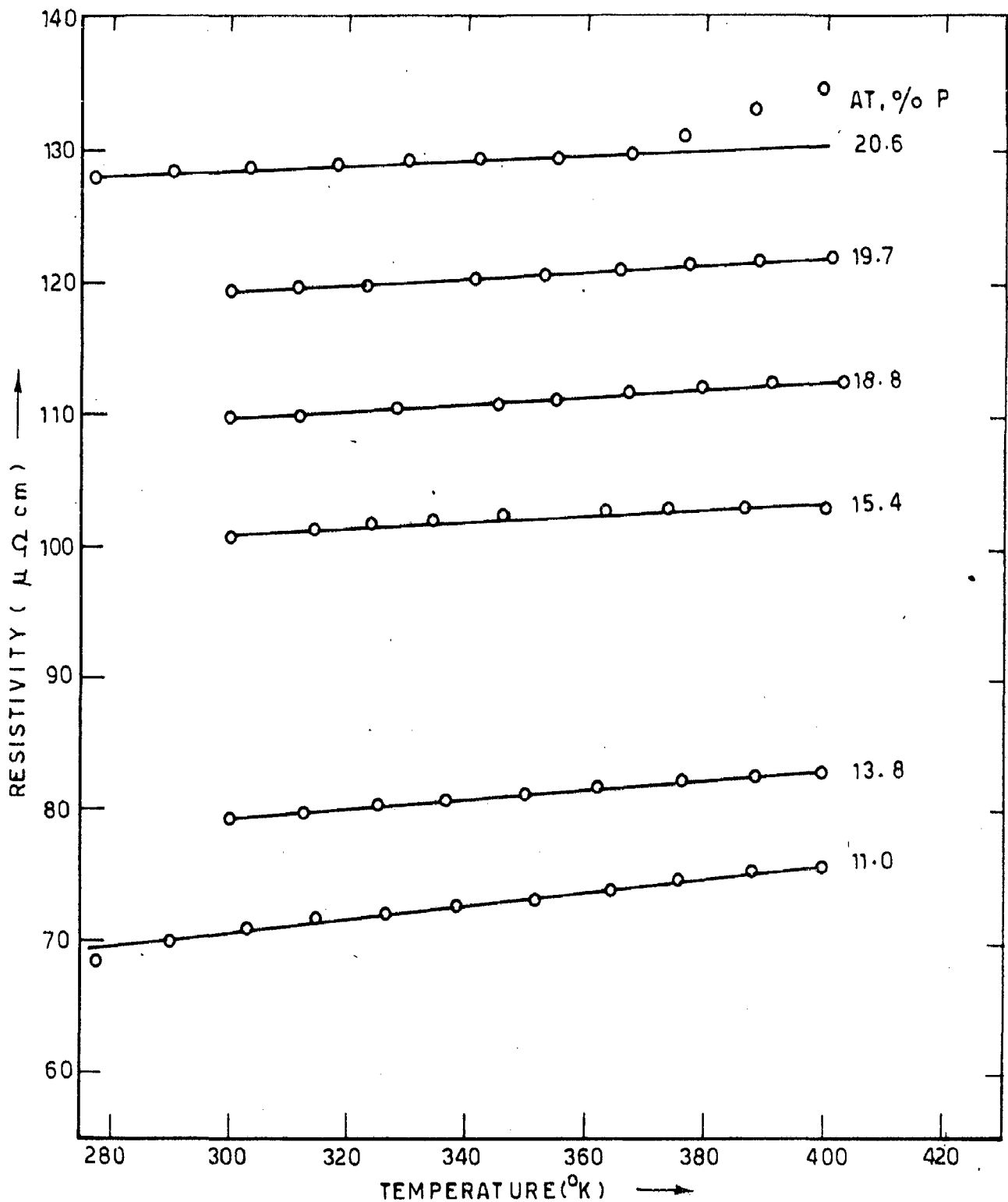


FIG. 5.12_ THE VARIATION OF RESISTIVITY WITH TEMPERATURE IN THE RANGE OF 280 TO 400 K FOR Ni-P SAMPLES CONTAINING 20.6 AT.% AND 11 AT.% P AND IN THE TEMPERATURE RANGE OF 300K TO 400K FOR SAMPLES WITH 19.7, 18.8, 15.4 AND 13.8 AT.% PHOSPHOROUS COMPOSITION. THE BEHAVIOUR OF RESISTIVITY IN THIS TEMPERATURE RANGE IS LINEAR WITH TEMPERATURE,

CHAPTER 6

ANNEALING BEHAVIOUR OF ELECTROLESS Ni-P SYSTEM

Metallic glasses or Amorphous Alloys are thermodynamically unstable and transform spontaneously to stable phases above the crystallization temperature. The driving force is the free energy difference between the amorphous phase and the corresponding stable phase or phases. The transformation takes place by nucleation and growth.

There are three different modes by which crystallization may take place: (i) polymorphous crystallization where there is no redistribution of atomic constituents, (ii) eutectic crystallization where two crystalline phases grow out of the amorphous phase in a coupled manner, and (iii) primary crystallization, where solutes are rejected from the growing crystals into the amorphous phase. However, the transition metal-metalloid system generally crystallizes through a sequence of metastable phases to its final stable phase. The steps involved in the crystallization of Ni-P amorphous alloys are still shrouded in mystery. Many investigators (28, 62, 79) took it up recently but consensus is yet to emerge. The crystallization behaviour of electroless Ni-P alloy is thus eminently

suitable for our investigation. The present chapter gives an account of our results and discusses the similarities or differences of our results with those obtained by others.

6.1 ANNEALING STUDIES USING HOT STAGE ELECTRON-MICROSCOPY AND X-RAY DIFFRACTION: RESULTS

The Ni-P films containing above 18 at % of phosphorous has been found to be amorphous as has been reported in Chapter-4. These films have been subjected to heating in the hot stage of electron-microscope and the changes in the microstructure have been noted. In order to understand the precise nature of the changes taking place at a given temperature, X-ray diffraction analysis has been carried out after heating the samples at that temperature in a furnace.

6.1.1 Hot Stage Electron-Microscopy:

Fig.6.1 shows the microstructure of the electroless Ni-P film containing about 20 at % phosphorous as it is heated from ambient temperature to 673K. The structure of the as-deposited film shown in fig.6.1(a) does not reveal any other detail than uneven thickness resulting in a film formed by lateral growth of islands. When this film is heated to 423K, and held for two minutes the thickness tends to become uniform and the thicker islands come out clearly in contrast as shown in fig.6.1(b). In addition there appears to be some change taking place in

the film which could not be clearly identified. When the film is further heated to 618K and held for 2 minutes one can clearly observe small crystallites formed in the film. On further heating to 673K and holding for 2 minutes the film appears to have become polycrystalline with a large grain size and dark precipitates of nickel phosphide have appeared, as shown in fig.6.1(c) and 6.1(d).

The changes in SAD pattern during continuous heating of the sample whose micro-structures are in fig.6.1(a) have been shown in fig.6.2(a) to 6.2(e). The SAD pattern of the as-deposited amorphous sample has been reproduced in fig.6.2(a) for the purpose of comparison. When the sample is heated to 423K the outer feeble diffuse ring of the as-deposited sample becomes a little more intense as shown in 6.2(b) but there are no three rings pattern characteristic of microcrystalline state or sharp diffraction rings or spot pattern indicating the onset of crystallization process. The sample when held at a higher temperature of 573K for 2 minutes, one observes co-existence of crystalline and amorphous state as observed in fig.6.2(c) but there had been no phosphide formation as yet. On heating to a still higher temperature of 618 K, one observes phosphide precipitation along with crystalline nickel but the process of crystallization is not yet complete as indicated by the presence of amorphous phase as also shown by the diffuse rings in fig.6.2(d). When the sample

is heated to 643K and held for 2 minutes, one finds that the crystallization has completed and phosphides have also formed. There are no diffuse rings and only spot pattern is obtained as shown in fig. 6.2 (e).

6.1.2 X-RAY Diffraction Studies

To confirm the changes taking place in the film as indicated by the SAD patterns, X-ray diffraction pattern has been taken for the amorphous Ni-P films heated at different temperatures for 30 minutes. The X-ray diffraction patterns are shown in fig.6.3(a). After half an hour heating at 473K, there is precipitation of almost pure crystalline nickel with the main peaks corresponding to $d = 2.024$ and 1.76 \AA . When heated at 573K, three additional lines appear at $d = 2.15$, 1.93 and 1.812 \AA . The appearance of a peak at $d = 1.812$ indicates that there might be the formation of Ni_7P_3 at intermediate temperatures but at 673 K the diffraction lines are those of Ni_3P and nickel. However the intensities of Ni_3P do not match with the theoretical calculation made by Makhsoos et.al(61). To compare it with the changes taking place in microcrystalline films the X-ray diffraction patterns of a sample containing 12 at % phosphorous after heating it to 473 and 673 K have been shown in fig.6.3(b). At 473 K the diffraction lines of nickel are becoming sharper but at 673 K one observes additional lines for Ni_3P .

6.2 THE ANNEALING STUDIES USING VSM: RESULTS

The appearance of crystallization is clearly detected from the magnetization vs temperature measurements. Different metastable phases at different temperatures can be seen from a continuous recording of magnetic moment with temperature. The crystallization of amorphous Ni-P alloys seems to progress through the formation of one or more new metastable crystalline phases as the material progresses towards the equilibrium during the annealing treatment. A very large number of new metastable crystalline structures may thus be generated by annealing an amorphous alloy of fixed composition.

In this section the results of a study of the annealing behaviour of electroless amorphous Ni-P alloys containing phosphorous from 5.4 to 23.5 at % have been reported. The annealing behaviour of polycrystalline electroless samples containing phosphorous upto 12 at % is presented in section 6.2.1, while the same for amorphous samples having phosphorous contents above 12 at % is given in section 6.2.2.

6.2.1 The Annealing Behaviour of Magnetization of Polycrystalline Ni-P system

Fig.6.4 shows the change in magnetization of Ni-P samples, containing phosphorous (a) 5.4 (b) 8.7, (c) 9.9 and (d) 12 at %, with temperature in the range of 300 K to 800 K.

The magnetization decreases continuously with temperature for all these four samples. However the sample containing 12 at.% phosphorous shows a slight increase in magnetization at two intermediate temperatures before the magnetization finally reduces approximately to zero at about 700 K. In the as-deposited samples magnetization at room temperature

steadily decreases from 27 emu/g (for 5.4 at.% phosphorous sample) to 6.25 emu/g (for a sample containing 12 at.% phosphorous) as the phosphorous content increases. The cooling curves in all the cases rise at about T_c of crystalline nickel (631 K), which are almost identical in shape. The final values obtained after cooling to room temperature are . 45.5, 37.5, 35 and 31.2 emu/g respectively for samples (a), (b), (c) and (d) respectively.

The systematic decrease in the final value of magnetization when the sample is cooled to room temperature is due to the decreasing content of crystalline nickel in the equilibrium mixture of Ni + Ni₃ P which is formed when the samples are heated beyond about 630 K. However, the temperature at which the transformation to equilibrium takes place has also been observed by the change in resistivity with temperature, i.e., the resistivity vs. temperature curve always show a sudden change in resistivity at all compositions of the sample right from 5.4 at.% phosphorous to 21.5 at.% phosphorous (the whole composition range studied) i.e. for samples containing less than 12 at.% as well as more than 12 at .% phosphorous at the temperature of formation of equilibrium phase.

6.2.2 The Annealing Behaviour of the Magnetization Of Amorphous Ni-P System

The Ni-P samples containing more than 12 at .%

phosphorous have been observed to contain amorphous phase as evident from the studies under electron-microscope and X-ray diffraction reported in chapter 4. It is further confirmed by the magnetization studies with temperatures, indicating some significant changes in the trend observed in sample containing 12 at.% phosphorous from those containing lesser phosphorous, but it was not clear enough. However, the onset of this new behaviour has been associated with the presence of amorphous phase and its crystallization. In this section, the observed changes in magnetization with temperature in different samples containing greater than 12 at.% phosphorous have been reported together without distinguishing the samples in a mixed micro-crystalline-amorphous states from those in fully amorphous state. But it should be remembered that the extent of crystallization observed in a sample of mixed state will depend on the amount of amorphous phase.

Fig.6.5(a) and 6.5(b) show the magnetization vs temperature behaviour of Ni-P samples containing (a) 13.0 at.% and (b) 15.0 at.% phosphorous respectively in the temperature range of 300 K to 800K. The slight increase in magnetization observed at intermediate temperature in the 12 at.% phosphorous sample, can now be clearly seen as two broad peaks in the temperature range (460 K-620K) and (630 K-700K) in 13 at.% phosphorous sample and (480K-580K)

in the 15 at.% phosphorous sample. The cooling curves are not shown. Samples (a) and (b) give values 28.5 and 23.5 emu/g respectively, when cooled to room temperature.

Fig.6.5(c) and 6.5(d) shows the variation of magnetization with temperature containing 16.4 at .% and 17.2 at .% phosphorous respectively in the temperature range of 300K-800K. The two peaks in magnetization can still be clearly seen in both these figures but initial magnetic moment of the as-deposited sample has now been decreased to a small paramagnetic value of 0.6 emu/g in the sample containing 17.2 at .% phosphorous,. Cooling curves are not shown in the figure, however, the magnetic moment values, for the two samples containing 16.4 and 17.2 at .% phosphorous, are 20.5 and 18.75 respectively, when cooled to room temperature.

Fig.6.5(e) and 6.5(f) show the change in magnetization with temperature in the range of 300 K to 800 K for Ni-P samples having 19.7 and 20.3 at. .% phosphorous respectively. In the former sample the two peaks appearing have come relatively closer, while in the latter sample with 20.3 at .% phosphorous, the second peak has become higher than the first one. Cooling curves are not shown; the magnetic moments of the samples containing 19.7 at .% and 20.3 at.% phosphorous are 12.9 and 11.1 emu/g respectively, when cooled to room temperature.

Fig.6.6 shows the magnetization behaviour of a non-ferromagnetic sample with 23.5 at .% phosphorous carried

out in the temperature range of 300 K-800K. The sample magnetization at 300 K (room temperature) in the as-deposited state is 0.006 emu/g at a 5 K Oe magnetic field, and displays only one hardly observable peak in the temperature range of 600 K - 690 K. The appearance of a single peak can be explained on the basis of only one phase transformation and the amorphous phase is stabilized upto a temperature of about 590 K; after which the sample passes over to the mixture of equilibrium phases of Ni + Ni₃P at about 620 K, without going through any non-equilibrium intermediate transition. The temperature range over which Ni + Ni₃P formation takes place and the height of the magnetization peak depends upon the rate of heating.

Annealing behaviour of Ni-P samples containing phosphorous from 12 to 23.5 at.% is shown in fig.6.7 on the same graph for the purpose of comparison, but the behaviour during cooling is not shown. As in the case of samples with less than 12 at .% phosphorous (Fig.6.4), the magnetization of the samples in the as-deposited state, decreases continuously from 6.2 to 0.006 emu/g with the increase of phosphorous. The samples are paramagnetic in their as deposited state with phosphorous content of 17.2 at .% and above. The peaks in magnetization which are first visible in the sample of 12.0 at .%, phosphorous becomes more prominent,

and as two distinct peaks in the intermediate phosphorous range; but with increasing phosphorous content these peaks come closer and finally merge into a single peak, which almost disappears as the phosphorous content reaches 23.5 at. %P.

The change in room temperature magnetization in Ni-P sample containing 15 at. % phosphorous when the samples were cooled from intermediate temperatures before the completion of equilibrium transformation are shown in fig.6.8(a). At the first step, the samples which had initial magnetization of 2.76 emu/g at 300 K is heated from 300 K to 460 K and then cooled to room temperature (300 K) with magnetization value rising to 4.75 emu/g. At the second step the sample is heated from 300 K to 525 K with magnetization dropping to 0.7 emu/g. The sample is then cooled to room temperature with the magnetization value 9.25 emu/g. At the third step the sample was heated from 300 K to 568 K and cooled again to temperature 300 K with magnetization value 12.5 emu/g. Finally the sample was heated from room temperature to 810 K where the magnetization has dropped to 0.05 emu/g. On cooling to room temperature, the magnetization value finally increases to 23.25 emu/g.

The heating has been carried out at the same rate of 4.6 K/minute at all steps.

Fig.6.8(b) shows the similar change in room temperature magnetization of Ni-P sample containing 17.2 at.% phosphorous when cooled from intermediate temperatures. At the first step, the sample which had a initial magnetization of 0.595 at room temperature, has been heated to 484 K and is then cooled to room temperature, i.e. 300 K with magnetization value increasing to 1.85 emu/g. At the next step the sample is heated from 300 to 536 K with magnetization dropping to 0.41 emu/g. The sample was cooled back to 300 K when magnetization is measured as 4.3 emu/g. At the third step the sample heating is done from 300 K to 585 K, the magnetization value is just, at the verge of increasing from lowest point, 0.48 emu/g. This sample on cooling to room temperature exhibits 8.54 emu/g magnetization. At the fourth step the sample heating has been done upto 614 K, with the magnetization value dropping to 0.3 emu/g, while the sample when cooled to room temperature gives magnetization value 15 emu/g. Finally the sample is heated from 300 K to 746 K with magnetization value only 0.27 emu/g and on cooling to room temperature again rises to a large value, i.e. 20.80 emu/g in this sample. The magnetization vs temperature behaviour of Ni-P sample containing 19.6 at.% phosphorous has been shown in fig.6.8(c) when the sample was cooled from several intermediate temperatures. At the first step, the sample

which is initially paramagnetic at room temperature, was heated to 495 K, but the sample remained non-magnetic. The sample was then cooled to room temperature, with an almost zero value of magnetization. It indicates that there has been no change in the non-ferromagnetic amorphous state of the sample. At the second step, the sample heating is done from 300 K to 570 K, the sample shows a magnetization of 0.60 emu/g. This sample when cooled to room temperature shows a magnetization of 3.11 emu/g. At the third step the sample is heated from 300 K to 600 K, the magnetization is reduced to 0.30 emu/g. The sample, on cooling to room temperature, shows a magnetization of 8.80 emu/g. The rate of heating of the sample is kept constant at 4.6 K/minute.

The increase in magnetization of the sample with phosphorous content 21 at.% when cooled from intermediate temperatures has been shown in fig.6.8(d). At the first step, the sample is heated from 300 to 570 K, the initial magnetic moment, which was about zero, remains the same. The sample on cooling to 320 K gives a magnetization value of 0.27 emu/g. At the second step, the sample heating is done upto 618 K starting from 320 K, with magnetization value decreasing to 0.08 emu/g. When the sample is cooled from 618 K to 300 K, magnetization increased to 6.8 emu/g. Finally the sample is heated to 800 K, giving 0.085 emu/g

magnetic moment and when cooled to 320 K again, the magnetization increases to 10.30 emu/g. The rate of heating was kept constant at 4.6 K/minute.

The variation in temperatures T_{f1} and T_{f2} at which the first and second magnetic peaks have been observed respectively with an increase in phosphorous content is shown in fig.6.9. T_{f1} may be identified as the temperature at which amorphous phase starts to undergo an intermediate reaction. T_{f2} may be related to the temperature at which the formation of equilibrium phases starts. T_{f1} although has a tendency to increase with increasing phosphorous contents but essentially remains constant upto about 17 at.% phosphorous. Beyond this level T_{f1} appears to rise more abruptly. The amorphous phase appears to remain stable upto about 443 K-473K in samples with upto 17 at.% phosphorous but remains stable even upto 503 K when phosphorous content is more. 17 at.% phosphorous is the composition at which as-deposited sample becomes almost paramagnetic. T_{f2} shows a weak tendency to decrease with increasing phosphorous content, but essentially remains around 600 K. The changes in temperatures at which the maximum value of magnetic moments corresponding to the two magnetic peaks, have been observed with the phosphorous content of Ni-P samples containing more than 12 at.%, is shown in fig.6.10. The graph shows that T_{p1} increases with increasing phosphorous contents while T_{p2} has a tendency to decrease with phosphorous.

The magnetic moments at T_{p1} and T_{p2} with the variation of phosphorous content have been shown in fig.6.11 for different Ni-P samples. It can be seen that the peak value of the magnetic moment in the first peak decreases as compared to that of second one, which has a tendency to increase with an increase of phosphorous. Fig.6.12 shows the change in magnetization after reactions indicated by the first and second peak. In both the cases one finds an increase in the change in magnetization with an increasing phosphorous content of the sample. Since T_{p1} , the temperature at which the first peak appears, increases with phosphorous, one assumes the evolution of the same amount of phase having enhanced magnetic moment in the sample with increasing phosphorous contents, the observed magnetic moment will be less because of its appearance at higher temperature. In fact with increasing phosphorous content of the sample the change in magnetization at T_{p1} will depend upon (i) the amount of precipitated phase of higher magnetization in this intermediate complex reaction and (ii) the temperature of appearance of this peak, T_{p1} .

In the second case the observed increase in the magnetic moment with increasing phosphorous content b can be explained by the fact, that the temperature at which peak is observed, decreases. However, it is known that the amount of crystalline nickel, remaining after, will be less and less with increasing phosphorous in the equilibrium reaction mixture of $Ni + Ni_3P$, it will contribute to a

decrease in magnetization. It has already been pointed out that as the phosphorous content in the sample increases, the height of the first peak decreases and that of the second peak increases. Heights of the peaks become equal for a sample at about 19.75 at.% phosphorous and after that height of the second peak looks higher than the first, although the absolute magnitude is small. The peak disappears in the samples with phosphorous content exceeding about 21 at.% and the height of these peaks is expected to be small, because although crystallized nickel is coming out, ~~but~~ its amount is quite small in these samples containing high phosphorous. In 25 at.% phosphorous samples the amount of nickel coming out is believed to be zero.

It appears that in samples with phosphorous 12 to 20 at.%, the transformation of the as-deposited samples to equilibrium mixture is formed through an intermediate complex reaction. But for samples with more than 20.5 at% phosphorous, the amorphous phase is stable and persists to a much higher temperature. As a result, it gets converted directly into equilibrium phases without passing through any intermediate transformation.

6.3 RESISTIVITY CHANGES ON ANNEALING: RESULTS

The temperature dependence of electrical resistivity of amorphous metals is very different from that of

crystalline metals as it has been discussed in chapter-5 and the temperature coefficient of electrical resistivity may be positive or negative, depending upon the composition. This behaviour implies Matthiessen's rule ceases to be valid in the amorphous region, but the changes of resistivity with temperature will indicate the transformation temperatures and quantitative informations about different transformations taking place. The present study is an attempt to understand the correlation between observed resistivity change and the structural transformation of electroless Ni-P alloys. In order to study the irreversible changes in resistivity during the annealing process, measurements were carried out while heating the samples to various temperatures upto 773 K (500°C) and then cooling these samples to room temperature.

6.3.1 Annealing Behaviour Of Resistivity In Polycrystalline And Microcrystalline Samples

The changes in resistivity of Ni-P film containing less than 12 at.% phosphorous have been shown in fig. 6.13. The representative sample of this category, whose results are shown in the figure, contains 11 at.% phosphorous. The sample is thus polycrystalline or microcrystalline and contains more phosphorous in solution than is permitted at equilibrium as it has been observed during investigations under electron-microscope and reported in chapter 4.

The figure shows that the resistivity increases with temperature till around 400 K due to increased vibrations

but beyond this temperature the resistivity becomes steady till 460 K. There is a drop in resistivity in the temperature range of 470-520 K. The resistivity again starts increasing but there is another drop in resistivity in the temperature range from 650 to 690 K. It is noteworthy that the resistivity remains quite steady also between 520 and 650 K. The initial drop in resistivity may be attributed to a stress relaxation in the films but then, the increase in resistivity with temperature has not been noticeable between 520 and 650 K. It may be due to balancing effect of lowering of resistivity by the grain growth in microcrystalline film. At a still higher temperature of 650 K the precipitation of Ni_3P may have been responsible for the sizable reduction of resistivity. The resistivity plotted in this fig.6.13 and other similar figures to be presented in this section is normalized with respect to the resistivity at ambient temperature. The changes in normalized resistivity while cooling has also been shown in fig.6.13.

6.3.2 Annealing Behaviour Of Resistivity In Amorphous Ni-P Alloys.

Fig.6.14(a) and (b) show the variation of resistivity with temperature while heating as deposited Ni-P samples containing 13.8 and 15.4 at.% phosphorous. These samples are in mixed state, as indicated in chapter 4, consisting of both microcrystalline as well as amorphous regions. The thermal behaviour of resistivity will be due to the changes taking place in both these regions while heating.

If one compares fig.6.14 with 6.13, one will be able to identify the features to be attributed solely to the amorphous regions of the film. In fig.6.14(a) the initial drop in resistivity in the broad temperature range between 380 to 500 K has been identified earlier with stress relaxation to the microcrystalline region. In addition now there will be atomic relaxation in the amorphous region of the film reducing its resistivity. Beyond this temperature the resistivity remains steady upto 562 K which may be explained in terms of grain growth in the microcrystalline regions. From 562 to 580 K there is quite a rapid drop in resistivity and again it happens in the temperature range between 586 to 630 K. The first drop at 562 K may be attributed to intermediate reactions in amorphous regions yielding transition phases and the second drop at 586 K shows the lowering of resistivity accompanying the final crystallisation reaction producing equilibrium phases in amorphous region and phosphide precipitation in microcrystalline regions. The cooling curve in resistivity is also shown in figure. Fig.6.14(b) shows qualitatively similar trends to those in fig.6.14(a) but the extent of resistivity drop during intermediate reaction and that during final crystallisation reaction are more here, because of an increased phosphorous content in the film resulting in larger amount of amorphous phase containing more phosphorous. The temperature of intermediate reaction has remained almost the same but the final crystallization

has started a little later above 600 K.

The samples containing more than 18 at .% phosphorous have been found to be amorphous and the resistivity changes of such films while heating will show the crystallisation sequence of amorphous alloy without getting mixed with changes taking place in microcrystalline region as it has been pointed out in relation to fig.6.14. The changes in normalized resistivity with temperature have been shown in 6.15(a), (b), (c), and (d) for films containing respectively 18.8, 19.7, 20.6 and 21.5 at.% of phosphorous.

In fig.6.15(a) one observe a lowering of resistivity at temperatures between 420 to 460 K but this lowering of resistivity is much less pronounced compared to that observed in microcrystalline or mixed films. In amorphous film there is atomic relaxation but the lowering of resistivity corresponding to this change is quite small and it becomes still less pronounced in films having a higher phosphorous content and consequently a higher disorder. In fig.6.15(b), (c) and (d) this effect has almost vanished. The second drop in resistivity in fig.6.15(a) is observed in the temperature range of 548 to 568 K just preceeding the major resistivity drop in the temperature range of 568 to 600 K. The second resistivity drop is quite distinct in respect of the slope of resistivity change as compared to that during the major drop, so the second drop in resistivity is attributed to intermediate reactions preceeding the the final reactions to equilibrium state corresponding to the major resistivity drop. The slope of resistivity change increases with the phosphorous content as it is observed in

fig.6.15(a), (b), (c) and (d). This slope indicates the stability with respect to intermediate reaction. In the crystallization of these amorphous samples a new feature of a resistivity drop after the major drop is observed and this feature has not been noticed in microcrystalline films. This drop is visible in the temperature range between 610 to 670 K in fig.6.15(a). It is present also in 6.15(b), (c) and (d). This small drop in resistivity has been attributed to grain growth in equilibrium phases.

6.4 DISCUSSION: THE CRYSTALLIZATION BEHAVIOUR

Since metallic glasses are thermodynamically unstable spontaneous transformation to stable phases occur at elevated temperature. In a Ni-P Phosphorous ^{amorphous alloy of the} ~~when dissolved~~ crystallization leads to finally a mixture of equilibrium phases of crystalline nickel and Ni_3P . Phosphorous when dissolved in nickel reduces its magnetic moment both in the crystalline and in amorphous state. In addition amorphous nickel has a lower magnetic moment as compared to that in its crystalline state (80). Thus, the crystallization of amorphous Ni-P alloys can be investigated by observing the change in magnetization in a Vibrating Sample Magnetometer as it has been done so extensively in present investigation.

The temperature dependence of electrical resistivity is another indicator conventionally used to investigate the sequence of crystallization (81).

A study of the results obtained from the change in magnetization in the crystalline and microcrystalline films containing 5 to 12 at .% phosphorous shows that there is

no discernible peak in magnetisation as shown in fig.6.4. But the resistivity behaviour of samples of this category as shown in fig.6.13 is marked by a resistivity lowering at around 470K and another major drop in resistivity at 644 K. The change in magnetization accompanying these resistivity drops is to such an extent that it is more than compensated by the decrease in magnetisation with an increase in temperature.

However, the resistivity measurement after cooling the sample clearly shows enhancement of magnetization of these samples.

The drop in resistivity observed at a relatively low temperature of 470 K may be attributed to stress relaxation and it does not reflect in the magnetization measurement. But the major drop in resistivity is associated with the precipitation of phosphides as can be seen from the X-ray diffraction patterns.

In earlier investigation of Maeda (20) it was observed that in polycrystalline films recrystallization occurs at 673 K along with precipitation of Ni_3P and some Ni_5P_4 and Ni_7P_3 . Although a faster grain growth may be taking place above 573 K causing the increase in height and reduction in width of (111) peak obtained in the X-ray diffraction pattern of a sample heated to 673K as shown in fig.6.3(b) but there is no evidence of any phosphide except Ni_3P . The enhanced height of (111) peaks at 400 K may also be attributed to the development of (111)

fiber texture as observed by Graham et.al (17).

It also may be pointed out that the present study finds no basis in the assumption of Albert et al that about 60 percent of phosphorous present is in the form of non-magnetic Ni_3P in the as-deposited state. Thus, the polycrystalline and microcrystalline nickel-phosphorous alloy containing less than 12 at.% phosphorous undergoes the following changes on heating.

1. Stress relaxation in the film causing a lowering of resistivity at around 450 K.
2. Phosphide precipitation from super-saturated f.c.c. nickel and its grain growth at around 650 K causing major drop in resistivity but no corresponding peak in magnetization.

In the films containing more than 12 at.% phosphorous the magnetization measurement has shown two peaks as given in fig.6.5(a), (b), (c) and (d). These samples contain less than 18 at.% phosphorous. It may be remembered that in chapter 4 it has been claimed that samples containing upto 14 at.% phosphorous remain microcrystalline. But the evidence of two magnetisation peaks indicate the presence of amorphous phase in the sample containing 12 at.% phosphorous which might have escaped the detection by electron microscopy. Also, the uncertainty in the determination of chemical composition of thin films prepared for electron-microscopy has made it impossible to determine the composition limit of microcrystallinity by this technique. But magnetization measurements have been done on thick samples and its composition is fairly accurately determined. So 12 at.% phosphorous

may be taken as the limit of stability of microcrystalline structure within the limit of detection of this experiment.

The peaks appearing in curve showing thermal behaviour of magnetization in films containing phosphorous exceeding 12 at.% may be attributed to the amorphous phase present in these films because the peaks are absent in polycrystalline and microcrystalline films. The evidence from resistivity behaviour as shown in 6.14(a) and (b) also confirms the presence of amorphous phase in films containing 13.8 and 15.4 at.% phosphorous by showing addition of features not present in polycrystalline or microcrystalline films. But these films are not totally amorphous because the characteristics observed in resistivity behaviour of microcrystalline are also present. But in films containing above 18at.% phosphorous there is no evidence of the presence of microcrystallinity. The conclusion of the earlier workers like Graham et al (17), Albert et al(19), Maeda (20) and Goldonstain et al (16) that even a film containing 12 at.% phosphorous is amorphous does not find confirmation in the present study. However, 12 at.% phosphorous is the composition at which amorphous phase start appearing in films.

The magnetization behaviour of films containing 19.7 and 20.3 at.% phosphorous as given in fig.6.5(e) and 6.5(f) show the presence of two peaks as observed in samples in mixed state with lower phosphorous content. But the sample containing 23.5 at.% phosphorous has a single peak in its magnetization-temperature curve. yet the resistivity-temperature curve of samples containing 18.8 to 21.5 at.% phosphorous as given in 6.15(a) to (d) is distinctly different from those

obtained from samples in mixed state. From the change in resistivity with temperature, ~~there~~ appears to be changes taking place in four steps in the films while heating to cause a lowering of resistivity.

- 1) A minor lowering of resistivity at 420 K.
- 2) A more significant lowering of resistivity as compared to that in (1) but with a relatively smaller slope.
- 3) A sharp drop in resistivity at around 580-600°K to a 75% of its original value.
- 4) A 5-10 % drop in resistivity at around 650 K at a rate faster than (2) but much slower than(3).

If one looks for the changes in magnetization one finds that there are peaks in magnetization corresponding to changes in resistivity in step (2) and step (3) but there is none accompanying step (1) or step (4). If these observations are combined with the evidence of X-ray diffraction and selected area diffraction under electron microscope as given in 6.2(b) and 6.3 the step 1 can occur only due to some structural changes within the amorphous phase. There might be atomic relaxation or local ordering which will be detected by resistivity but not by any other technique employed.

Fig.6.2 (c) and 6.3(a) indicate that the step (2) corresponds to precipitation of almost pure crystalline nickel from the amorphous phase as it can be observed in the electron micrograph shown in fig.6.1(b). Crystalline nickel will also have a higher magnetization to result

in the first peak obtained in fig.6.5(a) to (f). Several higher phosphides may also form at this phase like Ni_5P_4 and Ni_7P_3 as reported by Maeda (20).

The SAD patterns obtained have (fig.6.2(d)) indicated the formation of such intermediate precipitates but the exact identity of these phosphides could not be determined because of their small amount and the occurrence of peaks from many of these phosphides at similar d-values.

The extent of the reaction involved in this step reduces with an increase in the phosphorous content of the amorphous film as it will be evident from the extent of resistivity drop for these step shown in fig.6.15. The observation of a single peak in the magnetisation curve of Ni-P film containing 23.5 at.% phosphorous may also indicate a total absence of this step at that composition. However, Randin et.al(58) in DTA of Ni-P has observed the absence of the first reaction step in crystalline at about 18 at.% phosphorous itself which is contradicted by the present results. It is quite possible that due to a reduced extent of the reaction of this step DTA could not detect its presence beyond 18 at.%.

Step(3) can be identified with final crystallization and transformation to stable phases. The films will not show the presence of any amorphous phase after this step as evident in fig.6.2(d). The content of these films as determined by X-ray diffraction analysis given in fig.6.3(a)

are crystalline Nickel and Ni_3P .

Since the remaining amorphous phase is undergoing crystallization there will be an increase in the magnetization of the films giving rise to second peak.

The last step in the sequence of crystallisation is difficult to understand as it has not been identified by any other probe than resistivity, it has to do something with internal structure of phases present after crystallisation.

At such a low temperature the solid state transformation to crystalline nickel by nucleation and growth may be resulting into highly deformed nickel due to volume changes associated with the process. It is also possible that the deformed nickel is undergoing recovery, if not recrystallization to give rise to lowering of resistivity. But the present study does not have any direct evidence for this explanation.

When the phosphorous content of the amorphous samples is increased, the extent of enhancement of magnetisation, at the first peak, increases as shown in fig.6.12 and the temperature at which the peak is observed increases. Thus the extent of precipitation of nickel from amorphous phase increases with increasing phosphorous and the temperature for this intermediate reaction is pushed to higher temperature. In other words, the amorphous phase becomes more stable vis-a-vis this intermediate reaction. At a phosphorous content of 23.5 at.% the amorphous phase is so stable that nickel comes out of the amorphous phase only during step (3) and step (2) is not observed

independently.

The starting temperature for the peak in magnetisation remains fairly constant up to about 18 at.% phosphorous as shown in fig.6.9 and corresponding magnetisation is fairly linear in this range as shown in fig.6.11.

This may be an indication that the composition of amorphous state and microcrystalline state remains the same in the mixed state, only their relative amount changes with the overall phosphorous content of the film. In absence of EDX facility this matter could not be probed further.

Towards the end of this investigation Bakonyi et al(62) kindly provided with the manuscript of their paper on this topic. There are points of similarity and differences of his results with the observations of the present investigation. He finds the crystallisation behaviour in films containing less than 20 at.% phosphorous to be distinctly different from those having greater than 20 at.% phosphorous. For films containing less than 20 at.% phosphorous, there is precipitation/segregation of nickel in the remaining amorphous matrix with increased phosphorous content. The present study has identified this as step 2. but Bakonyi plots the temperature for this transformation for a film containing 10 % phosphorous. The present study indicates that below 12 at.% phosphorous the films are microcrystalline and does not show this reaction at all. The film transforms to stable phases of almost pure nickel and Ni_3P simultaneously.

For films containing more than 20 at.% phosphorous, Bakonyi claims that initially the amorphous alloy transforms completely to Ni_5P_2 and crystalline nickel subsequently and Ni_5P_2 recrystallizes to Ni_3P . The present investigation does not confirm these observations. If the sequence of transformation given by Bakonyi is correct, there will be only one peak in magnetisation because in the second step crystalline nickel will be consumed by Ni_5P_2 to become Ni_3P , so there will be a dip in magnetisation. The present investigation of two peaks in magnetisation of ~~of~~ 20.3 at.% phosphorous as shown in fig.6.5(f) is at variance with the sequence of transformation according to Bakonyi et al.

6.5 SUMMARY

The changes in structure and the crystallization of amorphous films have been investigated in Ni-P alloys containing 5.4 to 23.5 at.% phosphorous, by electron microscopy, X-ray and selected area electron diffraction, magnetisation and resistivity measurements.

The polycrystalline and microcrystalline films containing less than 12 at.% phosphorous undergo a stress relaxation at around 450 K and subsequently, around 650 K the precipitation of Ni_3P reduces the resistivity markedly and enhances the magnetisation. In the amorphous films containing more than 18 at.% phosphorous there is a very small reduction of resistivity at around 420 K and attributed to atomic relaxation.

A continued heating shows a lowering of resistivity over a broad temperature range and a corresponding peak

in the magnetisation. At the end of this temperature range there is a sharp drop in resistivity and another peak in magnetisation to correspond with it.

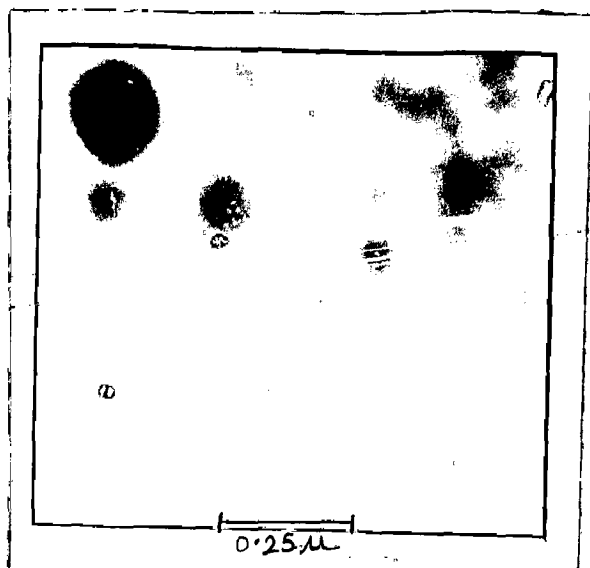
The former reaction taking place over a broad temperature range results in the precipitation of Nickel and its higher phosphides, the extent of this reaction reduces with increasing phosphorous content and it becomes non-existent in an alloy containing about 23.5 at.% phosphorous. The alloys with an intermediate phosphorous content of 12 to 18 at.% show a superposition of the characteristic reactions taking place in the micro-crystalline and the amorphous regions.

L I S T O F F I G U R E S

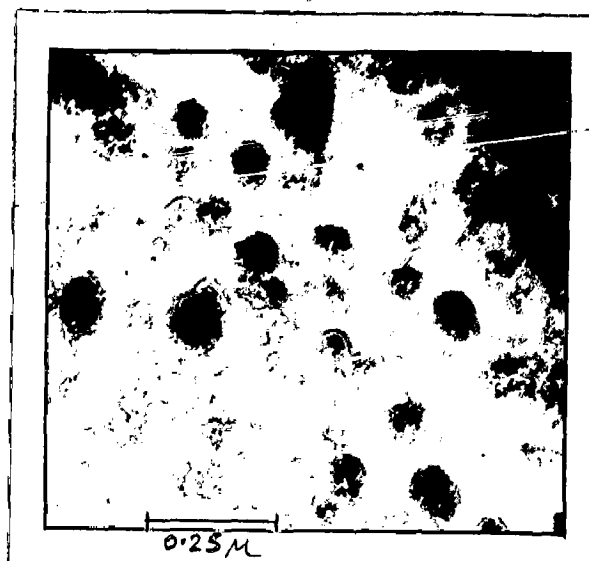
- 6.1 Microstructure of the electroless Ni-P sample III containing ^{about} 20 at.% P.
- (a) in the as-deposited state.
 - (b) when heated at 423 K for 2 minutes
 - (c) when heated at 618 K for 2 minutes
 - (d) when heated at 673 K for 2 minutes
- 6.2 SAD of the electroless Ni-P sample containing about 20 at.% P.
- (a) in the as-deposited state
 - (b) when heated at 423 K for 2 minutes
 - (c) when heated at 523 K for 2 minutes
 - (d) when heated at 618 K for 2 minutes
 - (e) when heated at 643 K for 2 minutes
- 6.3(a) X-Ray diffraction patterns of Ni-P sample-III containing 20 at.% phosphorous, heated for 30 minutes at (i) 473 K (ii) 573 K (iii) 673 K and (iv) 873 K
- (b) X-ray diffraction patterns of Ni-P sample I containing 12 at.% P, heated for 30 minutes at (i) 473 K and (ii) 673 K.
- 6.4 The variation of magnetization with temp.range 300K-780K containing 5.4, 8.7, 9.9 and 12.0 at.%P.
- 6.5 The variation of magnetization with temperature range of 300-800 K containing
- (a) 13 at.% P.
 - (b) 15 at.%P
 - (c) 16.4 at. %P.
 - (d) 17.2 at.% P
 - (e) 19.7 at.%P

- (f) 20.3 at.%P
- 6.6 The variation of magnetization with temperature range 300-800 K containing 23.5 at.% P.
- 6.7 The annealing behaviour of Ni-P samples containing phosphorous from 13.0 to 23.5 at.% .
- 6.8 (a) The variation of magnetization with temperature containing 15 at.% P.
- (b) Containing 17.12 at.% P.
- (c) Containing 19.5 at.% P.
- (d) Containing 20.7 at.% P.
- 6.9 Change in temperature at which I & II magnetic peaks appear, with the variation of P in the sample.
- 6.10 The variation of temperature corresponding to the two magnetic peaks with different phosphorous contents above 12 at.%.
- 6.11 The variation of magnetic moments corresponding to the magnetic peak temperature T_{p1} and T_{p2} with phosphorous above 12 at.%.
- 6.12 The change in magnetization after reactions indicated by I & II peak with increasing phosphorous.
- 6.13 The variation of P/P_{300K} with temperature in the range of 300-760 K containing 11.0 at.% P.
- 6.14(a) The variation of P/P_{300K} with temperature in the range of 300-760 K containing 13.8 at.% P.
- (b) Containing 15.4 at.% P.

- 6.15 (a) The variation of P/P_{300K} with temperature in the range of 300-760 K containing 18.8 at.% P.
- (b) Containing 19.7 at.% P.
- (c) Containing 20.6 at.% P.
- (d) Containing 21.5 at.% P.



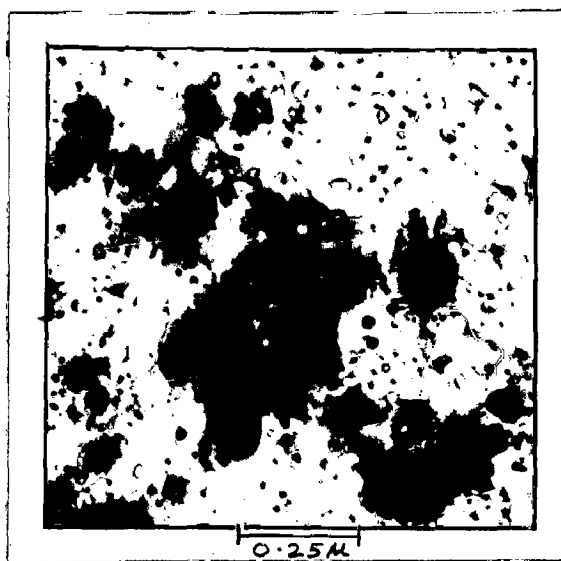
(a)



(b)



(c)



(d)

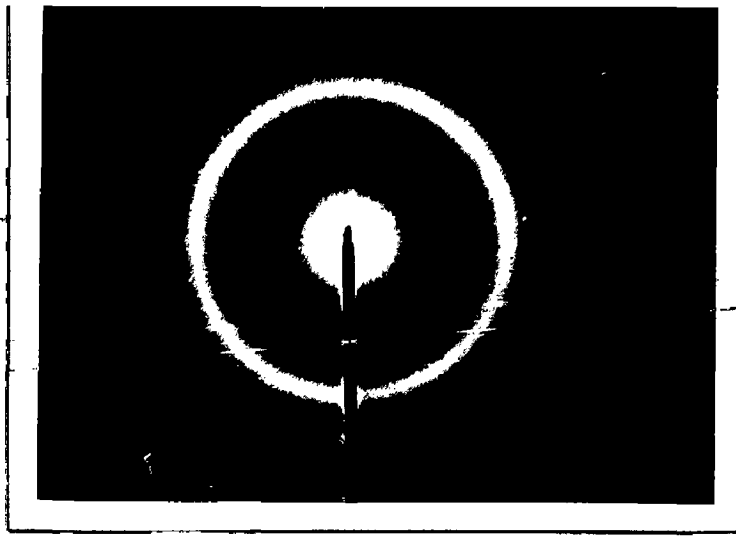
FIG. 6.1 MICROSTRUCTURE OF THE ELECTROLESS Ni-P SAMPLE III
CONTAINING 20 AT.% PHOSPHOROUS

(a) IN THE AS-DEPOSITED STATE

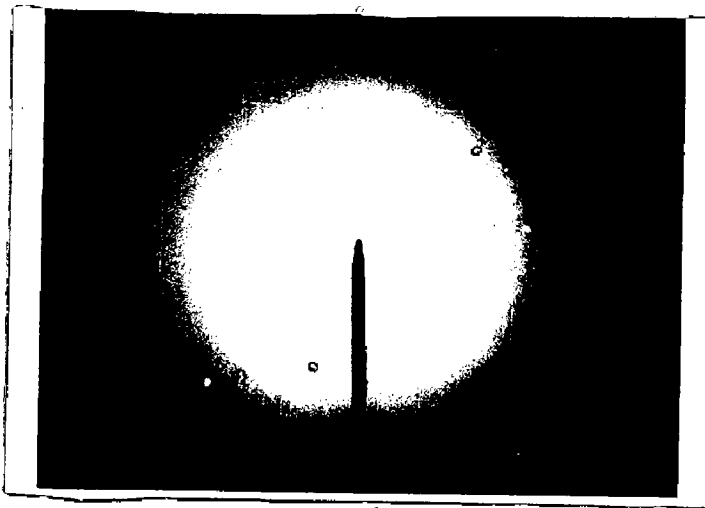
(b) WHEN HEATED AT 423 K FOR 2 MINUTES

(c) WHEN HEATED AT 618 K FOR 2 MINUTES

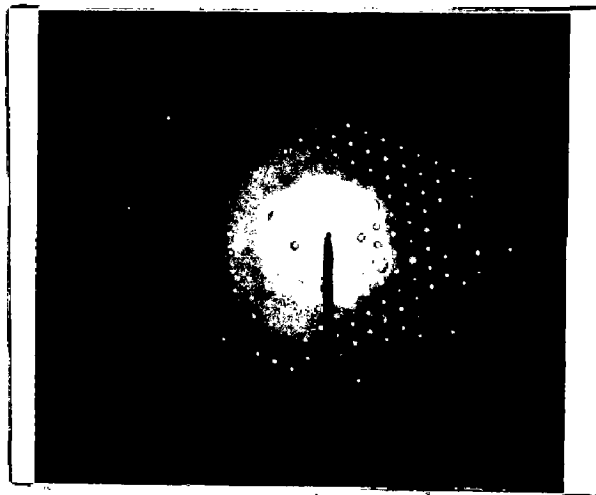
(d) WHEN HEATED AT 673 K FOR 2 MINUTES



(a)



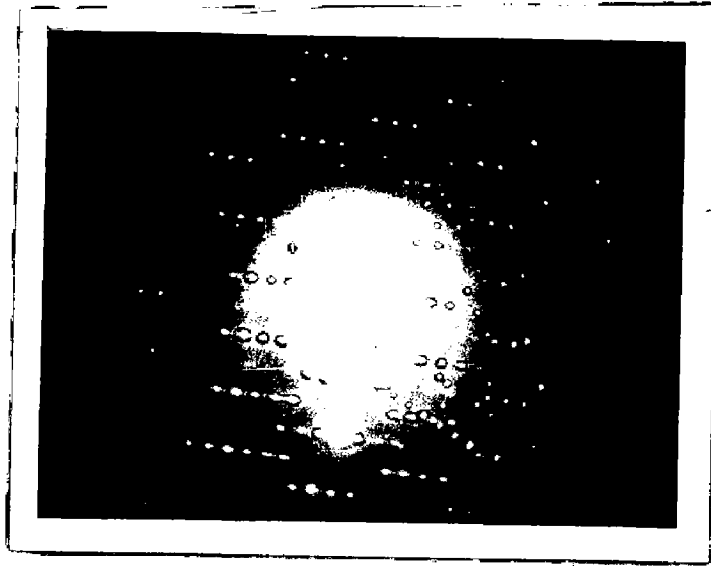
(b)



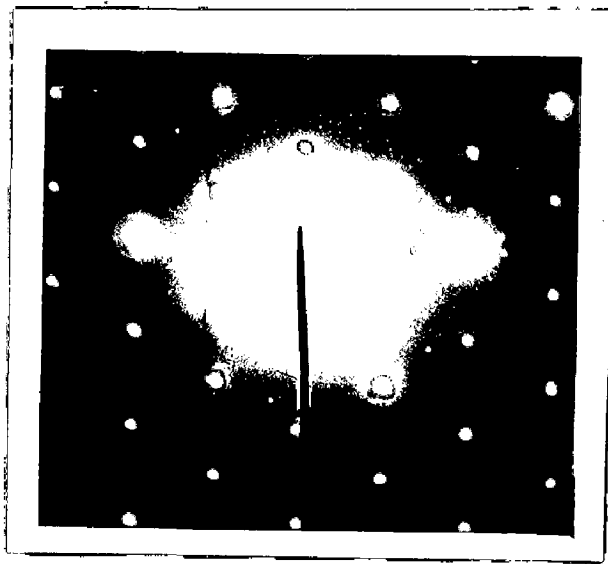
(c)

FIG. 6.2 SAD OF THE ELECTROLESS Ni-P SAMPLE CONTAINING ABOUT 20 AT. % PHOSPHORUS

- (a) IN THE AS-DEPOSITED STATE
- (b) WHEN HEATED AT 423K FOR 2 MINUTES
- (c) WHEN HEATED AT 573K FOR 2 MINUTES



(d)



(e)

FIG. 6.2 - SAD OF THE ELECTROLESS Ni-P SAMPLE III
CONTAINING ABOUT 20 AT. % PHOSPHOROUS

(d) WHEN HEATED AT 618 K FOR 2 MINUTES

(e) WHEN HEATED AT 643 K FOR 2 MINUTES

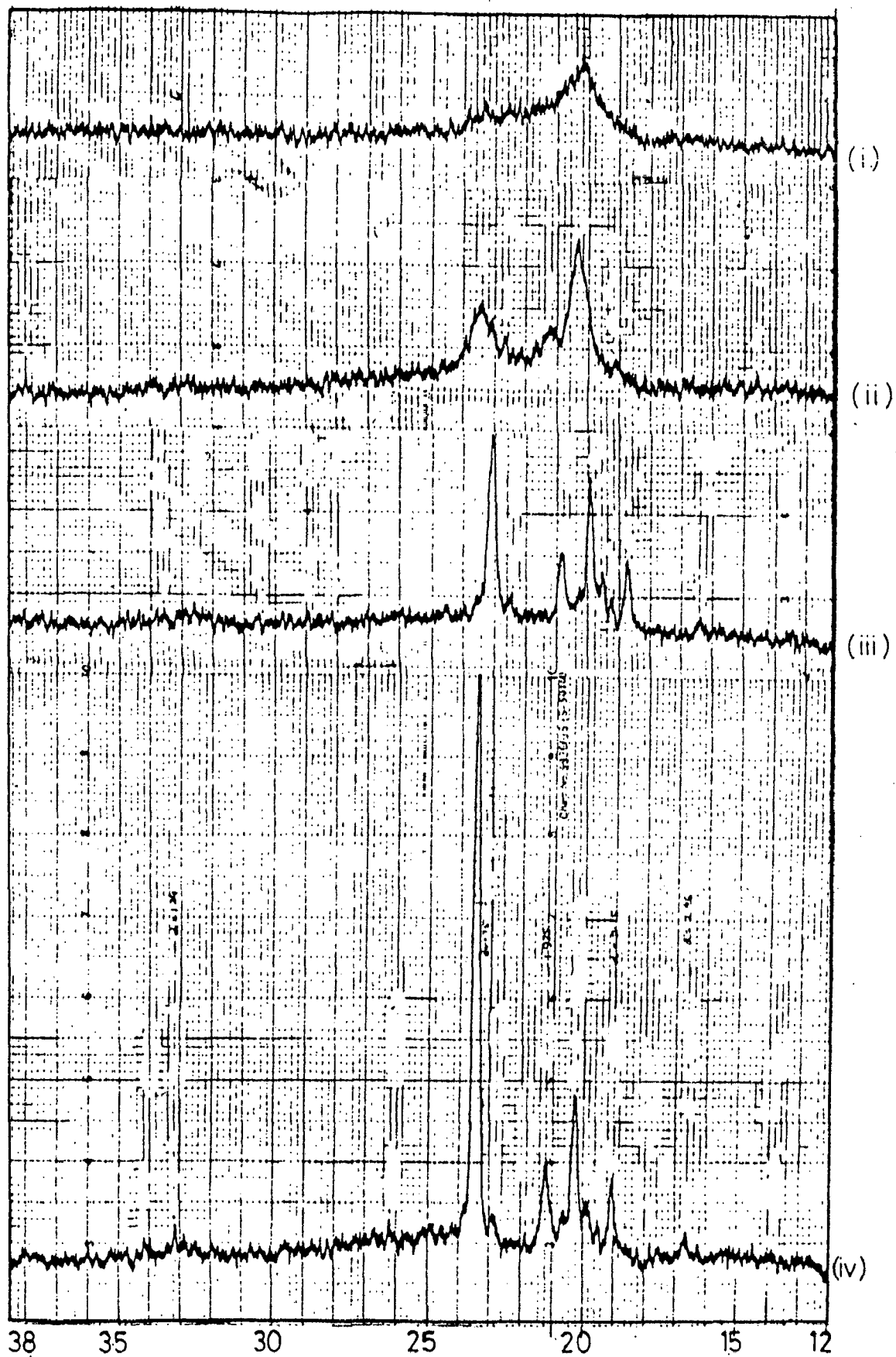


FIG.6.3(a) X-RAY DIFFRACTION PATTERNS OF Ni-P SAMPLE III CONTAINING 20 AT.% P, HEATED FOR 30 MINUTES AT (i) 473K (ii) 573K (iii) 673K AND (iv) 873K

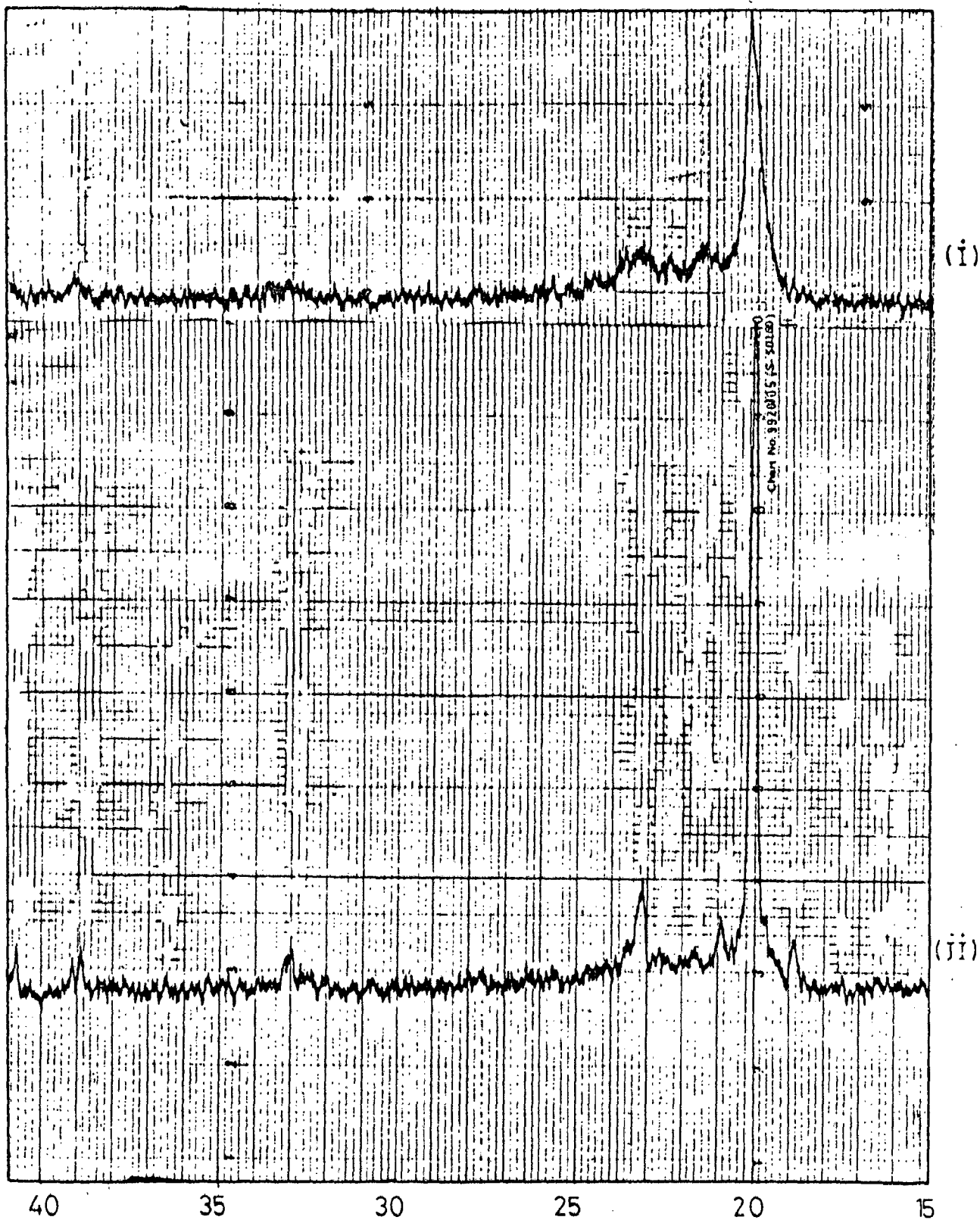


FIG. 6.3 (b) X-RAY DIFFRACTION PATTERNS OF Ni-P SAMPLE I CONTAINING 12 AT. % P, HEATED FOR 30 MINUTES AT (i) 473K AND (ii) 673K.

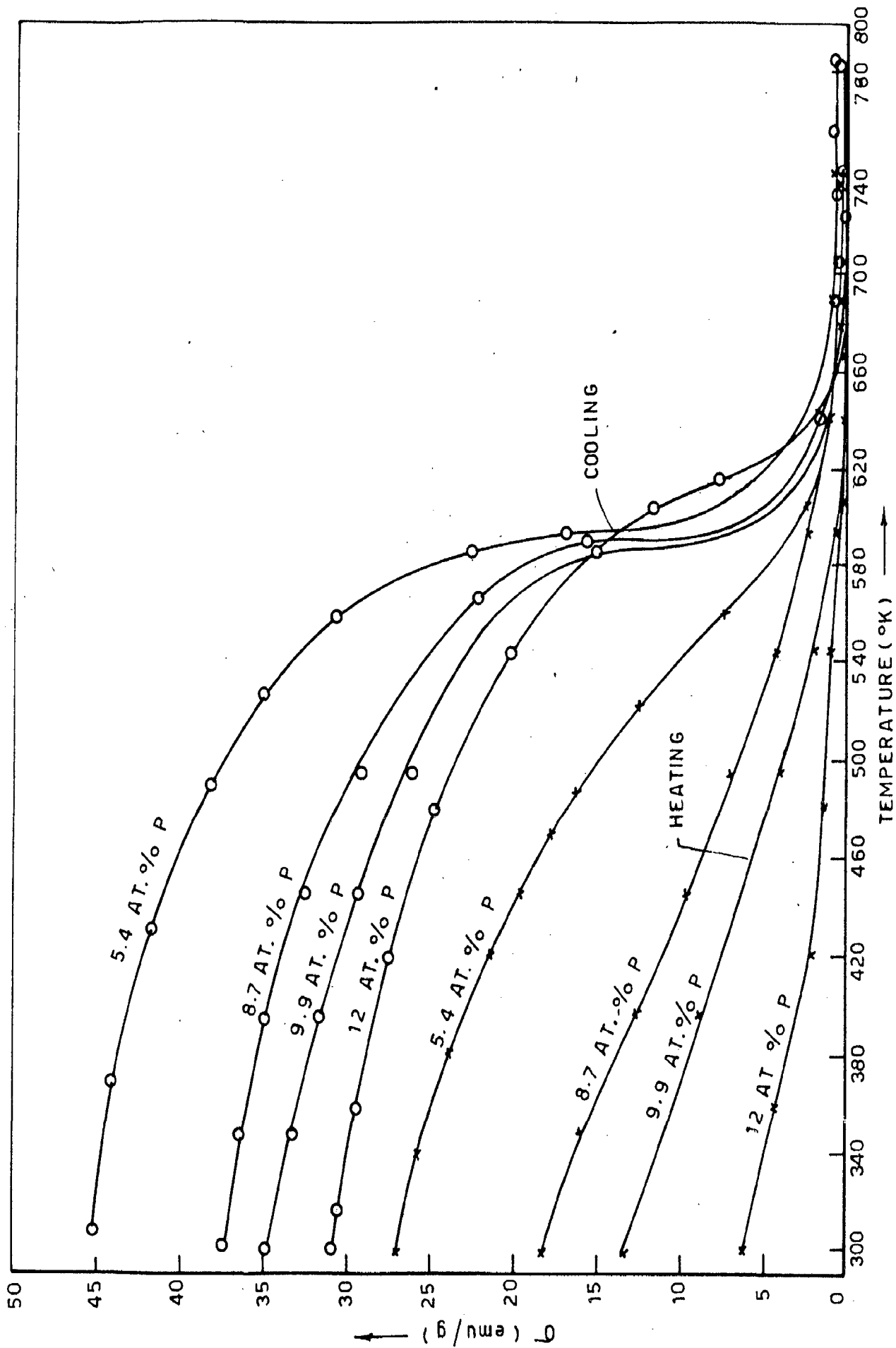


FIG. 6.4- THE VARIATION OF MAGNETIZATION WITH TEMPERATURE CONTAINING 5.4, 8.7, 9.9 AND 12.0 AT. % OF PHOSPHOROUS IN TEMPERATURE RANGE 300K-780K. THE COOLING CURVES ARE ALSO SHOWN IN THE FIGURE

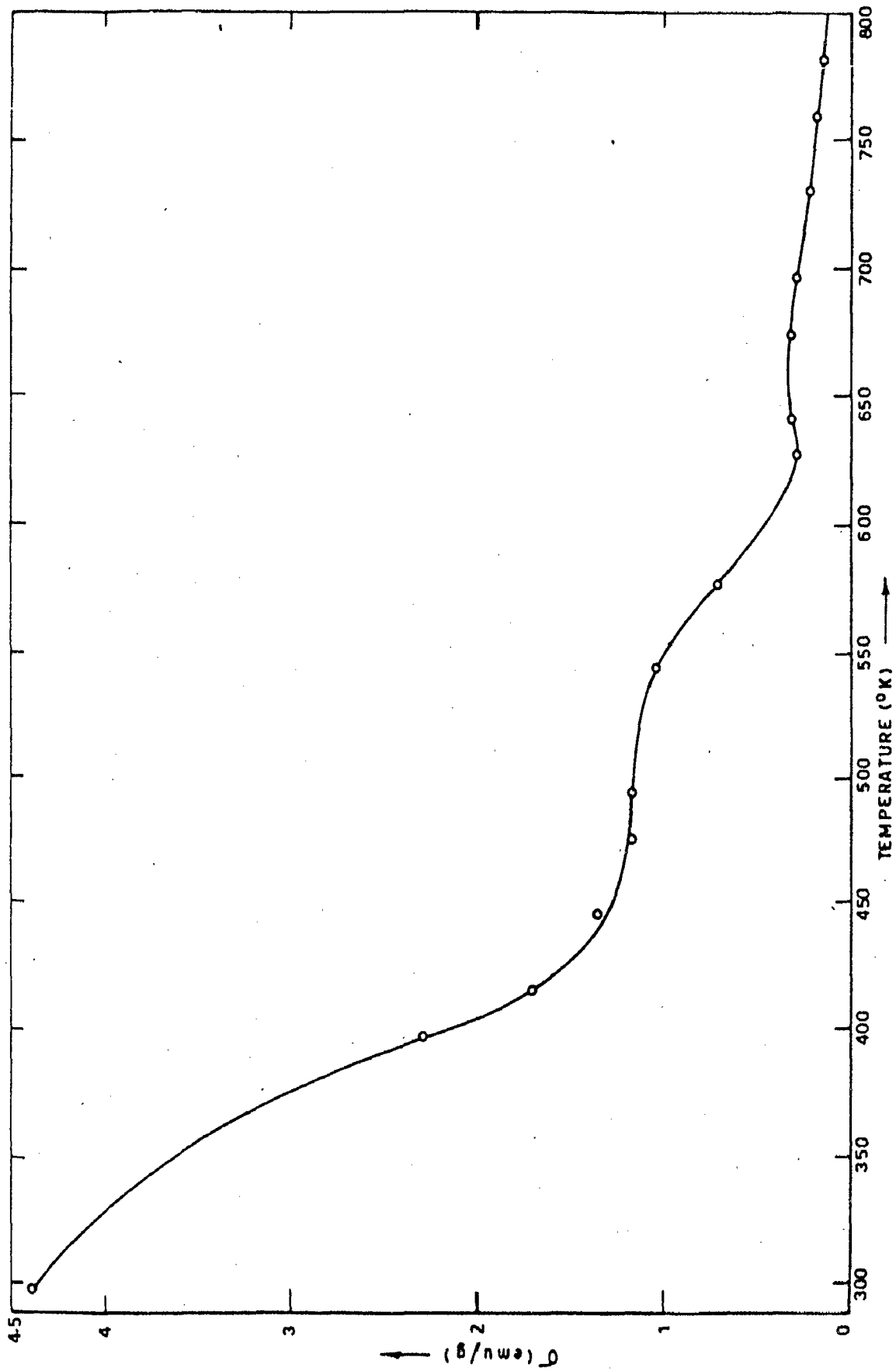


FIG. 6.5(a) - THE VARIATION OF MAGNETIZATION WITH TEMPERATURE OF THE Ni-P SAMPLE CONTAINING 13 AT. % PHOSPHOROUS IN THE TEMPERATURE RANGE 300K TO ABOUT 800K. THE COOLING CURVE IS NOT SHOWN IN THE FIGURE. THE VALUE OF MAGNETIZATION AFTER COOLING IS 28.5 emu/g

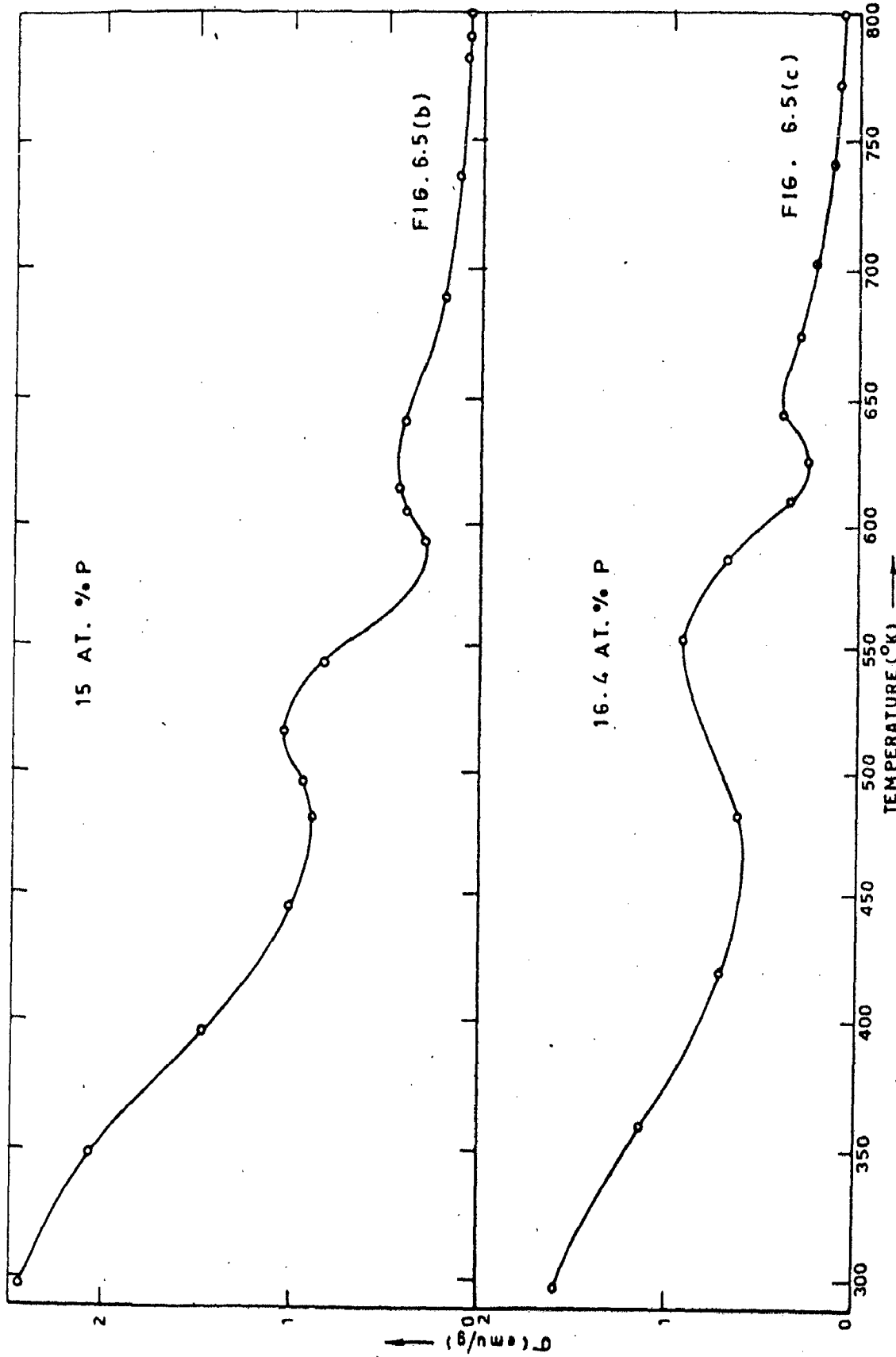


FIG. 6.5 (b),(c) - THE VARIATION OF MAGNETIZATION WITH TEMPERATURE OF NI-P SAMPLES CONTAINING 15 AND 16.4 AT. % PHOSPHOROUS IN THE RANGE OF TEMPERATURE 300K-800K. THE COOLING CURVES ARE NOT SHOWN; THE VALUES OF MAGNETIZATION AT 300 K AFTER COOLING ARE 23.5 AND 20.5 emu/g RESPECTIVELY

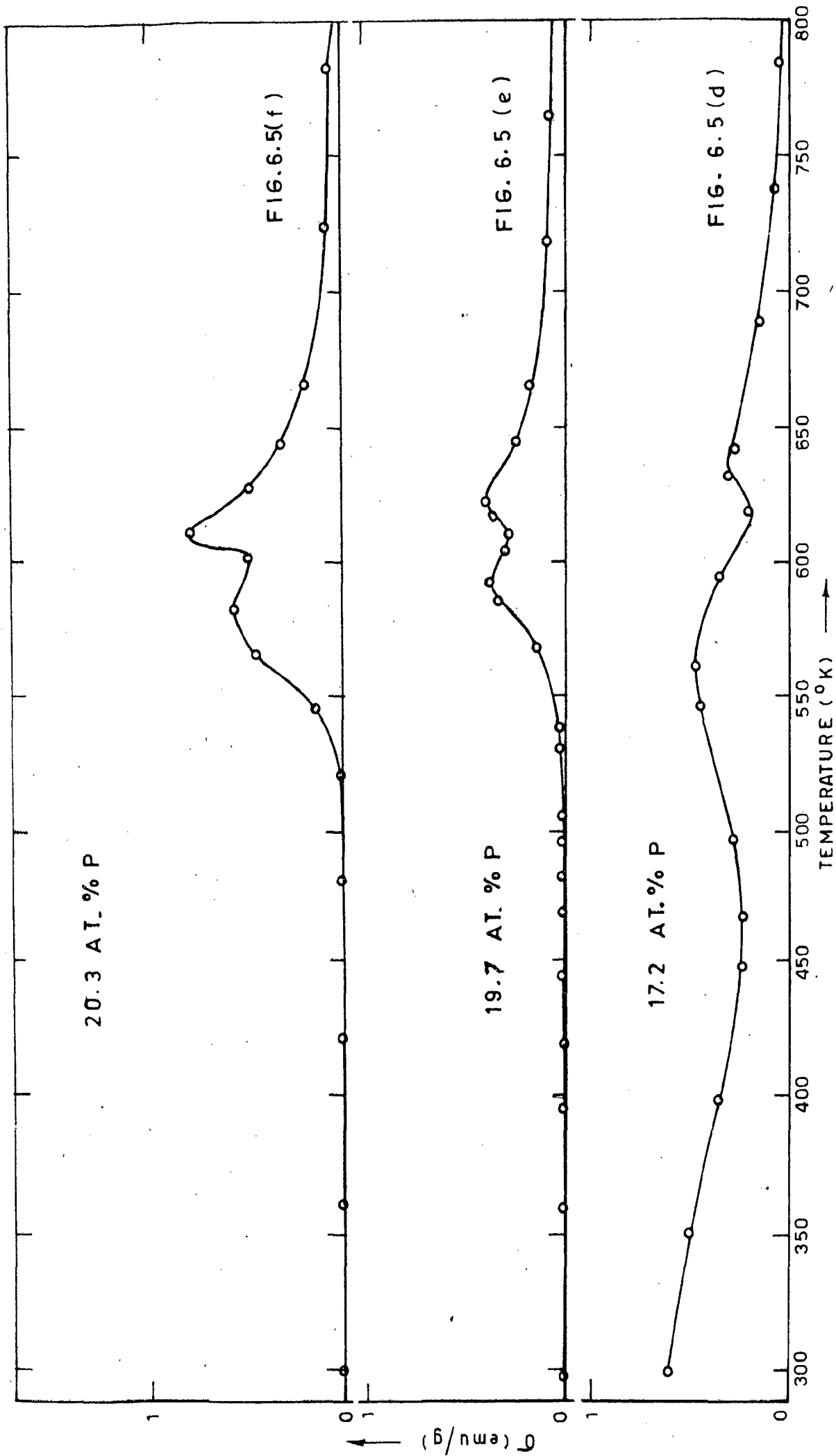


FIG. 6.5(d),(e),(f) - THE VARIATION OF MAGNETIZATION WITH TEMPERATURE, IN THE RANGE OF 300K-800K CONTAINING PHOSPHOROUS 17.2, 19.7 AND 20.3 AT.% RESPECTIVELY. COOLING CURVES ARE NOT SHOWN; THE MAGNETIZATION AFTER COOLING TO 300K ARE 18.75, 12.9 AND 11.1 emu/g RESPECTI

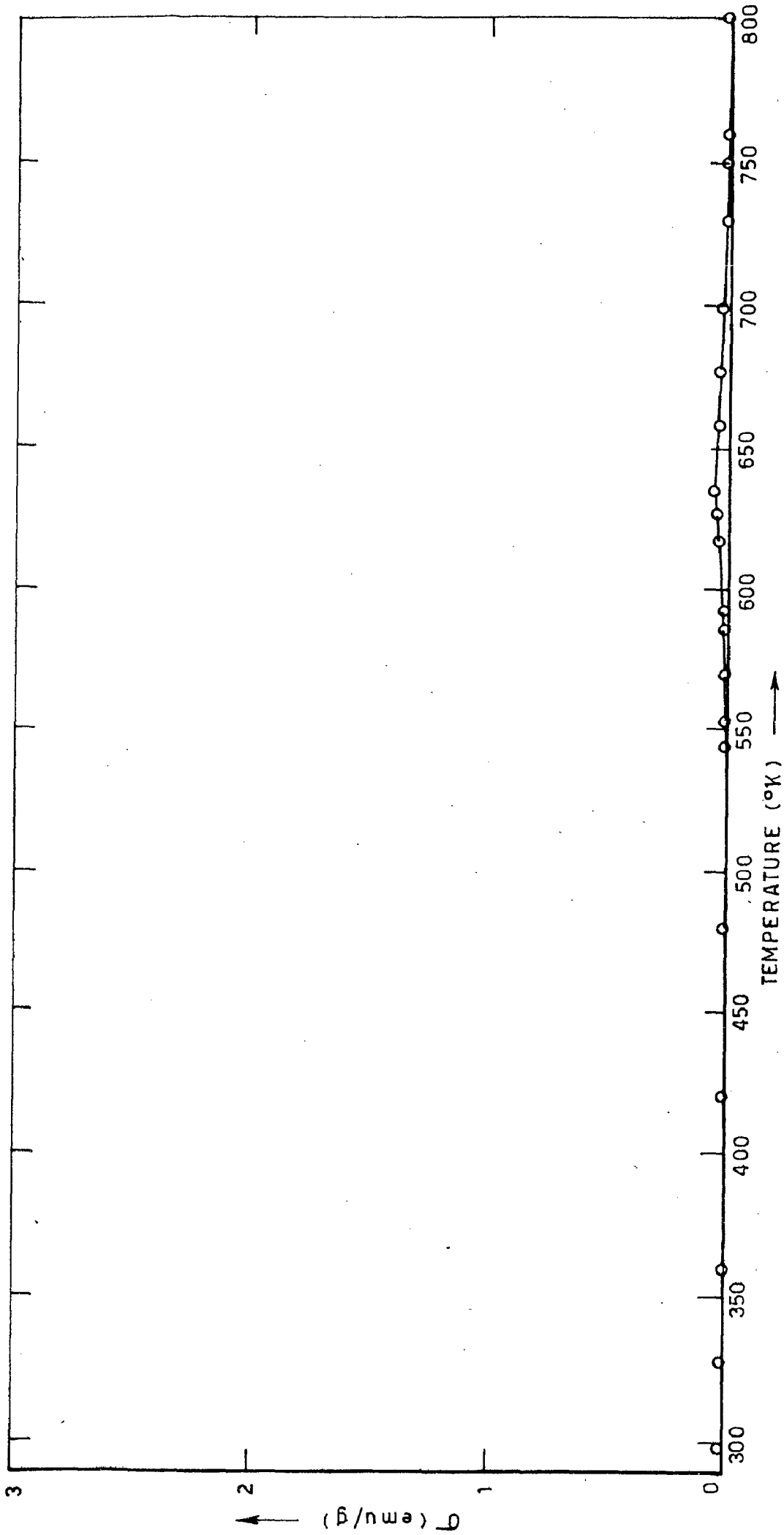


FIG. 6.6 - THE VARIATION OF MAGNETIZATION WITH TEMPERATURE OF THE SAMPLE CONTAINING 23.5 AT. % PHOSPHOROUS IN THE TEMPERATURE RANGE OF 300 K TO 800 K. THE INITIAL AS-DEPOSITED VALUE OF MAGNETIZATION IS 0.006 emu/g AT 300 K. THE COOLING CURVE IS NOT SHOWN IN THE FIGURE; THE MAGNETIZATION VALUE AFTER COOLING TO 312 K IS 3.3 emu/g

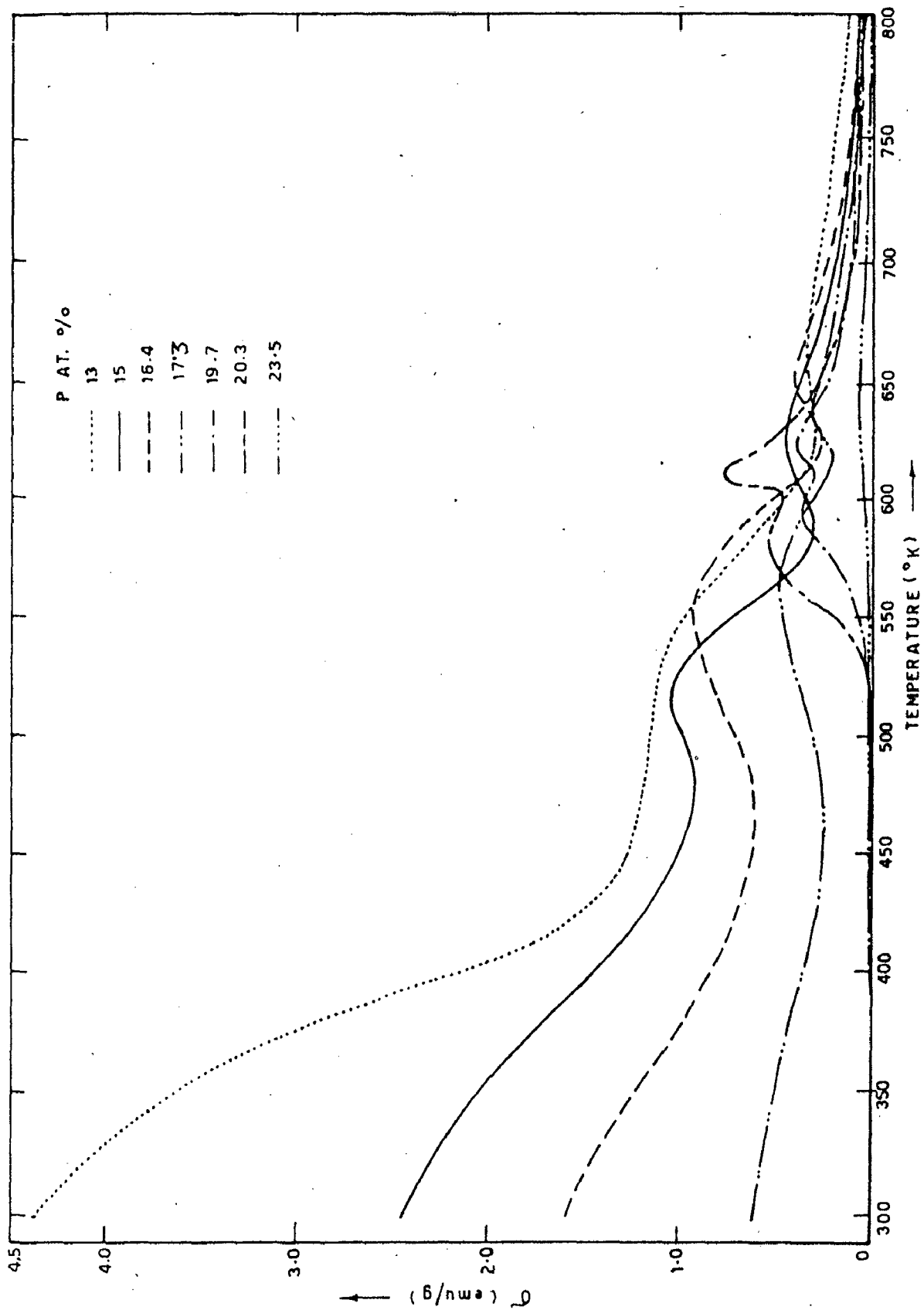


FIG. 6.7 - THE ANNEALING BEHAVIOUR OF Ni-P SAMPLES CONTAINING PHOSPHORUS FROM 13.0 TO 23.5 AT. % SHOWN ON THE SAME GRAPH FOR THE PURPOSE OF COMPARISON

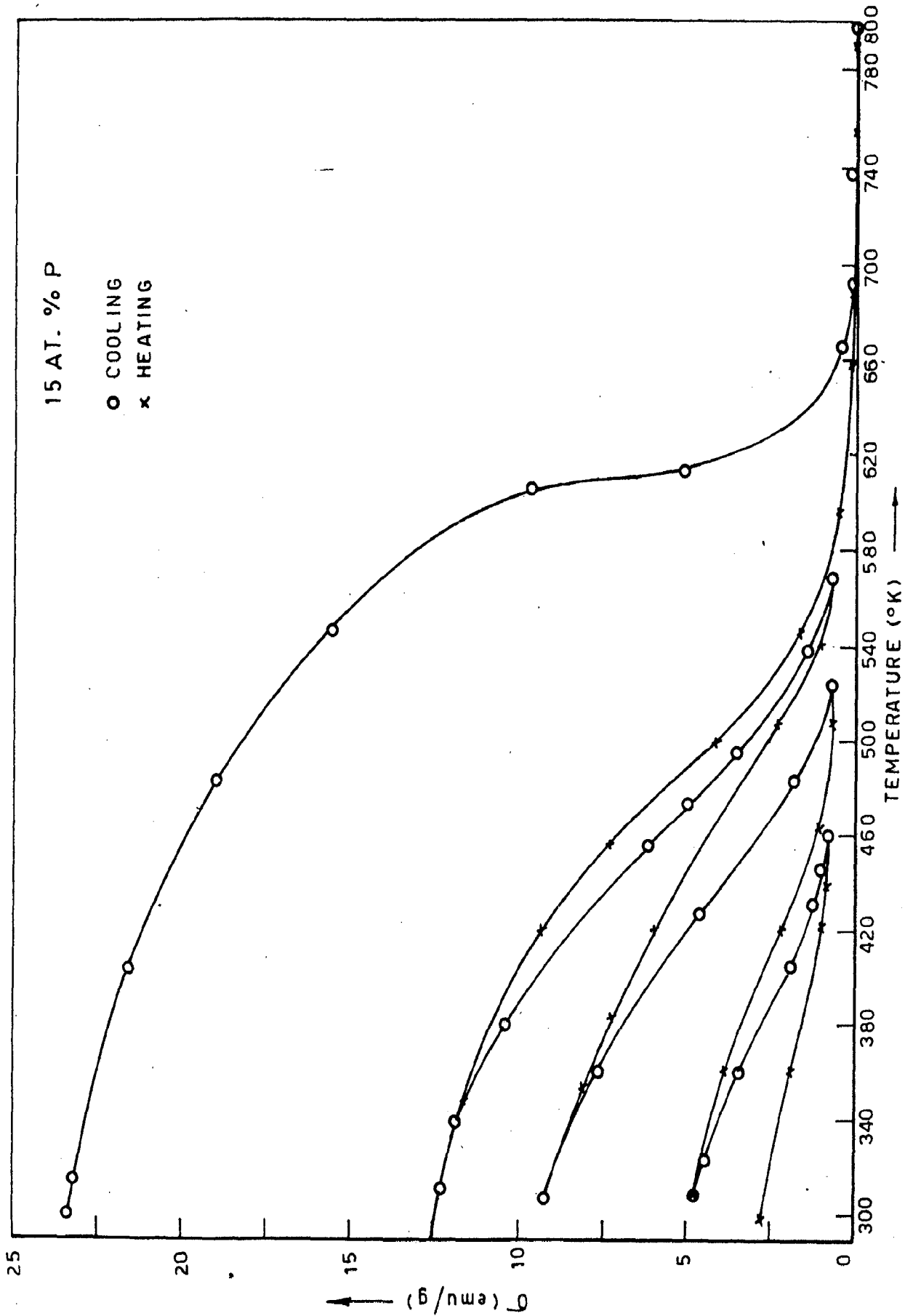


FIG. 6.8(a) - THE VARIATION OF MAGNETIZATION WITH TEMPERATURE OF A SAMPLE CONTAINING 15 AT.% PHOSPHOROUS WHEN THE TEMPERATURE IS INCREASED IN STEPS, E. G., TO 460 K, 525 K, 568 K AND FINALLY TO 810 K.

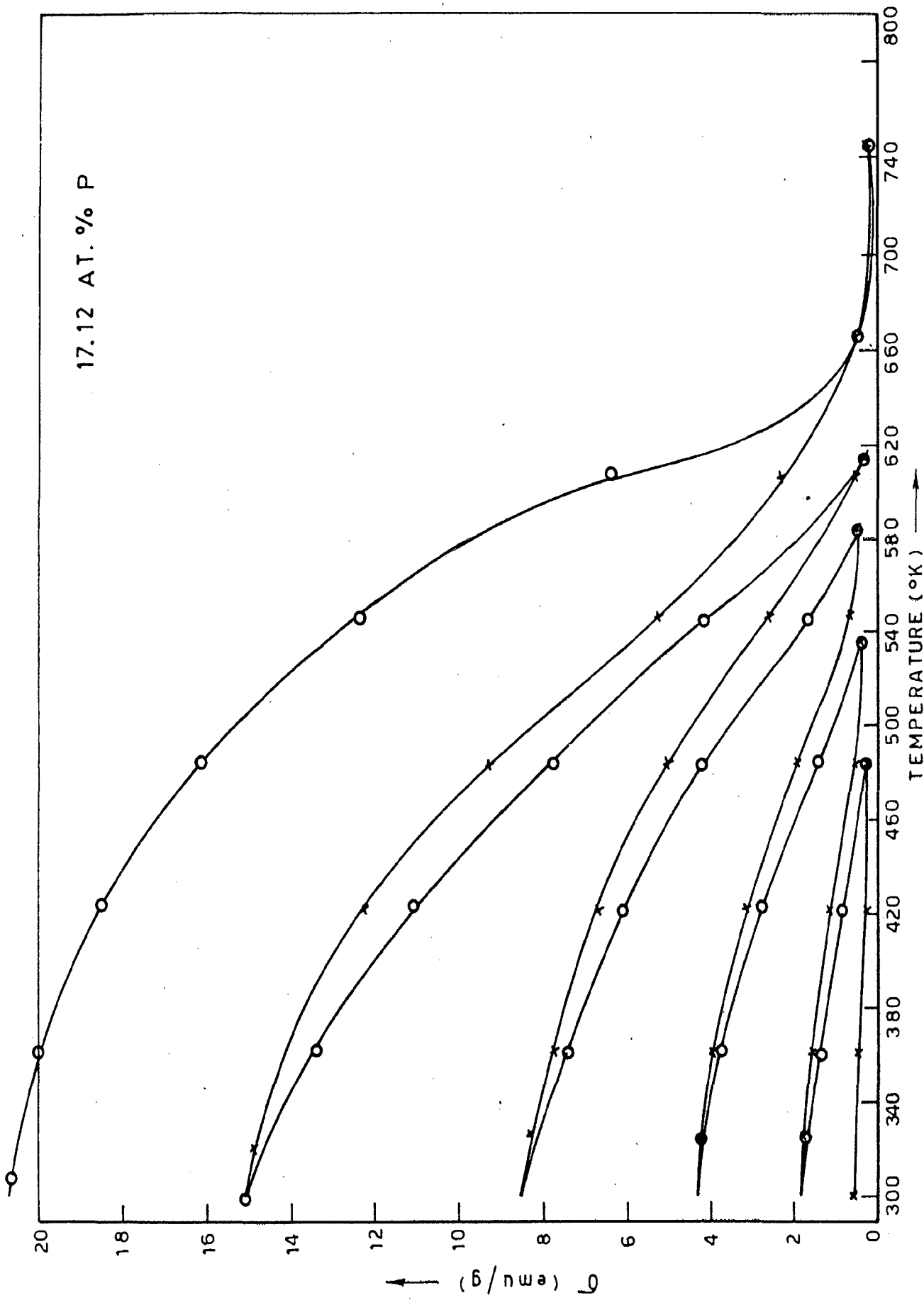


FIG. 6.8 (b) THE VARIATION OF MAGNETIZATION WITH TEMPERATURE, OF Ni-P SAMPLE CONTAINING 17.12 AT. % PHOSPHOROUS, WHEN IT IS HEATED AND COOLED IN STEPS.

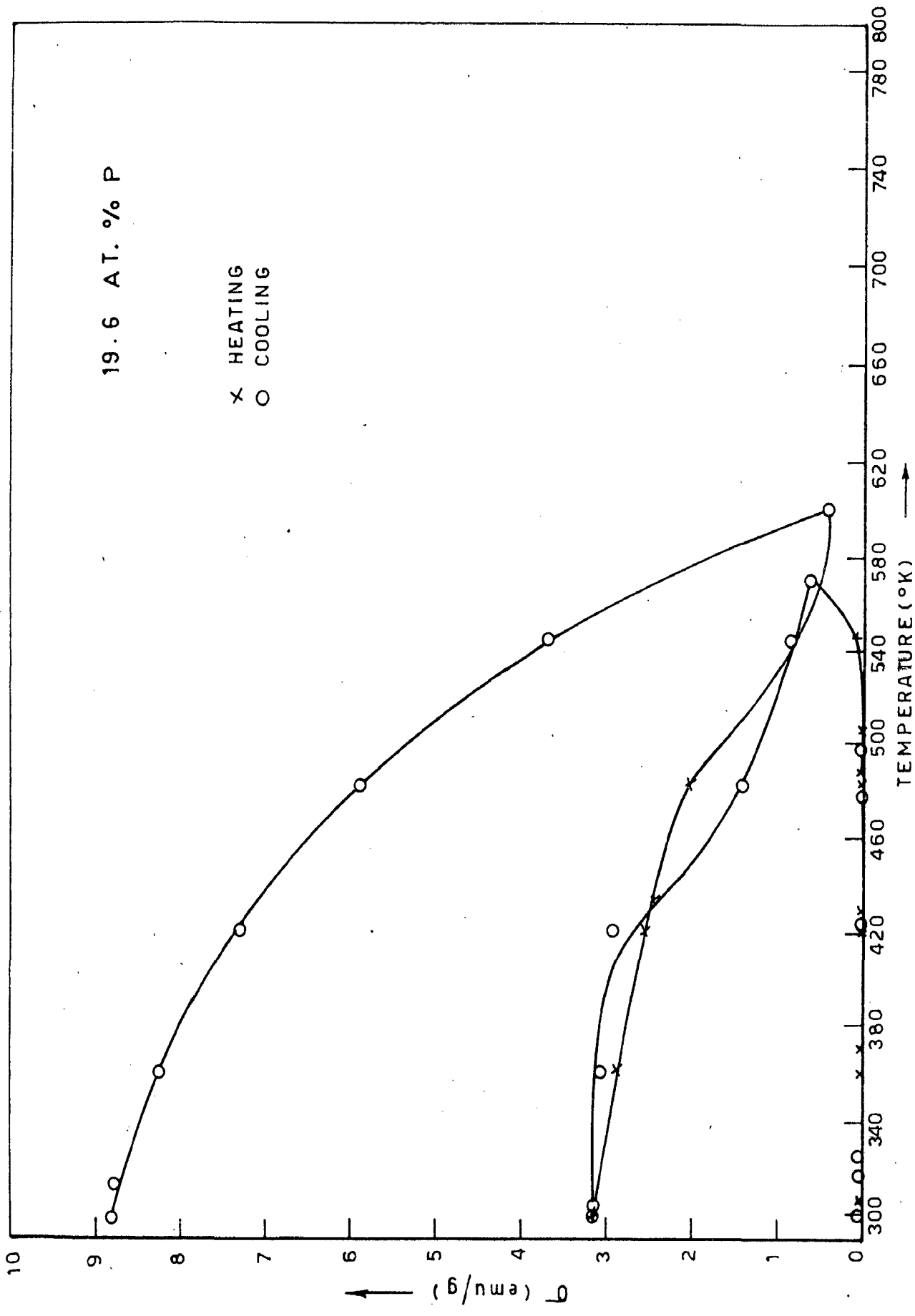


FIG. 6.8(c) - THE VARIATION OF MAGNETIZATION WITH TEMPERATURE, OF Ni-P SAMPLE CONTAINING 19.6 AT. % PHOSPHOROUS, WHEN IT IS HEATED AND COOLED IN STEPS.

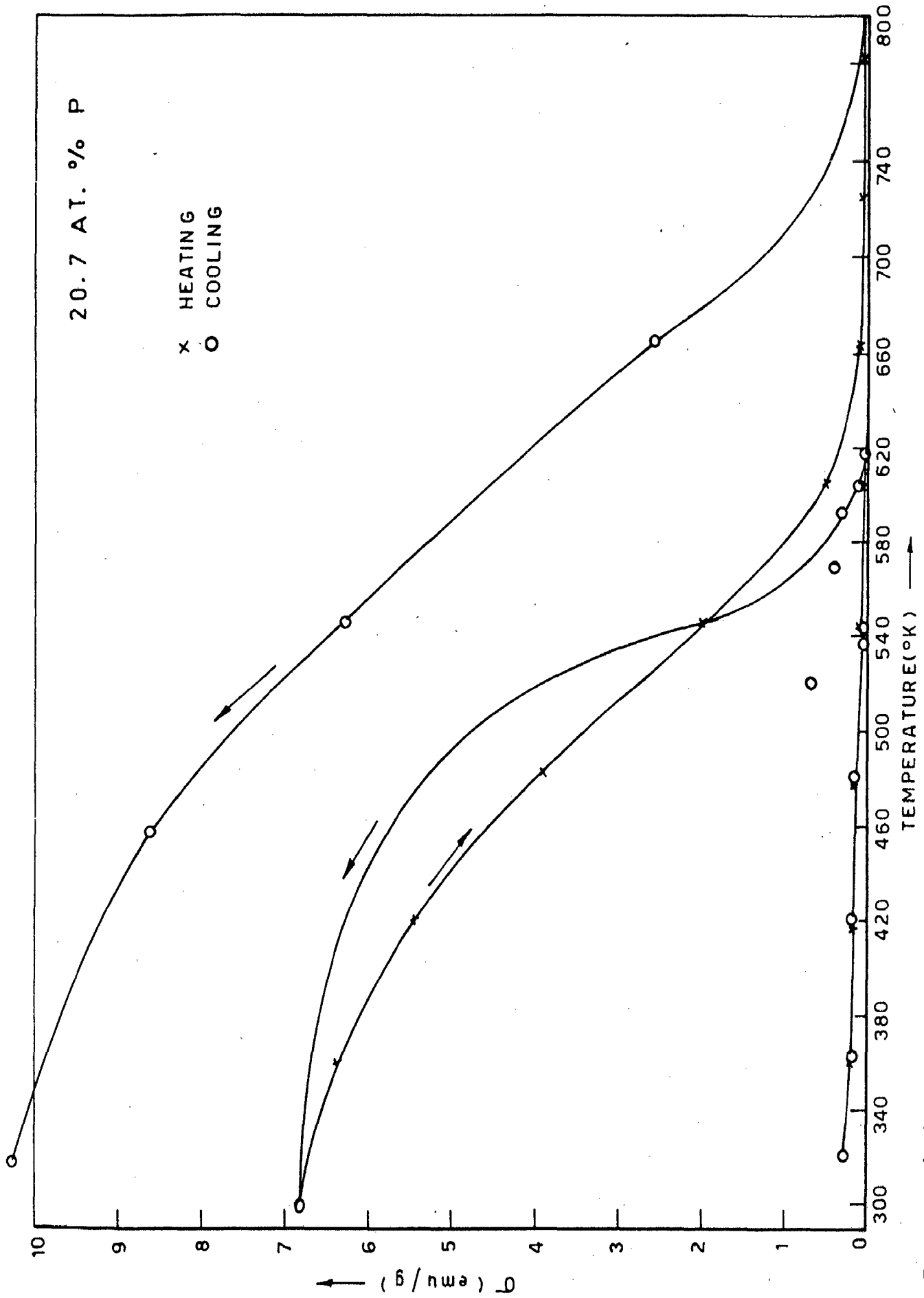


FIG. 6.8(d) - THE VARIATION OF MAGNETIZATION WITH TEMPERATURE, OF Ni-P SAMPLE CONTAINING 20.7 AT. % PHOSPHOROUS, WHEN IT IS HEATED AND COOLED IN STEPS.

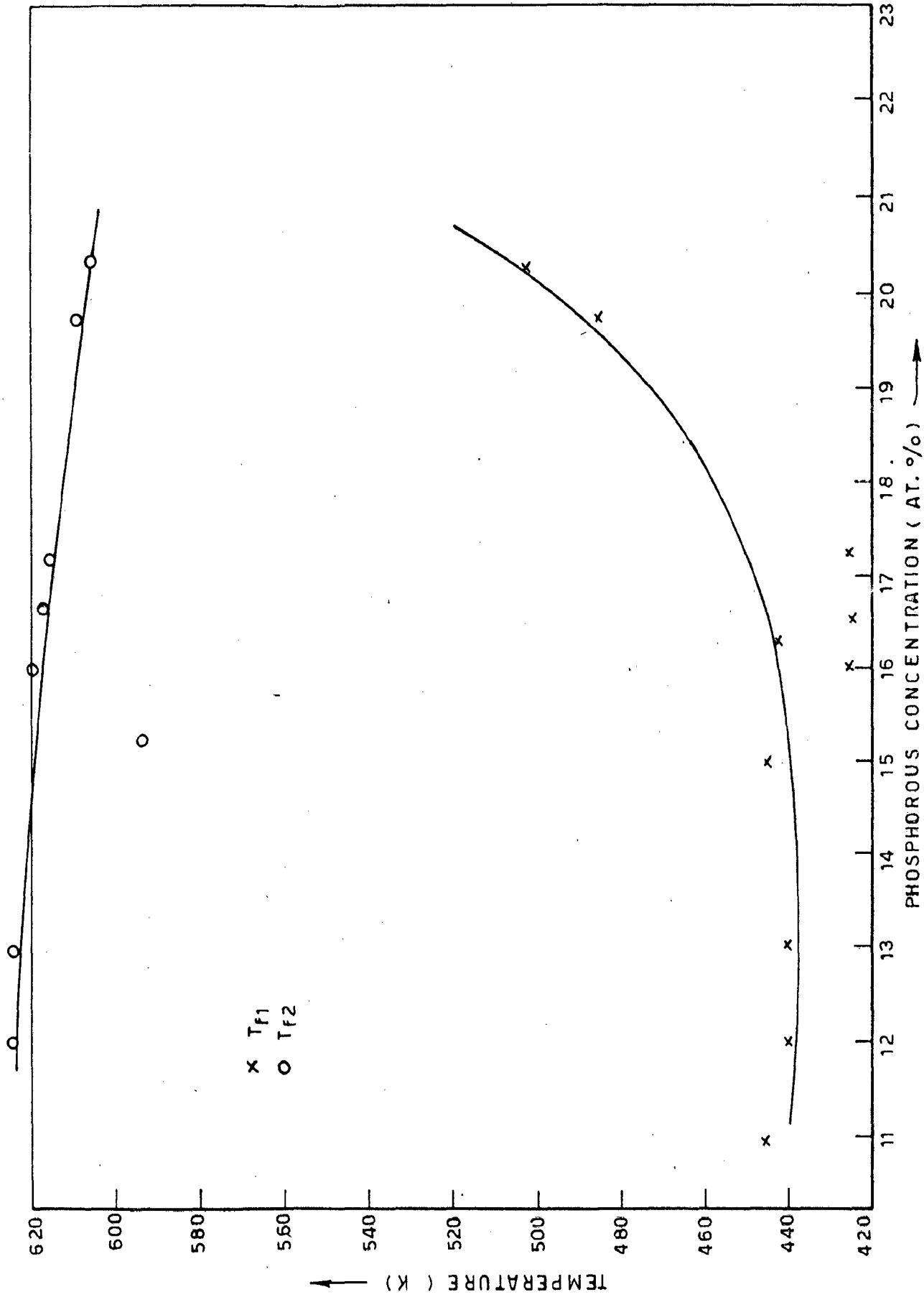


FIG. 6.9 - THE CHANGE IN THE TEMPERATURES AT WHICH FIRST AND SECOND MAGNETIC PEAKS APPEAR, WITH PHOSPHOROUS CONCENTRATION IN THE Ni - P SAMPLE ABOVE 12 AT.%.

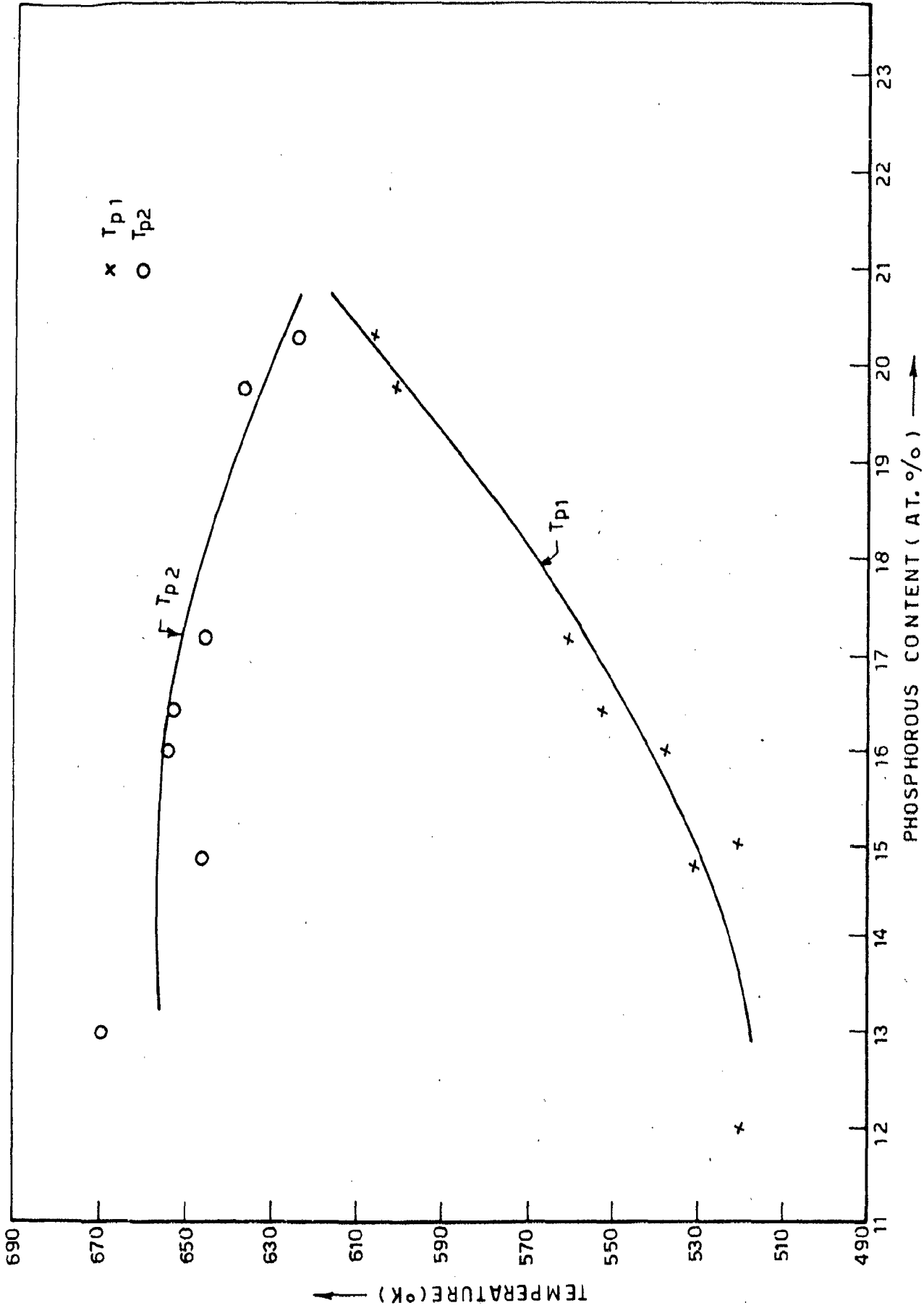


FIG. 6.10 - THE VARIATION OF TEMPERATURES, CORRESPONDING TO THE TWO MAGNETIC PEAKS, WHEN THE PHOSPHOROUS CONTENT IN THE SAMPLES CHANGES ABOVE 12 AT. %

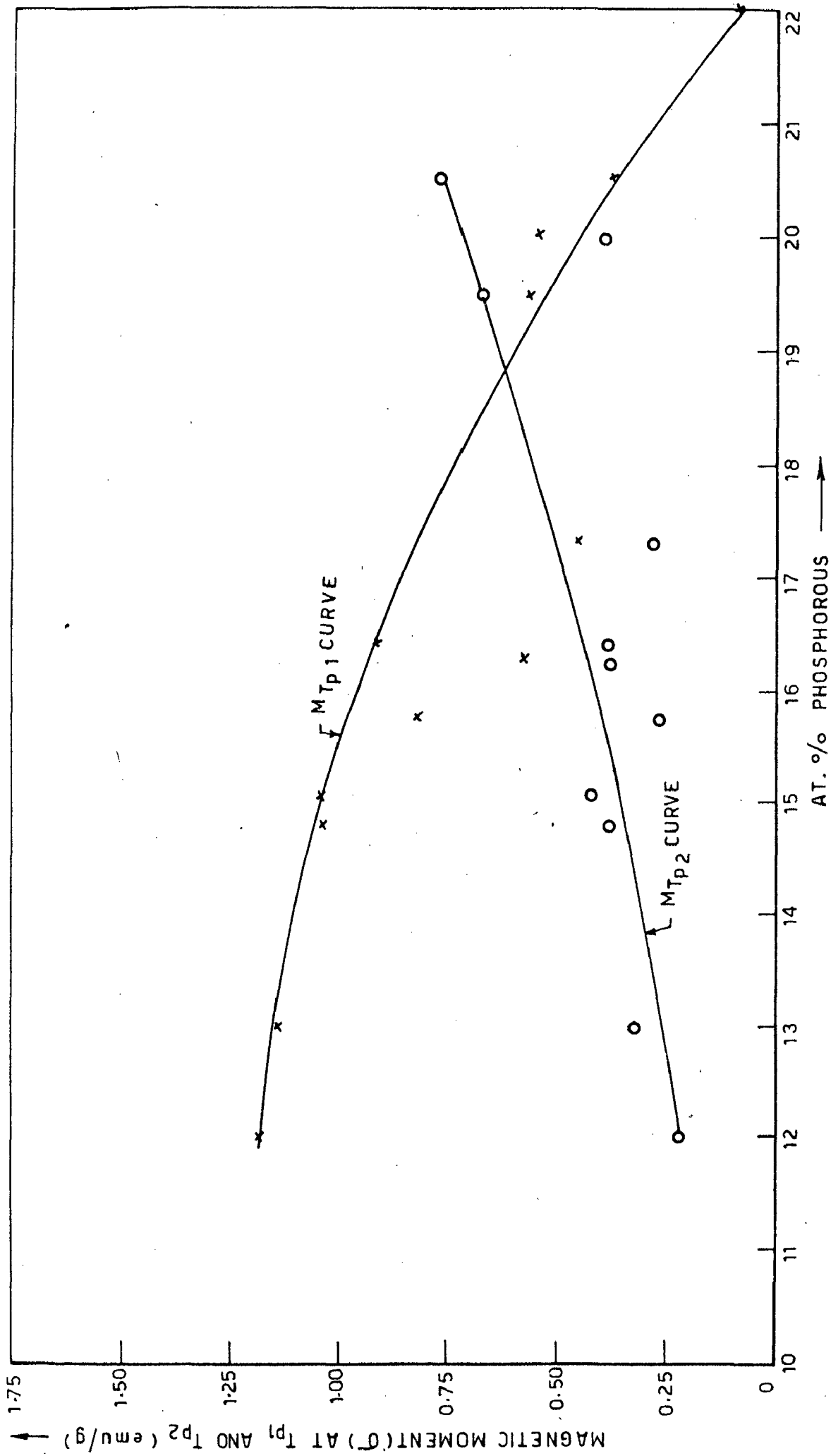


FIG. 6.11 - THE VARIATION OF MAGNETIC MOMENTS, CORRESPONDING TO THE MAGNETIC PEAK TEMPERATURES T_{p1} AND T_{p2} , WHEN PHOSPHOROUS IN THE SAMPLES IS CHANGING ABOVE 12 AT. %.

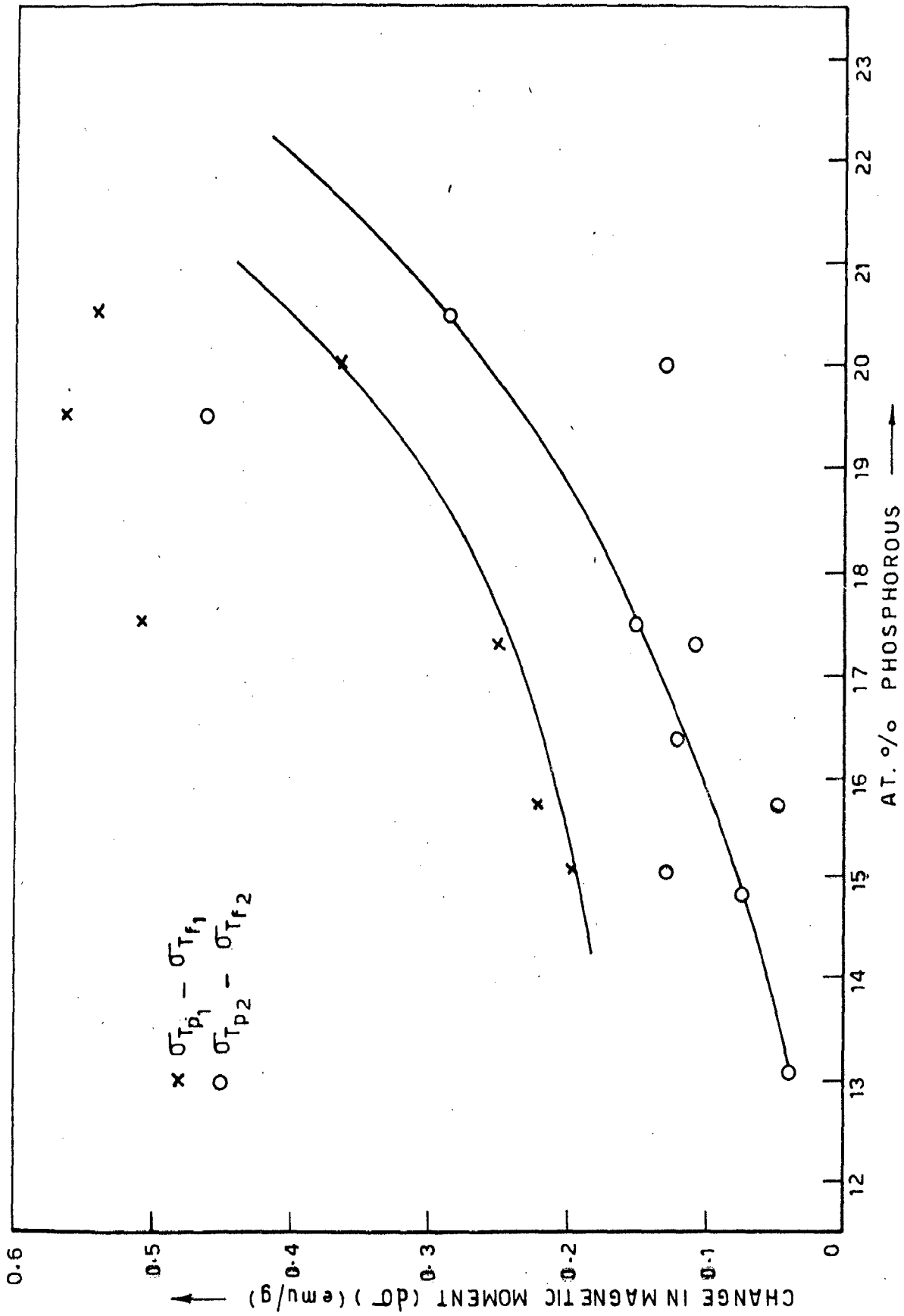


FIG. 6.12 - THE CHANGE IN MAGNETIZATION, AFTER REACTIONS INDICATED BY FIRST AND SECOND PEAK, WITH INCREASING PHOSPHOROUS IN Ni-P SAMPLES ABOVE 12 AT. %

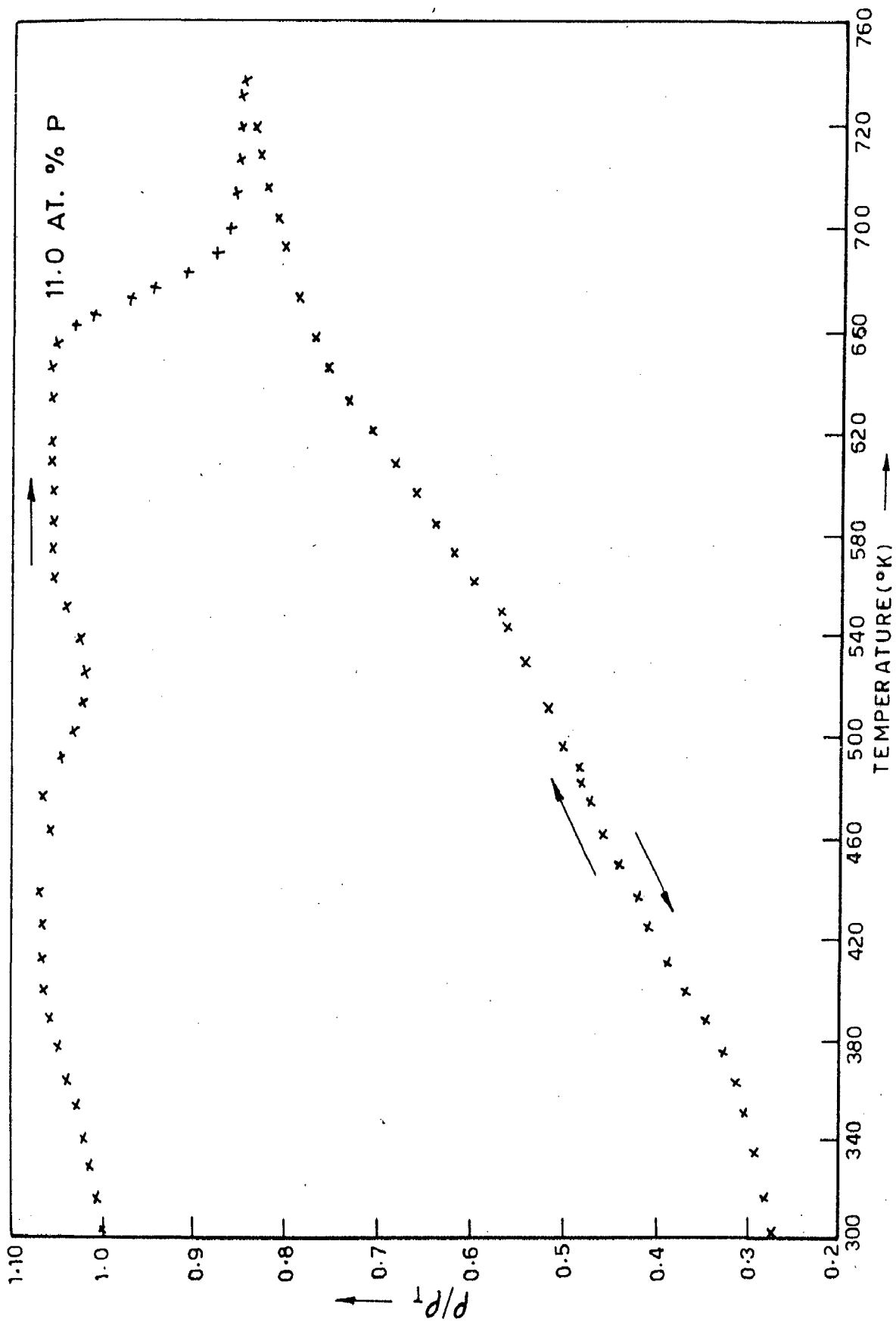


FIG. 6.13 - THE VARIATION OF ρ_1/ρ_{300K} WITH TEMPERATURE IN THE RANGE OF 300-760 K, OF THE Ni-P SAMPLE CONTAINING 11.0 AT.% PHOSPHOROUS

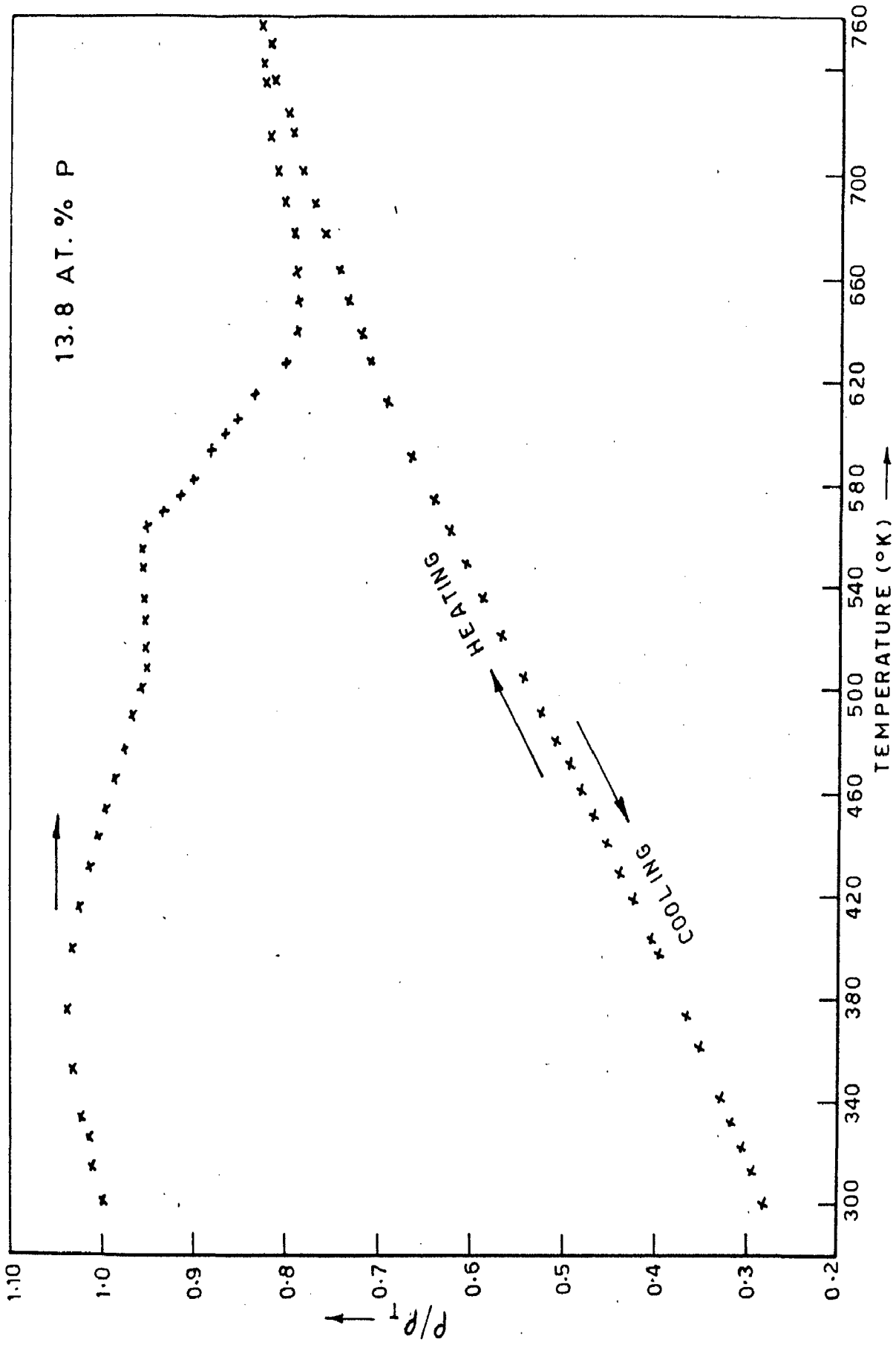


FIG. 6-14(a) - THE VARIATION OF ρ/ρ_{300K} WITH TEMPERATURE IN THE RANGE OF 300K - 760K, OF Ni-P SAMPLE HAVING 13.8 AT.% PHOSPHOROUS

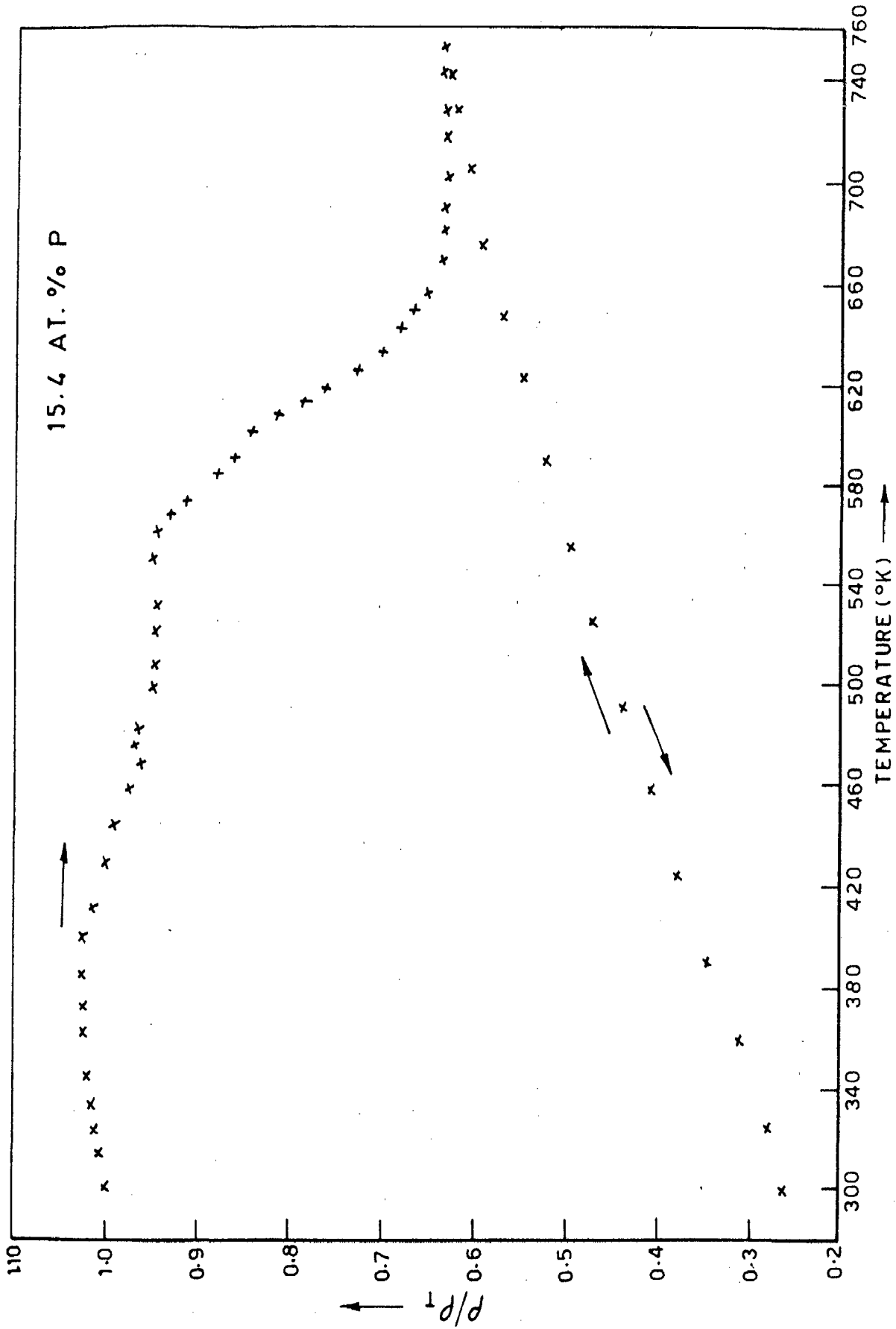


FIG.6.14(b) - THE VARIATION OF ρ/ρ_{300K} WITH TEMPERATURE IN THE RANGE OF 300K - 760K, OF Ni-P SAMPLE HAVING 15.4 AT. % PHOSPHOROUS

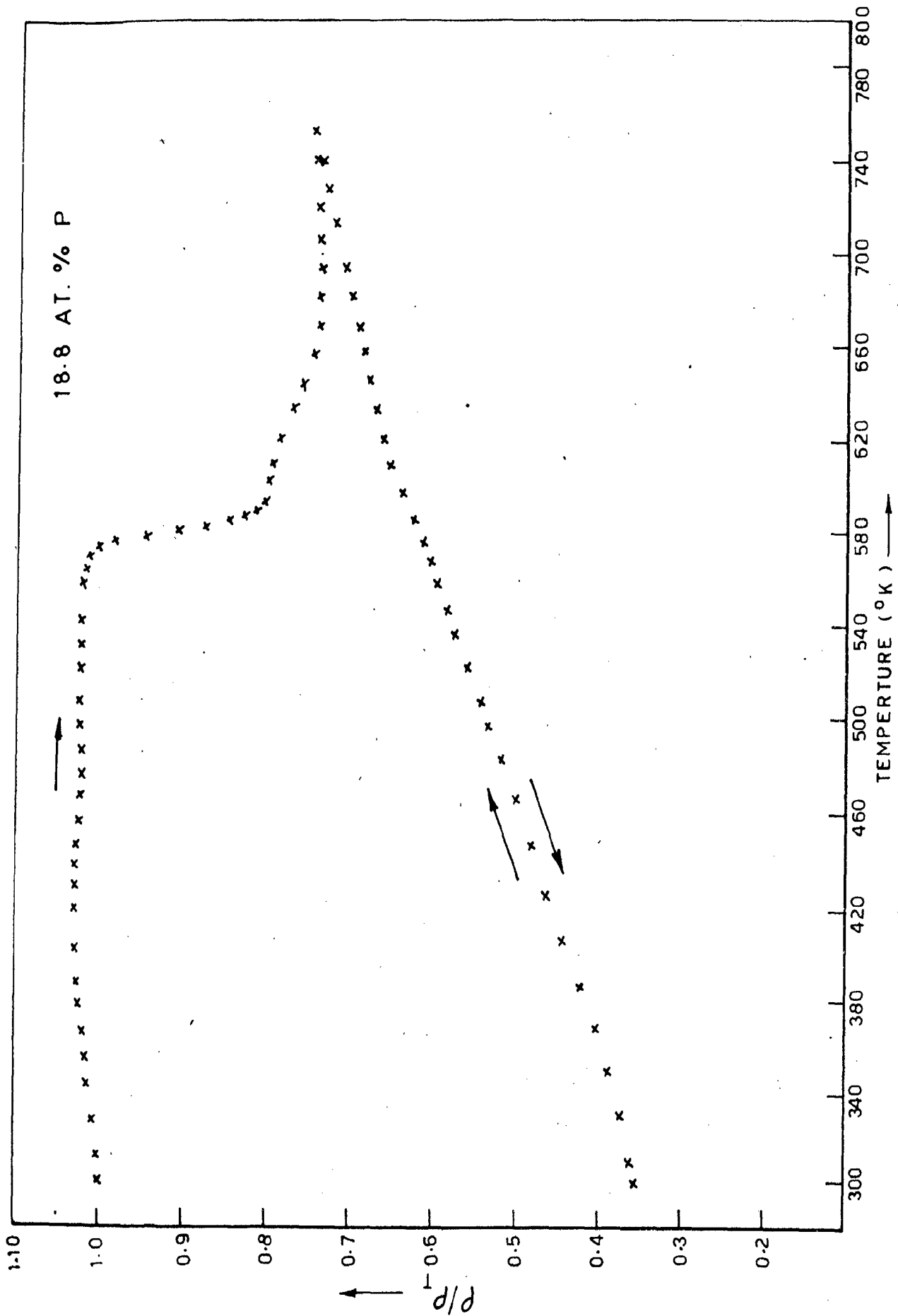


FIG. 6.15(a) - THE VARIATION OF ρ/ρ_{300K} WITH TEMPERATURE, IN THE RANGE OF 300K-760K OF Ni-P SAMPLES CONTAINING 18.8 AT. % PHOSPHOROUS

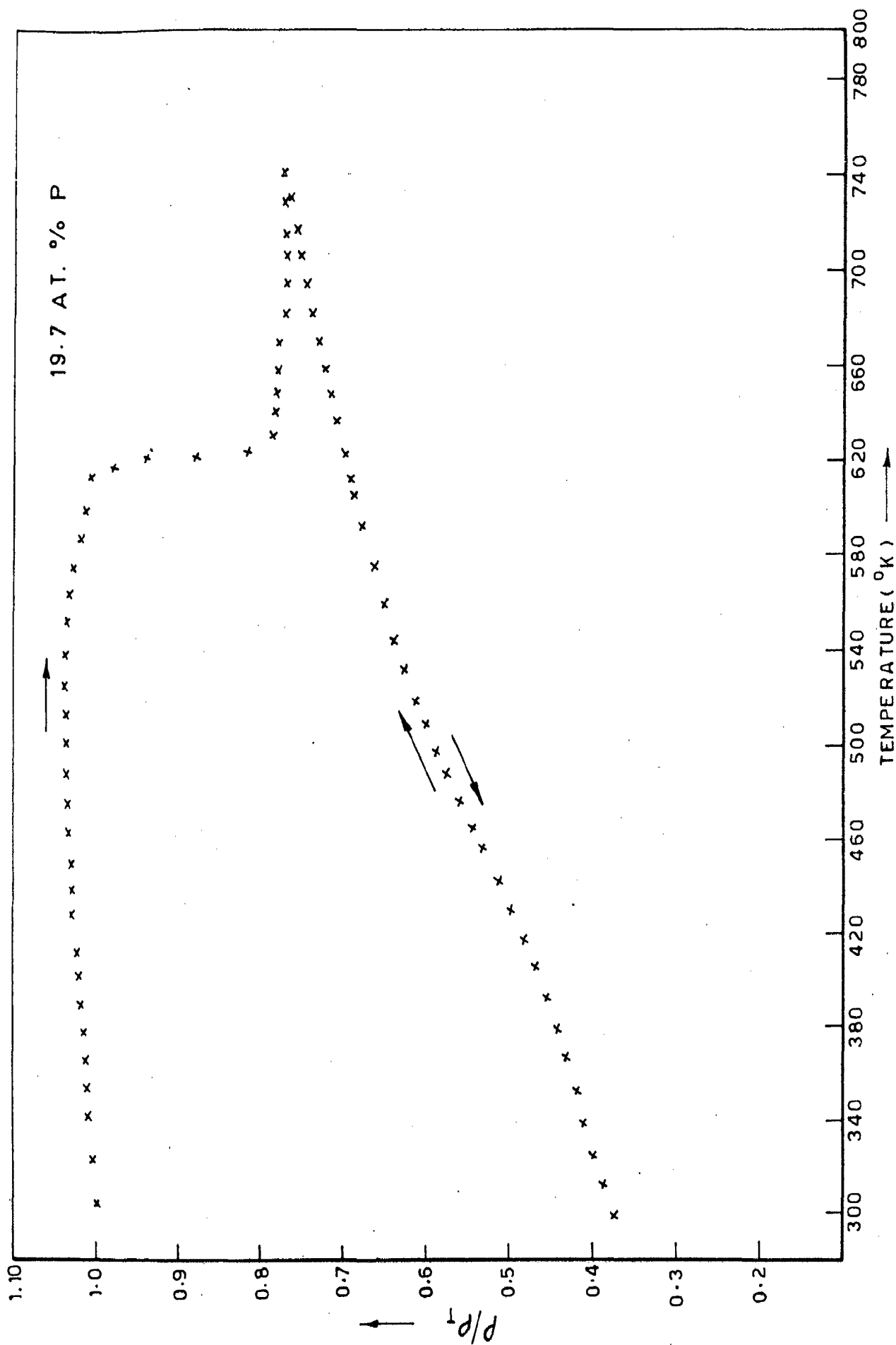


FIG. 6.15 (b) - THE VARIATION OF ρ/ρ_{300K} WITH TEMPERATURE OF Ni-P SAMPLE CONTAINING 19.7 AT. % PHOSPHOROUS, IN THE RANGE OF 300K-740K

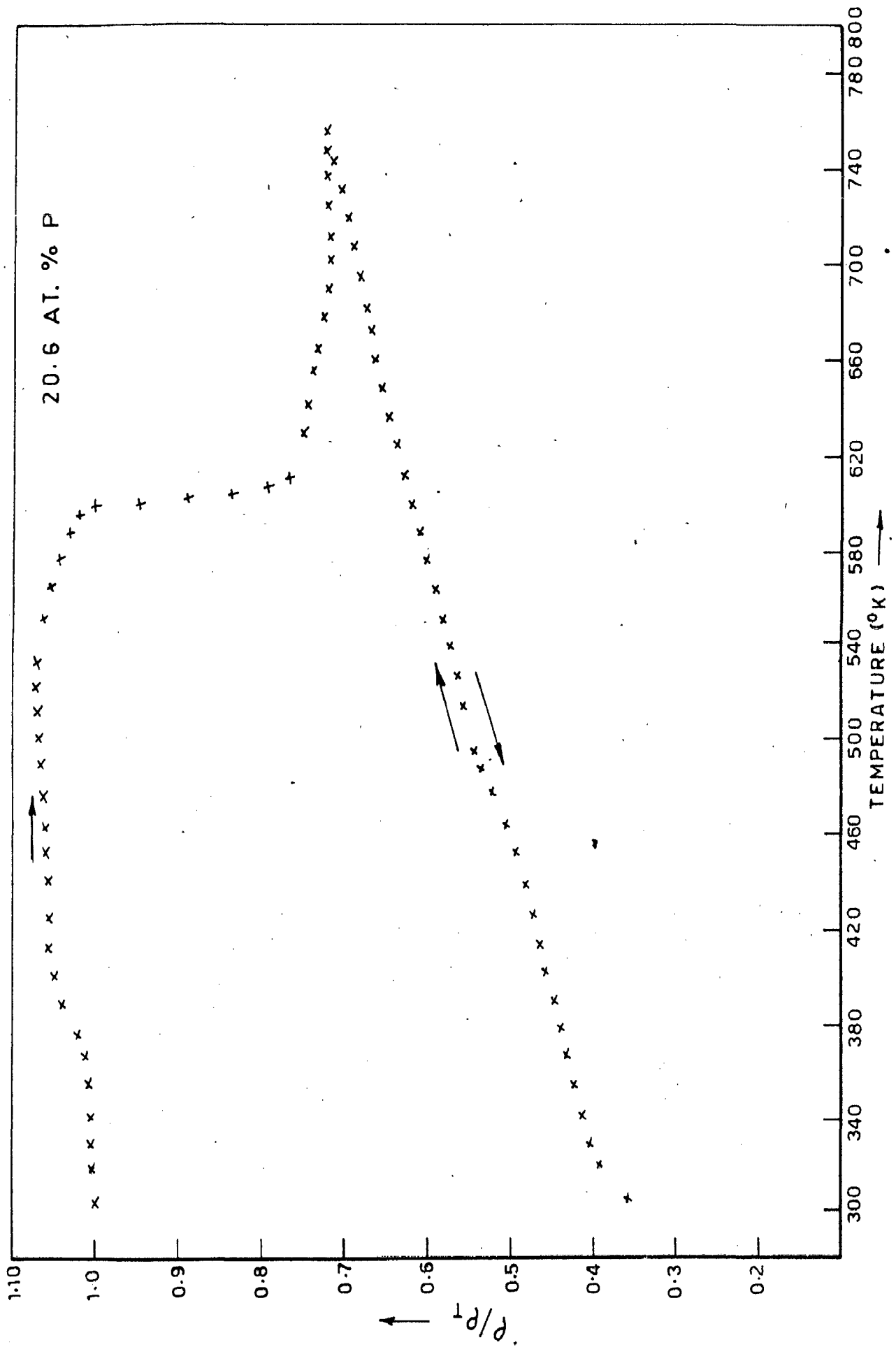


FIG. 6.15(c) - THE VARIATION OF ρ/ρ_{300K} OF Ni-P SAMPLE CONTAINING 20.6 AT. % PHOSPHOROUS, WITH TEMPERATURE IN THE RANGE OF 300K - 760 K

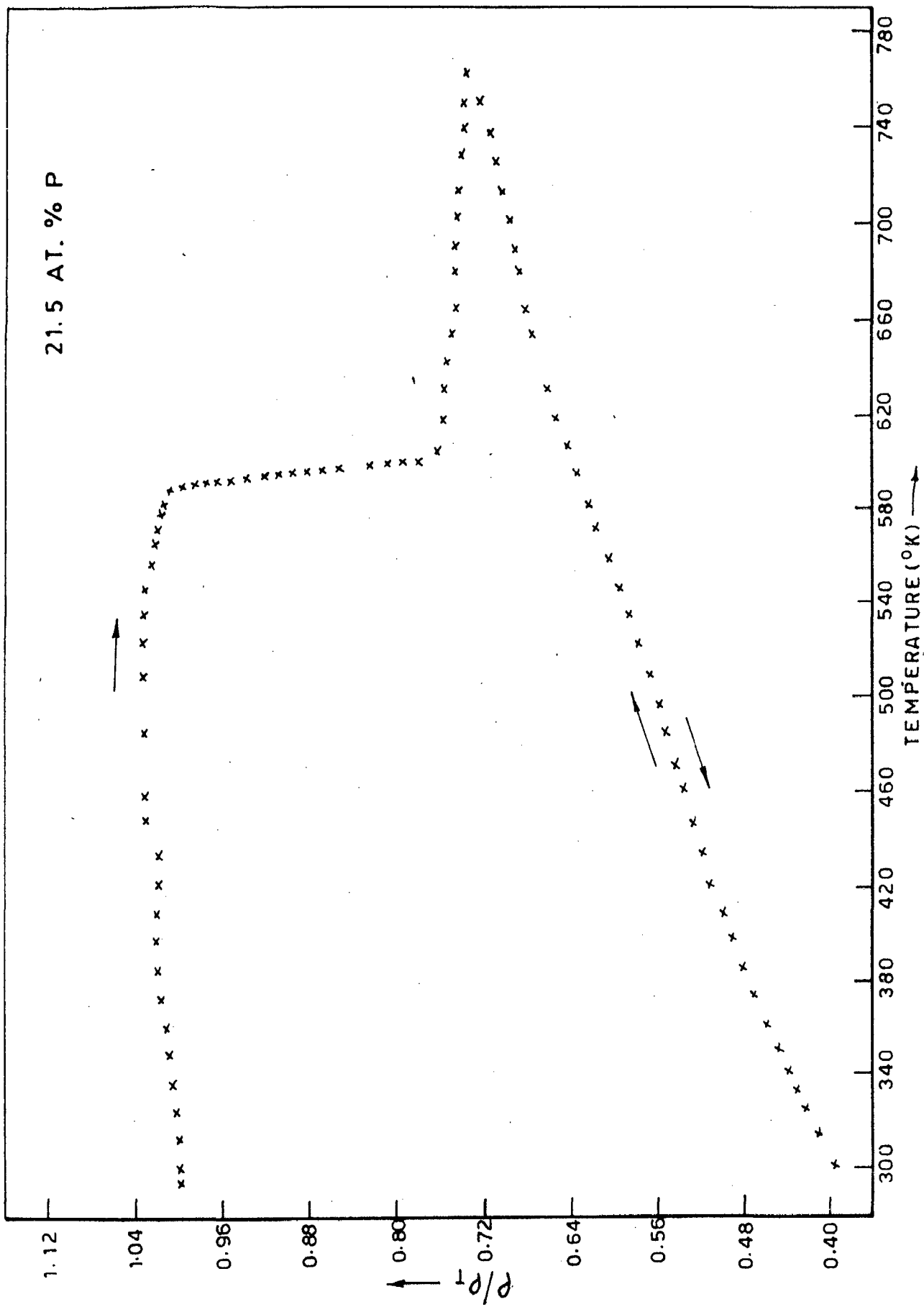


FIG.6.15(d) - THE VARIATION OF P/P_{300K} WITH TEMPERATURE IN THE RANGE OF 300K - 760K, OF Ni-P SAMPLE CONTAINING 21.5 AT. % PHOSPHOROUS

CHAPTER 7

CONCLUDING REMARKS

The chemical deposition of amorphous Nickel-Phosphorous film by Brenner et al in 1947 provides the second example of making noncrystalline alloys. Somewhat later Brenner and others (12) again made an important mark by electrodepositing amorphous Ni-P alloys. But it was not until the discovery of melt-quenched amorphous alloys by Pol.Duwez in 1959 that the widespread attention of the scientific community was drawn to explore the potential of these materials. Still, the electroless and electrodeposited amorphous alloys have received much less attention inspite of relative simplicity of these techniques.

In melt quenching or splat cooling amorphous alloys are made by kinetically suppressing the nucleation and growth process for crystallization. The most favourable glass forming composition range in this technique lies around the eutectic, the region of maximum stability of liquid structure. Schneider and Weisner (48) observed amorphous structure only in melt quenched Ni-18 at.% phosphorous but between 12 to 17 at .% phosphorous the alloys are microcrystalline. The mechanism of formation of amorphous structure in electroless and electrodeposited alloys are not clear and the most favourable range of composition

for amorphous alloys by these techniques need not be identical to that of melt quenching. Makhsoos(61), while summarizing the literature for electrodeposited alloys, concludes that those containing between 12 to 26 at.% phosphorous are amorphous. The structural studies of electroless films by electron microscopy, X-ray and selected area electron diffraction pattern reveals that the films containing less than 11 at.% are polycrystalline. Those having phosphorous between 11 to 14 at.% are microcrystalline and the films with 14 to 18 at.% phosphorous are in mixed microcrystalline-amorphous state. Finally, the films containing more than 18 at.% phosphorous are fully amorphous. The uncertainty in determining the limits of composition are reasonably high due to difficulties in the chemical analysis of these films. Also, the microscopy and X-ray techniques have a higher limit of detection. These results have been refined by magnetic measurements on thick films where compositions are known quite accurately. The films in mixed state are observed in a composition range of 12 to 18 at.% phosphorous. Thus, in the same system of Ni-P alloy the occurrence of microcrystalline and amorphous phase are observed over different ranges depending on its method of preparation. This aspect of formation of amorphous alloys requires a more deeper probing.

The selected area diffraction patterns of the amorphous phase are quite distinct from that of

microcrystalline alloys. The former contains one intense and another weak diffuse rings but the latter will show two relatively intense rings along with a weak diffuse ring. But it requires a careful observation for proper identification. Bagley and Turnbull(59) suggested that microcrystalline films will grow to coarser crystallites on heating but an amorphous film will transform by nucleation and growth. A simultaneous coexistence of crystalline and amorphous diffraction pattern should indicate a phase transformation. Fortunately, the precipitation of crystalline Nickel from amorphous alloy made it possible to observe the co-existence of diffuse rings and diffraction spots. The final crystallisation reaction is quite rapid as it has been observed in the annealing behaviour of resistivity. In sample of higher phosphorous say more than 24 at.% P it may not be practicable to identify amorphous phase by the suggestion of Bagley and Turnbull.

The electrical and magnetic properties of electroless films as it has been observed in the present investigation are quite similar to those of electrodeposited films. The amorphous films are weak itinerant ferro magnetic with Curie temperature and magnetisation reducing with an increasing phosphorous content. The reduction of

magnetisation takes place at a slower rate with phosphorous in the amorphous alloy as compared to that in the non-equilibrium crystalline Ni-P alloy. In the amorphous alloy strong magnetic clusters are observed to exist in the paramagnetic state upto paramagnetic Curie temperature which is observed to decrease with an increase in the phosphorous content of the alloy. The resistivity of the microcrystalline, mixed and amorphous alloys show a quadratic variation with temperature in the range of 140 to 280 K and a linear variation in the range of 280 K to 400K. However, it should be noted that the resistivity of electroless films are lower as compared to those observed in electrodeposited films upto a phosphorous content of about 18-20 at.% which may again be an indication of the fact that the electrodeposited films are amorphous at a phosphorous content beyond 12 at.% while the electroless films are in mixed state. The micro-crystalline regions act as shunt that reduces the resistivity of such alloys.

The transformations in non-equilibrium Ni-P films on heating have been intensively investigated in order to understand the crystallisation behaviour of amorphous Ni-P alloys. The films with less than 12 at% phosphorous when heated, relieves its stress at around 450 K. At a

still higher temperature of around 650 K the equilibrium Ni_3P precipitates out from supersaturated crystalline Nickel. The changes in magnetisation are not so high as to display a peak in magnetisation, but on cooling the alloy from above 650 K, one observes an enhanced room temperature magnetisation. The amorphous alloys on annealing shows an atomic relaxation reflected in the measured resistivity at around 420 K but at a still higher temperature one observes precipitation of crystalline nickel over a broad temperature range. On further heating the crystallisation of the amorphous alloy to equilibrium phases of Nickel and Ni_3P takes place above 680 K. Subsequent to crystallisation the alloys undergoes another transformation which has been attributed to recrystallisation of the crystallised phases. The extent of precipitation of crystalline nickel reduces with an increasing phosphorous content in the amorphous alloys and this reaction is not observed in a film containing 23.5 at % phosphorous. With increasing phosphorous the temperature for crystalline Nickel precipitation increases and that of crystallisation to equilibrium phases reduces. The electroless films in the mixed microcrystalline amorphous state shows a superposition of annealing behaviour of these constituent regions.

The present investigation has been an attempt to understand the structure and properties of electroless Ni-P alloys

in particular its crystallisation behaviour. The composition ranges of stability of crystalline, microcrystalline and amorphous alloys in electroless films have been established by diffraction analysis and microscopy, and it has been refined further by annealing studies by magnetisation and resistivity measurements. The existence of a mixed microcrystalline and amorphous state has been identified for the first time for an intermediate phosphorous content of 12 to 18 at% in the films. The high Curie temperature and lower resistivity of these films as compared to those in electrodeposited films, have been attributed to this mixed state. The sequence of transformation on annealing the crystalline, microcrystalline and the amorphous films have been determined in an integrated way by combining the results of microscopy, diffraction analysis, magnetization, and resistivity behaviour on annealing. It may very well be that the phosphorous contents in both the microcrystalline and amorphous regions for a mixed state remains almost constant but it could not be confirmed due to a lack of facility for microprobe analysis.

The purpose of the present investigation, to unravel the unique characteristics of electroless Ni-P alloys through the structure and property characteristics in

contrast to those obtained by electrodeposited and meltquench techniques and to understand the intermediate reactions leading to the formation of non-equilibrium phases during the crystallization, has been fulfilled to a large extent.

R E F E R E N C E S

1. Gubanov A.L., Quasi-classical theory of amorphous ferromagnetics, *Fiz.Tverd.Tela*, 2, 502, 1960.
2. Madar S. and Nowick, A.S., Metastable Co-Au Alloys: Example of an amorphous ferromagnet, *Appl.Phys.Letters*, 7, 57, 1965.
3. Cahn, R.W., Metallic glasses, *contemp.phys.*21, 43, 1980.
4. Chen, H.S., Glassy metals, *Rep.progr.phys.*43, 353, 1980
5. Wright J.G., Amorphous transition metal films, *IEEE trans.magn.MAG*, 12, 209, 1976.
6. Cargill G.S.III, Formation, structure and properties of metallic glasses, Research Report RC 8262 (=F 35514) 3/12/80 solid state physics.
7. Luborsky F.E. (Editor), Amorphous metallic alloys, Butterworths monographs in materials, 1983.
8. Luborsky, F.E., Ferromagnetic materials, Ed. Wohlfarth E.P. Vol.1, chap 6, North-Holland Pub.Co. Amsterdam, 1980.
9. Aboaf J.A., Kobliska R J and E.Kloholm, Properties of transition metal-metalloid Ferromagnetic thin films, *IEEE, trans. Mag. MAG-14*, 941, 1978.
10. Cargill III G.S., Structural Investigation of non-crystalline Ni-P alloys, *J.Appl.phys.*, 41, 12, 1970.
11. Cargill III G S and Cochrane R.W., Amorphous Co-P alloy: Atomic arrangements and magnetic properties, *J.de Physique*, C4 supplement au n^o5 Tome 35, C4-269, 1974.
12. Brenner A., Couch D.E., and Williams E.K., Electrodeposition of alloys of phosphorous with nickel or cobalt, *J.Res.Nat.Bur.Stand.*44, 109, 1950.

13. Berrada A., Lapierre M.F., Loegel B., Panissod P., and Robert C., A study of magnetic and transport properties of amorphous electrodeposited Ni-P alloys, *J.Phys.F.8*, 845, 1978.
14. Cote, P.J., Electrical resistivity of amorphous Ni-P alloys, *solid state commun.18*, 1311, 1976.
15. Bakonyi I, Vargal,L.K, Lovas, A., Toth-Kadar E., & Solyom A; Magnetization and NMR study of amorphous Ni-P alloys in the paramagnetic concentration range, *J.Magn. & Magn. Mat.*, 50, 111, 1985.
16. Goldstein, A.W., Rostoker W., and Schossberger F., Structure of chemically deposited nickel, *J.Electrochem. Soc.104*, 104, 1957.
17. Graham, A.H., Lindsay R.W. and Read J., The structure and mechanical properties of electroless nickel, *J.Electrochem. Soc.*, 112, 401, 1965.
18. Pai S.T. and Marton J.P., Annealing effects on the structure and resistivity of Ni-P films, *J.Appl.Phys.* 43, 282, 1972.
19. Albert P.A. Kovac Z., Lilienthal H.R., Mcguire T.R. and Nakamura Y., The effect of phosphorous on the magnetization of nickel, *J.Appl.Phys.*,38, 1258, 1967.
20. Maeda H, Perpendicular anistropy of electrodeposited Ni and Ni-P films, *J.Phys.Soc.Japan*, 29, 311, 1970.
21. Randin J.P; Chemical nature phosphorous in Ni-P deposits, *J.Appl.Phys.43*, 4834, 1972.
22. Schlesinger M., and Marton J.P., Electrical and optical properties of Ni-P films, *J.Appl.Phys.*,40,507, 1969.

23. Bagley B.G. and Turnbull D., The preparation and crystallization behaviour of amorphous Ni-P thin films, *Acta.Metall.*18, 857, 1970.
24. Bérada A., Gautier F., Lapiere M.F., Loegel B., Panissod P., Robert C., and Beille J., Magnetic properties of amorphous Ni-P alloys, *Solid State Commun.*, 21, 671, 1977.
25. Bennett L H., Schone H.E. and Gustafson, Nuclear magnetic resonance studies of amorphous Ni-P alloys, *Phys. Rev.B*, 18, 2027, 1978.
26. Cziraky A., Fogarassy B., Bakonyi I.Tompa K, Bagi T and Hegedus Z., Investigation of chemically deposited and electrodeposited amorphous Ni-P alloys, *J.De, Physique, Colloque C8, supplement au n°8, Tome 41, aout, C8-141, 1980.*
27. Yamasaki T., Izumi H., and Sunada H., The microstructure and fatigue properties of electroless deposited Ni-P alloys, *Scripta Metall.* 15, 177, 1981.
28. Cortiju , R.O. and Schlesinger M., Structural studies of electroless thin Ni-P films grown in an alkaline environment, *J. Electrochem Soc.*, 130, 234, 1983.
29. Fisher R.D. and Chilton W H., Preparation and magnetic properties of chemically deposited cobalt for high density storage, *J.Electrochem Soc.*109, 485, 1962.
30. Judge J.S., Morrison J.R. Speliotis D.E. and Bate G., Magnetic properties & Corrosion behaviour of thin electroless Co-P deposits, *J.Electrochem, Soc.*112, 681, 1965 .

31. Konbe T. and Kanematsu K., Magnetic properties of solid solution of cobalt with phosphorous, J.Phys.Soc.Japan, 24, 1396, 1968.
32. Pan D. and Turnbull D., Magnetic properties of amorphous Co-P alloys, J.Appl.Phys., 45, 1406, 1974.
33. Cargill III G S and Cochrane R.W., Amorphous Co-P alloys: Atomic arrangements and magnetic properties J.de Physique, C4, supplement au n°5, Tome 35, C4-269, 1974.
34. Chi G.C. and Cargill III G S, Perpendicular anisotropy of amorphous, electrodeposited Co-P alloy films , 21st Annual Conf. on magnetism and magnetic materials, Philadelphia, Pa, Dec.1975.
35. Cargill G.S.III and Kirkpatrick S., Structural ordering in some amorphous metals and alloys, AIP Conf.Proc., 31, 359, 1976.
36. Chi G.C. and Cargill G.S.III, Structural characterization of amorphous electrodeposited Co-P alloys, J. Appl.Phys., 50, 2713, 1979.
37. Riveiro J.M. and Sanchez-Trujillo M.C., Magnetic Anisotropy of electrodeposited Co-P alloys, IEEE Trans.Mag., MAG-16, 1426, 1980.
38. Riveiro J.M. and Rivero G., Multilayered magnetic amorphous Co-P films, IEEE Trans. Magn.MAG-17, 3083,1981.
39. Gorbunova K M, Ivanov M.V., and Moiseev V.P., Electroless Deposition of Ni-B alloys, J.Electrochem.Soc.120, 613, 1973.

40. Hedgecock N., Tung P., and Schlesinger M., On the structure and electrical properties of electroless Ni-B films, *J. Electrochem Soc.* 122, 866, 1975.
41. Takahashi M., Tateno Y., and Koshimura M., Observation of structures in rapidly quenched Ni-B alloys, I, *Jap. J. Appl. Phys.* 19, 2335, 1980.
42. Kaul S.N. and Rosenberg M., Magnetic properties of amorphous Ni-B alloys, *Phys. Rev. B*, 25, 5863, 1982.
43. Bakonyi I and Panissod P., Magnetic properties of glassy Ni_{81.5}B_{18.5} alloy, *J. Appl. Phys.* 53, 7771, 1982.
44. Bakonyi I. and Panissod P., Magnetic and NMR study of amorphous and crystalline Ni-B alloys, *J. of non-crystalline solids* 61 & 62, 1189, 1984.
45. Rhodes P. and Wohlfarth E.P., The effective Curie-Weiss constant of ferromagnetic metals and alloys, *Proc. Roy. Soc.* 273, 247, 1963.
46. Simpson A.W. and Brambley D.R. The temperature variation of magnetization of Bulk amorphous Ni₈₅P₁₅: An Amorphous Ferrimagnet?, *phys. stat. sol. (b)* 49, 685, 1972.
47. Pan D and Turnbull D., Magnetic properties of amorphous alloys: I. Co-P, II Ni-P, Research Report No.1, Division of engineering and applied physics, Harvard University, Under contract No.000 14-67-A-0298-0036, 1974.
48. Schneider J. and Wiesner H., Magnetic properties of rapidly quenched Ni-P alloys, *phys. stat. solids (a)* 29, K25, 1975.
49. Tamura K and Endo H., Ferromagnetic properties of amorphous nickel, *Phys. Lett.* 29 A, 52, 1969.

50. Fahnle M., Distribution of dipole fields in disordered crystalline and amorphous ferromagnetic alloys, Appl. Phys.21, 1, 1980.
51. Bakonyi, I., On the magnetism of nickel-metalloid alloys, Proc. 5th Int.Seminar on Magn.(Berggishubel, 161, 1984.
52. O'Handley R.C., Hasegawa R., Ray R., and Chow C.P., Magnetic properties of $TM_{80}P_{20}$ glasses, J.Appl.Phys. 48, 2095, 1977.
53. Boucher B.Y., Influence of phosphorous on the electrical properties of Pd-Ni-P amorphous alloys, J.Non-crystalline solids 7, 277, 1972.
54. Beeby J.L., Ferromagnetism in transition metals, Phys. Rev.B.141, 781, 1966.
55. Dreirach O., Evans R., Guntherodt H.J. and Kunzi H.U., A simple muffin tin model for the electrical resistivity of liquid noble and transition metals and their alloys, J.Phys.F Metal Phys.2, 709, 1972.
56. Meisel L V and Cote P.J., Structure factors in amorphous and disordered harmonic Debye solids, Phys.Rev.B 16, 2978, 1977.
57. Cote P.J. and Meisel L.V., Resistivity in amorphous and disordered crystalline alloys, Phys.Rev.Lett.39, 102, 1977.
58. Randin J.P., Maire P.A., Saurer E. and Hintermann H.E., DTA and X-ray studies of electroless nickel, J.Electrochem. Soc.114, 442, 1967.
59. Bagley B.G. and Turnbull D., Structure study of an amorphous electrodeposited nickel-phosphorous alloy, J.Appl.Phys.39, 5681, 1968.

60. Tyagi, S.V.S., Tandon V.K. and Ray S., Study of crystallization behaviour of electroless Ni-P films by electron and X-ray diffraction, *Z.Metallkde.*76,492,1985.
61. Makhsoos E.V., Thomas E.L. and Zoth L.E., Electron-microscopy study of crystalline and amorphous Ni-P electrodeposited films : In-situ crystallization of an amorphous solid, *Met.Trans.A.9A*, 1449, 1978.
62. Bakonyi, I.Cziraky, A. Nagy I and Hosso M., Crystallization characteristics of electrodeposited amorphous Ni-P alloys, *Z.Metallkde.*66, 5291, 1986.
63. Gorbunova K.M. and Nikiforova A.K., *Zhurnal Fizicheskoi Khimii*, 28, 883, 1984.
64. Gorbunova K.M. and Nikiforova A.K., Mechanism of reduction of phosphorous in the formation of Ni-P coating, *Protection of Metals*, 5, 163, 1969.
65. Mooij J.H., Electrical conduction in concentrated disordered transition metal alloys, *Phys.Stat.Sol.,A-17*, 521, 1973.
66. Yamauchi K and Mizoguchi T., The magnetic moments of amorphous metal-metalloid alloys, *J.Phys.Soc.Japan Lett.*, 39, 541, 1975.
67. Harris R., Plischke M. and Zuckermann M.J., A model for magnetism in amorphous metals, *J.de Physique*, 35, C4-265, 1974.
68. Harris R., Plischke M., Zuckermann M.J., A new model for amorphous magnetism, *Phys.Rev.Lett.*,31, 160, 1973.
69. Handrich K., Some general thermodynamic properties of amorphous magnets, Preprint QM 2/72, Tu Dresden, 1972.

70. Handrich K. Hemmerling J & Abdallah N., Thermodynamic behaviour of a one-dimensional amorphous Ising Model, *Acta.Phys.Pol.*, A41, 663, 1972.
71. Edwards D.M. and Wohlfarth E.P., Magnetic Isomers in the band model of ferromagnetism, *Proc.Roy.Soc.A*, 303, 127, 1968.
72. Malozemoff A.P., Williams A.R. and Moruzzi V.L., Band gap theory of strong ferromagnetism: Application to concentrated crystalline and amorphous Fe and Co-metalloid alloys, *Phys. Rev.B*, 1620, 1984.
73. Evans, R., Greenwood D.A. and Lloyd P., Calculations of the transport properties of liquid transition metals, *Phys.Lett.* 35 A, 57, 1971.
74. Nagal S.R. and Tauc J., Nearly free electron approach to the theory of metallic glass alloys, *Phys.Rev.Lett.* 35, 380, 1975.
75. Rao K.V., Malmhall R., Bhagat S.M., Backstorm G., and Chen H.S., Magnetic and transport properties of transition-metal based glassy ribbons, *IEEE trans.Mag.*, MAG-16, 896, 1980.
76. Rapp O., Bhagat S.M. & Johannesson Ch. Measurements of the electrical resistivity of amorphous ferromagnets, *solid state commun.* 21, 83, 1977.
77. Maitrepierre P., Electrical resistivity of amorphous Ni-Pd-P alloys, *J.Appl.Phys.* 41, 498, 1970.
78. Hasegawa R. and Dermon J.A., Electrical resistivity and Curie temperature of amorphous (Fe-Ni)-P-C alloys, *Phys. Lett.* 42A, 407, 1973.
79. Lagarde P., Rivory J. and Vlaic G., Structural studies of amorphous Co-P and Ni-P by EXAFS, *J.of non-crystalline solids*, 57, 275, 1983.

80. Wright J.G., Amorphous transition metal films, IEEE Trans. Magn. MAG-12, 95, 1976.
81. Rao K.V., Electrical Transport properties, Chap.21 of book on amorphous metallic alloys, edited by F.E. Luborsky, Butterworths monographs in materials, 401, 1983.

